Università degli Studi di Ferrara

PH.D. Course
in
Evolutionary Biology and Ecology

In cooperation with:
Università degli Studi di Parma
Università degli Studi di Firenze

CYCLE XXXI

COORDINATOR Prof. Barbujani Guido

Evolution of UV-photoreception and DNA repair systems in blind cavefish

Scientific/Disciplinary Sector (SDS) BIO/05

Candidate

Dott. Di Mauro Giuseppe

Supervisor

Prof. Bertolucci Cristiano

Years 2015/2018

INDEX

Abstract 2

Chapter 1: *General Introduction* 4
1.1 - Fish as model for study light-related mechanisms 5
1.2 - Evolution in absence of light 8
1.3 - Ecological roles of UV light 9
1.4 - Impact of UV-light on the zebrafish physiology 11

Chapter 2: *Evolution of UV photoreception in fish* 13
2.1 - Introduction 14
2.1.1 - Ocular and Extra-ocular perception of UV light 14
2.1.2 - Circadian clock 22
2.1.3 - Phototaxis 26
2.2 - Aim 30
2.3 - Material and Methods 31
2.3.1 - Entrainment of circadian clock 31
2.3.2 - Phototactic behaviour 32
2.3.3 - Statistical analysis 33
2.4 - Results 34
2.4.1 - Entrainment of the behavioral locomotor activity 34
2.4.2 - Behavioural phototactic response 37
2.5 - Discussion 39

Chapter 3: *Evolution of DNA repair mechanism in Somalian cavefish* 44
3.1 - Introduction 45
3.1.1 - Shine on DNA repair by photolyase 45
3.1.2 - Other DNA repair mechanisms 50
3.1.3 - Molecular adaptation of subterranean species 53
3.1.4 - DNA repair in fish 57
3.2 - Aim 59
3.3 - Material and Methods 60
3.3.1 - Embryo survival 60
3.3.2 - Immunofluorescence assay in cell lines 60
3.3.3 - Gene expression of blue-light inducible genes in embryo 61
3.3.4 - Estimation of synonymous and non-synonymous substitution rates 62
3.3.5 - Statistical analysis 63
3.4 - Results 64
3.4.1 - Loss of light-driven DNA repair in Somalian cavefish 64
3.4.2 - Light fails to protect cavefish from UV-treatment 66
3.4.3 - Loss of function mutations in cavefish photolyase genes 69
3.4.4 - Loss of light-inducible DNA repair gene expression in cavefish 72
3.4.5 - Loss of D-box-regulated transcription in *P. andruzzii* 74
3.4.6 - Molecular evolution of cavefish photolyases 79
3.4.7 - Dark function for CPD photolyase 80
3.5 - Discussion 82

Supplementary Information 87

References 103

Acknowledgments 128

Pubblications during the PhD 129

Abstract (English)

Light has dominated animal biology since the origin of life. It serves as the primary source of energy, has an impact on metabolism and coordinates the behavior of animals. Excess exposure to sunlight also represents a major source of damage for complex biomolecules and thereby underlies pathology. Light is known to have a crucial effect on many aspects of fish physiology ranging from development and growth to sex determination, behavior and reproduction. Recent discoveries have revealed the presence of different types of photoreceptors in fish. The extreme phenotypes of cavefish which have evolved in the complete absence of light are a testimony to how much light shapes fish evolution. Using the zebrafish and two species of cavefish, *Phreatichthys andruzzii* and *Astyanax mexicanus*, evolved in different ecological niches, we investigated the evolution of UV perception and DNA UV-damage repair mechanism. The main elements of these processes are highly conserved: UV photoreceptors are expressed in eye, brain and peripheral tissues of almost all fish, while the photolyases, blue-light activated DNA repair enzymes, are essentially preserved throughout the animal kingdom. Comparing the light-related mechanisms of species inhabiting surface habitat with species linving in subterranean habitat, we can learn much details about how light and related biological mechanisms evolve in response to their environmental conditions. In the following thesis, we attempt to illustrate how the use of behavioral, molecular and computational tools lead the answer on this question.

Keywords: circadian clock, UV-photoreception, DNA repair, UV damage, cavefish, zebrafish.

Abstract (Italian)

La luce ha dominato la biologia animale sin dall'origine della vita. Serve come fonte primaria di energia, ha un impatto sul metabolismo e coordina il comportamento degli animali. L'eccessiva esposizione alla luce solare rappresenta anche una delle principali fonti di danno per biomolecole complesse e quindi è alla base di patologie. È noto che la luce ha un effetto cruciale su molti aspetti della fisiologia di pesci, che vanno dallo sviluppo alla crescita, dalla determinazione del sesso al comportamento e alla riproduzione. Recenti scoperte hanno rivelato la presenza di diversi tipi di fotorecettori nei pesci. Gli estremi fenotipi dei pesci di grotta che si sono evoluti in completa assenza di luce sono una testimonianza di quanto la luce modella l'evoluzione dei pesci. Utilizzando zebrafish e due specie di pesci di grotta, *Phreatichthys andruzzii* e *Astyanax mexicanus*, evoluti in diverse nicchie ecologiche, abbiamo studiato l'evoluzione della percezione UV e il meccanismo di riparazione del danno al DNA causato da UV. Gli elementi principali di questi processi sono altamente conservati: i fotorecettori UV sono espressi negli occhi, nel cervello e nei tessuti periferici di quasi tutti i pesci, mentre le fotoliasi, enzimi di riparazione del DNA attivati dalla luce blu, sono essenzialmente conservati in tutto il regno animale. Confrontando meccanismi relazionati alla luce di specie che vivono nell'habitat di superficie con specie che risiedono nell'habitat di grotta, possiamo apprendere molti dettagli su come la luce e meccanismi biologici connessi evolvono in risposta alle loro condizioni ambientali. Nella seguente tesi, tentiamo di illustrare come l'uso di strumenti comportamentali, molecolari e computazionali conducano la risposta a questa domanda.

Parole chiave: orologio circadiano, fotorecezione UV, riparazione del DNA, danno da UV, pesce ipogeo, zebrafish.

Chapter 1

General Introduction

1.1 - Fish as model for study light-related mechanisms

Fish are wonderfully diverse as consequence of adaptation on different aquatic environments. In order to understand the biology of a species appears essential realize how the environment and ecological niche shaped organisms. Though the comparison of different species occupying different habitats we can learn how molecular and behavioral mechanisms change during the evolution to excellently adapt to their environment. Earth's environment is dominated by cyclic changes, namely seasons, day-night cycles, lunar cycles and tides, that are all driven by geophysical properties of the planet. The type of cycle in the ecological niche where an organism lives can pose a major risk to survival. Therefore, during the evolution of animals and plants occurred several survival and adaptation strategies. Essential to this strategy are endogenous timing mechanisms, according to which organisms can optimally coordinate physiological and behavioral adaptations required for survival to the environmental changes. The most common biological timing systems is the circadian clock which allows anticipation of the day-night cycle. The circadian rhythmicity generated by this endogenous clock dominates most aspect of the biology of plants, animals, even fungi and unicellular organisms (Pittendrigh, 1993). Normal clock function involves regular resetting by environmental signals such as light and temperature indicative of the time of day, to ensure its entrain with the natural day-night cycle. (Roenneberg et al., 2003; Roenneberg and Foster, 1997). Consecutively, the clock communicates with most features of physiology and behavior through a combination of cell autonomous as well as systemic signals such as cyclic hormone production (Schibler et al., 2015).

Photoreception in fish are well studied. As well as eyes, they posses a photosensitive pineal gland, deep brain photoreceptors, and dermal melanophores that are light responsive (Doyle and Menaker, 2007). In mammals, a central circadian clock located in the suprachiasmatic nucleus (SCN) of the hypothalamus is indirectly synchronised by light perceived by intrinsically photosensitive retinal ganglion cells (ipRGCs) in the retina, cells which express the melanopsin photoreceptors (Lucas et al., 2012). Light signals are conveyed from the eye to the SCN clock via the retinohypothalamic tract. The SCN in turn relays timing information to an array of peripheral clocks distributed in most tissues via complex

systemic signal (Ko and Takahashi, 2006). Interestingly, in the case of teleost fish, light directly entrains the peripheral clocks in tissues, organs and even cell lines as well as in central pacemaker structures such as the photosensitive pineal gland. Indeed, most cell types express photoreceptors and exhibit directly light inducible gene expression (Sassone-Corsi et al., 2000). Thus, fish and related fish cell lines have become reasonable models for inferring the mechanisms whereby biological clocks respond to light. Many questions still remain concerning the directly light-sensing peripheral clocks of fish. What are the photoreceptors? How do they signal intracellularly? Does light influence other aspects of cell biology independently of the circadian clock? In order to provide answers to these basic questions, many studies have exploited the fish genetic model species such as the zebrafish *Danio rerio* (Figure 1A) and the medaka *Oryzias latipes* (Figure 1B) using a combination of genetic and in vitro tools. Precisely because of their fast and transparent modality of growth and well-known genetics, zebrafish is widely used to study the development and functions of the visual system in vertebrates (Foulkes et al., 2016). From an overview, fish are optimal for exploring how light shape the organisms over the course of evolution in response to changes in environmental conditions. Biodiversity of Teleost are the largest, with about 30.000 know species successfully adapted to a full range of aquatic habitats. They are the most diverse group of vertebrates. Each habitats differs considerably in terms of the ambient lighting conditions depending on geographical location, quality and depth of water, photoperiod length, and wavelengths and intensity of light (Loew and McFarland, 1990). Fish, have also successfully colonized perpetually dark habitats such as subterranean caves and abyssal marine environments. These particular kinds of environment are affected by extremes temperature and food deprivation. One poorly understood issue is how long-term changes in environmental lighting conditions have shaped the evolution of the light-related mechanisms. Blind cavefish represent good models to study this issue due to their set of striking adaptations (so-called troglomorphisms), resulting from evolution under perpetual darkness. Most notably, with increasing time isolated in a dark environment, cavefish progressively lose dedicated photoreceptive organs such as the eyes and pineal organ (Stemmer et al., 2015), instead relying on enhancement of non-visual senses to navigate and find food. Troglomorphic phenotypes also include loss of body pigment, as well as reduced metabolic rate (Foulkes et al., 2016). There are a

number of unique and remarkable features which make fish models suitable and it is not only the genetics and screening tools that they offer but also the biology which make them highly relevant models.

One important model is the blind Somalian cavefish *Phreatichthys andruzzii* (Berti and Messana, 2010; Colli et al., 2009) (Figure 1C), which exhibits an extreme troglomorphic phenotype as the result of evolution for approximately 2.5 million years in complete isolation from sunlight beneath of the Somalian desert (Calderoni et al., 2016). Previous study have documented the general loss of light induced clock gene expression in the cavefish *P. andruzzii*. This lack of a gene expression response to light is due to the accumulation of loss of function mutations in key non-visual opsin photoreceptors OPN4m2 (Calderoni et al., 2016; Cavallari et al., 2011). Importantly, recently study revealed the presence of additional mutations affecting a light-responsive, the core circadian clock component PER2 gene (Ceinos et al., 2018).

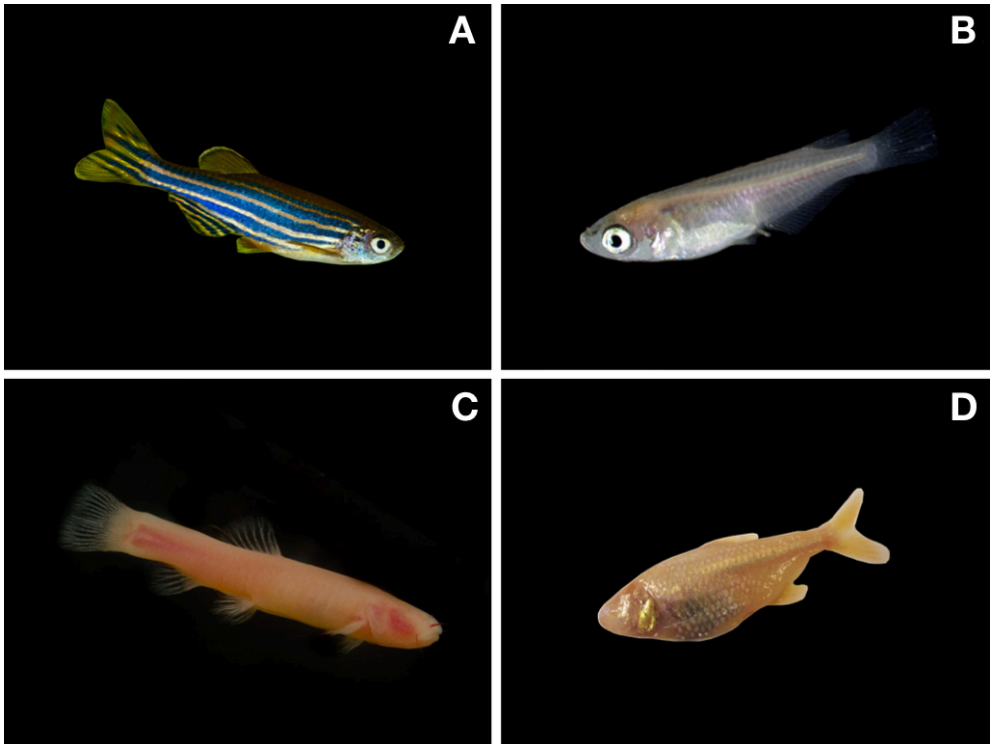

Figure 1. Zebrafish *D. rerio* **(A)** and medaka *O. latipes* **(B)** represents an ideal model for gaining mechanistic insight into the full range of light dependent mechanisms. Potential models for exploring these mechanisms adapted to the perpetual darkness: cavefish *P. andruzzii* **(C)** have evolved in absence of sunlight in the phreatic layers of the Somalian desert and cavefish *A. mexicanus* **(D)** have evolved in constant darkness environment in the karstic area of Mexico.

Another important model for the study of light-related mechanisms is the blind Mexican cavefish *Astyanax mexicanus* (Figure 1D). Most recently a microsatellite polymorphism analysis has suggested that surface and cave populations may have diverged 20.000 years ago (Fumey et al., 2018). The cavefish *Astyanax* compared to *P. andruzzii* show a low troglomorphic phenotype level. It has been shown that the blind Mexican cavefish populations retained a robust circadian rhythm like in the surface counterpart but with substantial alteration (Beale et al., 2013). Therefore, the cavefish *Astyanax* raised in the lab have the capacity to generate molecular oscillation of PER1 and PER2. This altered expression of light-inducible genes could provide a selective advantage in the cavefish systems and may be witnessing at the first stages of a process that previously occurred in *P. andruzzii* (Ceinos et al., 2018). Surprising the blind Mexican cavefish populations showed light-responsive in the DNA repair genes. It was speculated that the conserved functionality in DNA UV-damage repair mechanisms under constant darkness may provide a selective advantage. For example, life in the hypoxic and slightly acidic water may lead to an increase of intracellular oxidative stress and thereby elevate DNA damage that need to be repaired urgently (Beale et al., 2013).

1.2 - Evolution in absence of light

Not all aspects of living in hypogean habitats are negative. Caves may provide shelter from the outside environment. A multitude of organisms retreated into these cave habitats due to selective evolutionary pressure and currently inhabit diverse niches. Those inhabitants are defined as troglobites and they evolved from epigean ancestors. These were forced by evolutionary selective pressure to colonize the hypogean habitat. In general, other groups deriving from these ancestors who could not adapt to the exotic habitat became extinct, whereas their cave inhabiting counterparts remained conserved (Proudlove, 2010). So far troglobiontic species have been encountered in habitats featuring high salinity, high temperatures, hypoxia, and high concentrations of natural toxins (Carveth et al., 2011; Tobler et al., 2011; Timmerman and Chapan, 2004). Therefore, known cavefish species exhibit significantly high tolerances to harsh environments. Cave animals are completely isolated from light and do not use this energy and information. For these reasons an animal evolved in absolute darkness are extraordinary and show

regression of eyes, low body pigmentation, elongated barbels, well-developed electric sense organs and peculiar behavioral traits. Usually the common ancestor of cave specie is night-active morph (troglophiles) which was predated to cave life because of already having acquired improved traits necessary to live in light-poor environments or to be active at night. For example, whereas among teleost the diurnal characin fish (Characiformes) are only represented by 3 cave species. The mostly nocturnal catfish (Siluriformes) contain at least 151 cavefish species (Proudlove, 2010). For such troglophiles, life in light-poor or lightless environments is not extreme. They adapted morphological, physiological, and behavioral traits by which they are able to find food and propagate.

1.3 - Ecological roles of UV light

In almost all the ecosystem the light serves as main energy source and has a major impact on animal physiology and behavior. The visible light that arrives on our planet consists of many monochromatic components ranging from red (750-620 nm), to green (570-495 nm), and to blue-violet (475-380 nm). The focus on the ecological tasks of Ultra-Violet (UV) solar radiation has been discovered in the last half century. UV light-spectrum is divided into three portions: UV-A (400–315 nm), UV-B (315–280 nm), and UV-C (280–100 nm), and has long been known to cause adverse effects to aquatic organisms (Nigel and Dylan, 2003). The energy carried by a single photon is inversely proportional to its wavelength, thus UV-C and UV-B compared to UV-A are the most dangerous radiations causing cytotoxic effects. The UV-C radiation is absorbed by oxygen and ozone in the atmosphere, so it does not penetrate through it. UV-B radiation and UV-A radiation penetrate the biosphere, although only UV-B is absorbed by atmospheric ozone and therefore increases as a consequence of the stratospheric ozone depletion (Häder et al., 2003). The exposure of an organism or an ecosystem can be quantified as the instantaneous UV intensity incident on a surface called irradiance and typically expressed in W m^{-2} sec^{-1}. Studies on ozone depletion have focused on both the harmful effects of UV in animals and on photosynthetic processes (Häder et al., 2003). As for plants, one of the most obvious responses to UV-B radiation is the change in physiological processes and the production of metabolites that strongly absorb these wavelengths. However, this may have other ecological roles, such as

defense against herbivores animal and pathogens (Meijkamp et al., 1999). The worries due to ozone depletion and the consequent increase in UV-B radiation, have made the attention focus on the effects of these wavelengths in different organisms. For example, in zebrafish, it has been shown the UV-B dangerous effect on embryos (Dong et al., 2007). In amphibians, the embryos and larvae are also sensitive to UV-B solar radiation and adults could be vulnerable to sublethal effects from UV-B (Ankley et al., 2002). Terrestrial animals are well protected from damage caused by UV radiation through their exoskeleton, fur or plumage, and / or because they have effective mechanisms to repair UV damage.

While most animals have evolved mechanisms to minimize the effects of UV damage in their natural environment, it is also evident that many species use UV radiation, especially UV-A, as part of the visual system. From a behavioral point of view, UV vision has a great evolutionary significance for the development of trophic associations between plants and animals, choice of the partner, escape from a predation event, these in vertebrates and in invertebrates (Hunt et al., 2001). The absorption of light in an aquatic environment is selective depending on the wavelength and depth, making the weaker radiation disappear in order: first the red, then the green-blue, and finally the violet and UV. Sensory systems provide crucial information about the external environment in which organisms live, and are often subject to strong natural selection. The spectral sensitivity of the visual pigments of many fish species depends on the wide variability in intensity and in the light spectrum of the aquatic environment where they live, thus identifying different visual systems (Loew and McFarland, 1990). The survival of an organism depends critically on the ability to gather information in their natural environment. Although this information may come from a variety of senses, vision is essential for day organisms that evaluate a bright scene. Therefore, the visual discrimination of objects is strongly influenced by the environment in which they are found, whether it is bright water, murky water or dark cave. In order to understand how organisms have developed different visual systems along the evolutionary time, protective colors, mimicry and warning signs have been well documented (Marshall and Vorobyev 2003; Ferrari, 1993). In particular, the color sensitivity provided by the visual pigments can differ drastically between animals that need to live in specific photic environments (Yokoyama and Yokoyama, 1996). Many studies have demonstrated the use of UV light in fish behaviors such as foraging, orientation,

mate selection and communication (Rick et al., 2012; Siebeck et al., 2010; Leech et al., 2009; Cummings et al., 2003).

1.4 - Impact of UV-light on the zebrafish physiology

Almost of our knowledge on effects of UV light in teleost fish come from studies conducted on zebrafish model. The retina of many vertebrates, including fish, amphibian, reptile, bird and small mammals, has a photoreceptor cone most sensitive to UV light, in the range between 360 and 390 nm (UV-A). This sensitivity in this light spectrum is determined by the combination of UV-sensitive visual pigment SWS1 opsin and a chromophore derived from vitamin A, which together form the visual pigment absorbing the light expressed in UV cones (Hunt et al., 2014). Zebrafish show monochromatic sensitive responses in a study that relationship between physiological and behavioral color processing and the visual processing of UV light have a spectral sensitivity function (Risner et al., 2006). Physiological, molecular and morphological studies on zebrafish larvae have shown that the zebrafish retina has photoreceptors sensitive to UV light. The UV-sensitive cones appear to be the first to become functional in zebrafish larvae, presenting sensitivity to UV wavelengths about 4 days post fertilization (dpf) (Saszik et al., 1999). UV opsin in zebrafish is the first expressed in the retina at 50 hours post fertilization (hpf). Furthermore, while zebrafish has four types of cones responsive to wavelengths (362 nm, 420 nm, 480 nm, and 560 nm), approximately 25% of the cones photoreceptors in the retina of the adult zebrafish are sensitive to UV wavelengths (Takechi and Kawamura, 2005; Robinson et al., 1993; Branchek and Bremiller, 1984). However, the number of photoreceptor types in an animal's retina is not always directly correlated with color vision and perceptual abilities. Several factors, such as the photic conditions and the development plasticity may influence how the signals of the retina are processed in the brain by different types of photoreceptors (Jacobs, 1981). For example, similarly to zebrafish, the redfish retina contains four different types of photoreceptor cones, but only the goldfish shows a tetrachromatic vision under high intensity illumination, while below lower levels of light show a trichromatic view (Neumeyer, 1992). In some species of fish only larvae and juveniles show UV visual sensitivity, presumably used to detect prey as zooplankton (Job and Bellwood, 2006). For some species of Salmonidae,

visual sensitivity to UV in larvae is necessary for prey research, whereas in adults, UV sensitivity disappears and presents considerable plasticity in association with habitat and diet changes (Allison et al., 2003). Zebrafish clearly maintains its UV photoreceptors even in adulthood (Robinson et al., 1993). In a recent study of Novales Flamarique (2016) has been demonstrated how zebrafish mutant for UV cones population compared with the wild-type strain have diminishing foraging performance. Computing the ecological function of the UV cones that may explain why small zooplanktivorous fishes retain UV cones throughout their lives.

The UV-B exposure have an impact on oxidative stress and mortality in embryonic and young zebrafish (Charron et al., 2000). Recently, it has been evaluated the effects of UV-B and temperature interaction on physiology and locomotory activity of zebrafish. The chronic exposure to UV-B alters the selection of thermal microhabitats of zebrafish (Seebacher et al., 2016). Today, there are limited data pertaining to photorepair in zebrafish. From one work that correlate the synergic effects of UV-B and UV-A irradiation on zebrafish embryos emerged that UV-B have strong effect on hatching and mortality rates, as well as development and presence of malformations. Considerably, zebrafish embryos exposed to UV-B followed by UV-A post-exposure point out a competent photorepair system. Pigmentation from UV-absorbing chromophores is a common injury-prevention strategy seen in developing embryos, and pigment cells in zebrafish can be identified within 24h of development (Dong et al 2007). Post-exposure mechanisms for UV repair include photorepair refers to the specific light-induced activity of photolyase and the other mechanism of nucleotide excision repair of DNA (Sancar, 2016). Zebrafish and their ability to tolerate UV was linked with circadian rhythms, where incubation in total darkness or constant light reduced survival rates (Tamai et al., 2004).

Chapter 2

Evolution of UV photoreception in fish

2.1 - Introduction

2.1.1 - Ocular and Extra-ocular perception of UV light

Generally, non-mammalian vertebrates share all the photosensitive activity in the lateral eyes that reveal the image for the vision and in extraocular receptors that mediate the detection of irradiation allowing to animals the regulation of circadian rhythms. However, it is not entirely valid. Although the lateral eyes do not necessarily serve to control the day-night cycle, their presence significantly increase sensitivity to regulation, as clearly demonstrated in most animals. Extraocular photoreceptors, mostly developing from the forebrain, are classified as pineal complex and deep brain photoreceptors. The pineal complex consists of the (*i*) intracranial pineal organ or pineal body; (*ii*) intracranial parapineal organ found in lampreys and teleost fish; (*iii*) extra-cranial ‘‘third eye’’ named frontal organ in anuran amphibians and parietal eye in reptiles (Figure 2) (Bertolucci and Foà, 2004). The ability to detect and use the light is ubiquitous in nature, and is an important element of feature detection in visual scenes (Kelber et al., 2003). Color vision begins with the wavelength selective absorption of light by the eye’s photoreceptors. Activation of these cells triggers a signaling cascade that propagates the transduced light information into several layers of processing, both at the retinal level and beyond (Pichaud et al., 1999). The detection and perception of color has been studied at many of these levels and in a variety of organisms, but we still do not understand many of the basic principles governing color vision (Conway et al., 2010). In vertebrates, light sensitivity is achieved in the retina by the presence of rods and cones photoreceptor. These are composed of internal and external segments connected by a cilium. Sensitivity to light is transmitted by visual pigment molecules incorporated into the membrane disc of the outer segment; each type or class of photoreceptors contain a visual pigment differing from the others by the peak of spectral sensitivity (λ_{max}). A single class of rods is often present, containing a pigment with λ_{max} generally around 500 nm in the green-blue region of the spectrum. The rods are functional with low intensity of light and form the basis of the scotopic system. In contrast, the cones are involved for vision with normal light levels (phototopic vision). The presence of two or more different classes of cones, each with a different λ_{max} allows the visual system to test light

levels at different spectral areas. In all taxa except in mammals, there are more than three types of visual pigment cones, each belonging to different classes of cones. The classes of cones are distinguished on the basis of the amino acid sequence of their respective opsins and approximately correlated to the spectral sensitivity: long waves (LWS) with λ_{max} 500-570 nm, medium waves (MWS) with λ_{max} 480-520 nm, short waves (SWS) with λ_{max} 415-470 nm and violet/ultraviolet (V/UV) light with λ_{max} between 355-435 nm. The harvesting of photons by the different type of photoreceptor cones provide the basis of color vision in the neural system. Therefore, photoreceptors in the visual pigments are fundamental for light sensitivity. These pigments, called opsins, are part of the superfamily of receptors coupled to G proteins, which functionality depend by the activation of a protein G and an enzyme that changes the level of a second messenger in the cytoplasm of the cell. Each visual pigments are composed by the same basic structure of one chromophore linked with the opsin. In vertebrates, the chromophore may be 11-*cis*-retinal or 11-*cis*-3,4-dehydroretinal, respectively the derivatives of vitamin A1 and A2 (Parry and Bowmaker, 2000; Bridges, 1972).

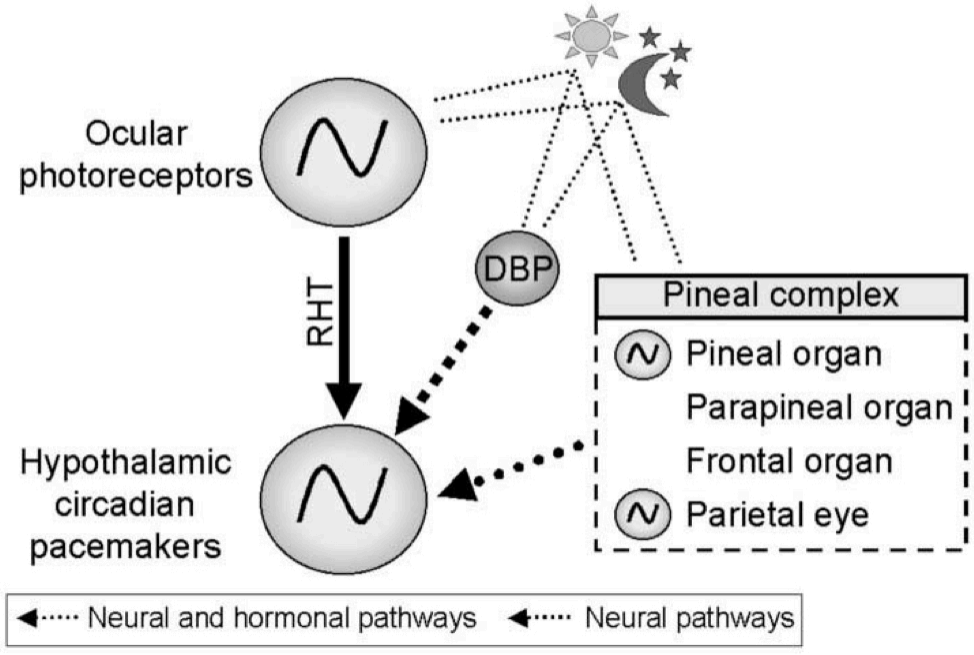

Figure 2. Schematic representation illustrating ocular and extraocular photoreceptive structures involved in the vertebrate circadian system. Arrows indicate pathways between circadian oscillators and photoreceptors. DBP: deep brain photoreceptors; RHT: retino-hypothalamic tract. Image from Bertolucci and Foà, 2004.

Sensitivity to UV light is reached through eye photoreceptors that include class of visual pigment extremely sensitive to long-wave lower then 400 nm. Sensitivity to UV light is not a constant characteristic of the visual system. In many vertebrates, the UV-sensitive pigment (UVS) is replace by a violet-sensitive pigment (VS) with the major absorption between 410 and 435 nm. Analysis of amino acid sequence of VS/UVS pigments in vertebrate, indicate that ancestral pigment is UVS with the lost of UV sensitivity in mammalians, amphibian and birds. Subsequently, some species of birds reacquired UVS pigments by replacing a single amino acid. Conversely, no loss of UV sensitivity occurred in the UVS pigment of insects. The electromagnetic spectrum extends from radio waves with longer wavelength and low energy to gamma rays with shorter wavelengths and high energy. However, only a small part of this spectrum is visible to animals as light. Radiation below 320 nm (UV-B) is largely filtered by the ozone layer, therefore is not available to the visual system, but radiation upper to 320 nm and below to 400 nm (UV-A) can be perceived by many animal species. In human, the sensibility of short wavelength ends nearby 400 nm. Thus is not the case for many other species in which the cornea and lenses are transparent below 400 nm, and the sensitivity in this region can be further enhanced by the presence of retinal photoreceptor cells that are most sensitive to the UV region of the spectrum (Hunt et al., 2001).

In non-primate mammals, this complement is reduced to only two classes, long and short waves, an event that is believed to have been a nocturnal lifestyle that mammals have experienced during their evolution and in which the others classes of cones have been discarded (Gerkema et al., 2013). Vision in the region of the short waves of the spectrum is therefore subjected to the class of V/UV visual pigments and these are coded by members of the same family of opsins. In primates the vision is trichromatic with cones sensitive to short wavelengths (420 nm), medium (530 nm) and long (565 nm). The short wave sensitive opsin, despite a wavelength of about 420 nm, has a spectral sensitivity that would extend into the UV if the cornea and lenses transmitted light within small region of the spectrum (Yokoyama et al., 1998; Jacobs et al., 1991).

The function of UV vision has been extensively studied in the non-mammalian vertebrate taxa. In birds, the presence of UV pigments is relatively common, especially in the passerines and an adaptive role in the selection of the partner has been shown in the blue tit and zebra finches (Hunt et al., 1999; Bennett et al., 1996).

In both species the reflection of the UV from the feathers was shown to be an important factor in the selection of the male partner by the females. There is also evidence that UV sensitivity is important in some species to find food, for example in the identification of prey by the kestrel (Viitala et al., 1995) and for the collection of nectar in the hummingbirds (Goldsmith , 1980).

UV pigments are also present in many freshwater and marine fish, with examples distributed through major orders such as in cyprinids (Bowmaker et al., 1991; Avery et al., 1983), in the beloniforms (Hisatomi et al., 1997), in the perciforms (Carleton et al., 2000) and in the salmonids (Bowmaker and Kunz, 1987). A common feature in UV cones is that they are present in young fish but may be lost in adults. For example, in *Salmo trutta*, the UV cones can only be found in fish older than 1-2 years (Bowmaker and Kunz 1987) and in *Oncorhynchus nerka*, the number of UV cones decreases drastically when the specimens pass from the larval stage to juvenile, although in this case they still increase in adults (Novales Flamarique, 2000). UV sensitivity was also detected in many coral reef fish species (McFarland and Loew, 1994). The presence of UV cones in young fish can be related to plankton feeding, through the sensitivity to UV light that enhances the detection of zooplankton (Browman and Hawryshyn, 1994). While their loss in older animals can be correlated with a change in foraging habits because larger fish move to deeper waters where UV light is less available. Another important role is linked to the recognition of conspecifics (Loew and McFarland, 1990). In mammal, the V/UV cones frequency is generally lower compared with medium and short wavelength cones, despite the retina of the squirrel *Spermophilus beecheyi* is rich of cones (Kryger et al., 1998). Primates have violet cones that are distributed throughout the retina. The longer wavelength cones are limited to the dorsal retina where they are predominant, while the cones expressing both opsins show a gradation in the increase of UV opsins from the dorsal to the ventral retina. This phenomenon was reported for the first time by Szèl et al (1996), who demonstrated that all the cones express the pigment of short wavelengths in a ventral region of variable width. The meaning of this asymmetry is unknown. Raymond et al. (1993) and Robinson et al. (1993) showed that the blue and UV-sensitive cones in zebrafish are alternate along the single cone rows and that the red and green cone members are alternate along the double cone rows so that the red member of the double cone is always adjacent to the UV cone whereas the green member is adjacent to the blue cones. Although

the UV photoreceptors pattern varies from species to species (Bowmaker et al., 1991; Bowmaker and Kunz, 1987; Avery et al.,1983). From a more recently research we know well that the UV cone photoreceptors in zebrafish are occupy specific, invariant position in the retina. In zebrafish, the genetic disruption of the transcription factor Tbx2b eliminates most of the cone subtype maximally sensitive to UV wavelengths and also perturbs the long-range organization of the cone lattice (Raymond et al., 2014).

The gene sequences of V/UV opsins have been found in more than 20 species. This range extend from violet opsins of primate (Hunt et al., 1995) and chicken (Okano et al., 1992) to the real UV pigments in many fish (Hisatomi et al., 1997; Carleton et al., 2000), birds (Yokoyama et al., 2000; Wilkie et al., 1998), mammals (Yokoyama et al., 1998) and in a reptile species (Hauzman et al., 2017; Yewers et al., 2015; Kawamura and Yokoyama, 1998).

A molecular phylogenetic analysis of the opsin sequences confirmed that the V/UV pigments belong to a single class of opsins, coherent with their single evolutionary origin. Teleost fish generally have an UV pigment, while all the amphibians studied so far have only violet pigments. The chameleon *Anolis carolinensis* posses a UV pigments (Kawamura and Yokoyama, 1998), and both V/UV pigments are present among different avian and mammalian species. The ancestral pigment is the UV and, during the evolution, there have been movements within the violet spectrum and secondarily in the ultra-violet spectrum, these series of event in a separate way in the different taxa. It follows that the molecular basis of these spectral shifts may not be the same in fish, reptiles, birds and mammals with regard to UV pigments.

Recent sequencing of vertebrate and invertebrate genomes has revealed that animals express diversified opsin genes in addition to visual pigments (Davies et al., 2015; Koyanagi et al., 2014). These opsins are expressed in retinal interneurons, including horizontal, bipolar, amacrine, and ganglion cells and multiple brain regions, which indicates that these opsins are responsible for non-image-forming photoreceptions. Opsins identified so far are classified into several groups based on amino acid sequence. In the photosensitive activities that extraocular photoreceptors effectively conduct there are something more than a simple irradiance survey. For example, the pineal gland of the salamanders, the frontal organ of the frogs and the parietal eye of the lizards have been demonstrated in the detection of the horizontal direction of a light source, specifically the azimuth

of the sun, which is essential for orientation. The azimuth of the sun can also be determined under overcast conditions by detecting the *e*-vector of the polarized-light plane, as does the pineal gland of the salamander. In general, the orientation with the sun, also classified as a photomenotaxia (Fraenkel and Gunn, 1940), results in rather sophisticated behavioral performance by detecting the amount of light in the environment. One of the intriguing questions that has not yet been found response in this field is the reason why the central nervous system of the non-mammalian species contains different types of photopigments expressed in many distinct areas. Roenneberg and Foster (1997) suggested that multiple photopigments, which differ in their spectral responses, can be used to obtain information on spectral changes within the environment. Sunrise and sunset are the moments of the day when both changes in the spectral composition are maximal, and the signals of the photic regulation involved in circadian rhythms are more relevant (Aschoff et al., 1982). Thus, multiple photic channels, each extracting spectral information slightly different from the same ambient light. These, can be adopted by the circadian system to extract reliable information on sunrise and sunset, with the adaptive meaning of very accurately adjusting the physiological and behavioral rhythms to that reference phase (Foster and Hankins, 2002; Philp et al., 2000b). So far, there are few cases in which a well-localized group of deep cerebral photoreceptors has revealed that it can directly mediate the photic regulation of circadian behavioral rhythms. This is evident in neurosecretory cells, all confined between the periventricular area of the hypothalamus in the *Podarcis sicula* lizard (Pasqualetti et al., 2003). Since the discovery that fish cells and tissues are clock regulated by direct light exposure, they represent a good model to study the “peripheral” clock. Although the identity of the teleost peripheral photoreceptor remains unclear, candidates include the opsins Melanopsin (OPN4m2) and Teleost-Multiple-Tissue opsin (TMT-opsin) that are widely expressed in most zebrafish tissues (Moutsaki et al., 2003; Bellingham et al., 2002). Melanopsin was originally isolated from the photosensitive melanophores of *Xenopus* (Provencio et al., 1998). TMT-opsin was originally identified by virtue of its opsin sequence homology (Moutsaki et al., 2003). Subsequently, orthologs of melanopsin were isolated from other non-mammalian vertebrates (Bellingham et al., 2006). Mutations affecting melanopsin photoreceptors in the cavefish *P. andruzzii* could also account for the blind clock (Cavallari et al., 2011).

Opsin classification correlates well with the diversity of their molecular properties. Among opsin groups, the OPN5 (neuropsin) group has members originally found by using a bioinformatics approach on mouse and human genomes and forms one independent opsin group (Tarttelin et al., 2003). Since then, multiple OPN5-related genes have been found from non-mammalian vertebrates, and the corresponding proteins were phylogenetically clustered into some distinct subgroups (Tomonari et al., 2008). Mammals have only one OPN5 gene, OPN5m (mammalian type), and non-mammalian vertebrates have additional OPN5 genes (OPN5L1 and OPN5L2) (Ohuchi et al., 2012). The OPN5m gene can be found widely in vertebrates from fish to mammals. Previous reports showed that OPN5m functions as a G-coupled UV-sensitive pigment and that this property is common to OPN5m from various vertebrate species (Yamashita et al., 2014; Kojima et al., 2011; Yamashita et al., 2010). In addition, the analysis of its distribution patterns in birds and mammals revealed that OPN5m is localized to retinal interneurons, including the amacrine and ganglion cells, and several brain regions including the hypothalamus (Nakane et al., 2014). Therefore, it is thought that OPN5m can regulate various non-image-forming photoreceptions in these animals. In fact, avian OPN5m modulates a photoperiodic response in the hypothalamus and mammalian OPN5m photoentrain the local circadian clock in the retina (Buhr et al., 2015; Nakane et al., 2014; 2010; Buhr and Gelder, 2014).

In a recently study by Sato et al., 2016 it was characterized additional OPN5, OPN5m2, found exclusively in ray-finned fishes (including zebrafish and *Astyanax*) and closely related to OPN5m. This UV-light photoreceptor would contribute directly to non-visual functions in retinal interneurons and ganglion cells with visible light inputs by other non-image-forming opsins. The analysis of expression patterns in the brain showed that OPN5m-positive cells are localized not only in the hypothalamus but also in other brain regions of ray-finned fishes, some of which are responsible for reproductive activities in vertebrates. In the medaka fish and spotted gar brains, OPN5m was distributed in the preoptic area, which is consistent with the expression pattern of OPN5m in the mammalian brain (Yamashita et al., 2014). The expression patterns of several genes in the preoptic area of both mammals and fishes indicate sexual dimorphism (Hiraki et al., 2013; Forger, 2009). This suggests that OPN5m plays a conserved role in vertebrate brains, probably in the regulation of sexual behavior or reproductive activity. OPN5m was also

expressed abundantly in the medaka fish pituitary gland. Thus, medaka fish OPN5m may directly regulate the production and secretion of pituitary hormones such as gonadotropin (Zohar et al., 2010). Moreover, OPN5m was localized to the tuberal nucleus of medaka fish and in the periventricular nucleus of zebrafish. Previous reports showed that kisspeptin is expressed in the tuberal nucleus and periventricular nucleus of medaka fish and zebrafish (Servili et al., 2011; Kitahashi et al., 2009; Kanda et al., 2008). Kisspeptin plays a crucial role in regulating the activity of the hypogonadotropin neuron in mammals (d'Anglemont de Tassigny et al., 2007). Whereas knockouts of kisspeptin1 or 2 does impair reproductive activity in zebrafish (Tang et al., 2014). Recent reports showed that kisspeptin2 cells in the periventricular nucleus of zebrafish have fibers that form a wide network projecting to several brain regions (Song et al., 2015). Thus, OPN5m may be related to the unknown physiological function of kisspeptin in medaka fish and zebrafish.

In conclusion, OPN5m and OPN5m2 diverged by gene duplication early in the evolution of ray-finned fishes, exhibit common UV light-sensitivity, and exhibit different affinities to retinal isomers. In addition, the distribution patterns of OPN5m and OPN5m2 in ray-finned fishes revealed that these opsins are localized in multiple retinal interneurons and ganglion cells with a dorsal-ventral gradient of expression levels, and also in several brain regions, including the hypothalamus (Sato et al., 2016). Therefore, in contrast to only a small number of UV light-sensing visual cells for visual photoreception, a wide range of cells in the retina and brain have the potential to respond to UV light. This finding suggests the importance of UV light information for various non-visual photoreceptions in ray-finned fishes. As seen in retinal interneurons, it has been reported that melanopsin, VA opsin and TMT opsin are also expressed in multiple teleost brain regions, such as the optic tectum and hindbrain (Fischer et al., 2013; Drivenes et al., 2003; Kojima et al., 2000). By using a variety of non-image-forming opsins, the teleost brain would be capable of sensing a wide range of wavelengths from UV to visible light for modulating long-term activities, such as neuroendocrine activities, and short-term activities, such as sensory inputs.

2.1.2 - Circadian clock

One of the most impressive features of the circadian clock is that its basic properties are highly conserved across immense distances of evolution. Essentially all species have developed cellular oscillations and mechanisms synchronized by environmental cycles. Such environmental cycles in biotic (e.g. food availability and predation risk) or abiotic (e.g. temperature and light) factors may occur on a daily, annual or tidal time scale. Internal timing mechanisms may facilitate behavioral or physiological adaptation to such changes in environmental conditions. These timing mechanisms commonly involve an internal molecular oscillator (a clock) that is synchronized (entrained) to the environmental cycle by receptor mechanisms responding to relevant environmental signals (*zeitgeber*, i.e. German for time-giver) (Hut and Beersma, 2011). The circadian timing system in all organisms is essentially composed of three distinct elements (Menaker et al., 1978): (*i*) the core oscillator, that is the central cell-autonomous pacemaker which generates the circadian rhythm; (*ii*) the input pathway, which detects the zeitgebers and entrains/resets the core oscillator; (*iii*) the output pathway, which allows the pacemaker to control many behavioral and physiological activities (Figure 3).

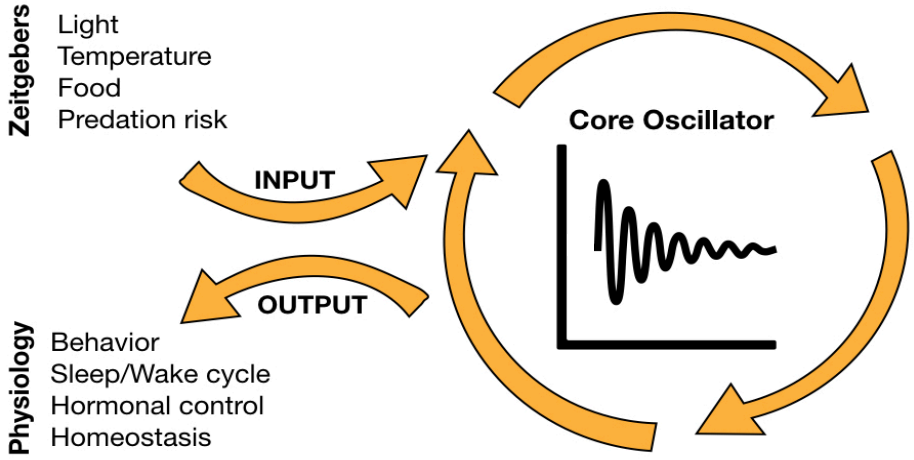

Figure 3. Schematic representation of the circadian timekeeping mechanism. By day and night environmental signals, the input pathways synchronize the circadian pacemaker with natural cycles and generates cell autonomous circadian rhythms. Through multiple output pathways, the circadian pacemaker is able to control and regulate various physiological aspects in all living organisms.

At the molecular and cellular level, what is a clock? In most organisms, the clock mechanism consists of a core of interconnected transcription-translation negative feedback loops that is made up of so-called core clock genes and proteins and requires about 24 h to complete one cycle (Reppert and Weaver, 2001). In the case of vertebrates, two key core clock proteins are CLOCK and BMAL. These are transcription factors which form heterodimers and thereby bind to E-box enhancer elements and activate transcription. E-box enhancers are located in the promoters of a broad range of genes including the negative elements of the core clock mechanism: the period (PER) and cryptochrome (CRY) genes (Figure 4). Upon activation of PER and CRY expression and their translation, the PER and CRY proteins translocate to the nucleus where they interact with the CLOCK/BMAL heterodimers, interfering with their transcriptional activation function and thereby down-regulating E-box-driven activation. As a result, PER and CRY gene expression is reduced and levels of these negative regulators fall. At a critical reduced level of PER and CRY proteins, CLOCK and BMAL are once again able to direct activation and the cycle can be repeated. This whole process takes about 24 h to complete one cycle and by stringent genetic analysis, this regulatory network has been pinpointed as the primary genetic source of circadian rhythmicity. However, it is now clear that the clock is not so simple. The BMAL gene itself is rhythmically expressed under the control of a second “stabilizing” feedback loop involving the two orphan nuclear receptors, REV-ERB and ROR (Figure 4) (Preitner et al., 2002). Furthermore, reinforcing this core cycling gene-regulatory network, additional layers of regulation provided by post-transcriptional and post-translational modifications (Lim and Allada, 2013; Vanselow and Kramer, 2007), epigenetic regulation, and metabolic networks (Asher and Sassone-Corsi, 2015) serve to reinforce the core transcription-translation feedback loop and make it more robust. Clock genes and a functional circadian clock are characteristically expressed in most tissues and cell types. However in vertebrates, certain dedicated clock structures, for example, the suprachiasmatic nucleus (SCN) of the hypothalamus in mammals, and the pineal gland in birds, reptiles, amphibia, and fish, appear to serve as “master” clocks (Menaker et al., 1997) that coordinate the activity of the other “peripheral” tissue clocks via a complex set of cycling systemic signals (Mohawk et al., 2012; Schibler and Sassone-Corsi, 2002). Therefore, the

circadian timing system can be considered like an orchestra with the master clock serving as the conductor.

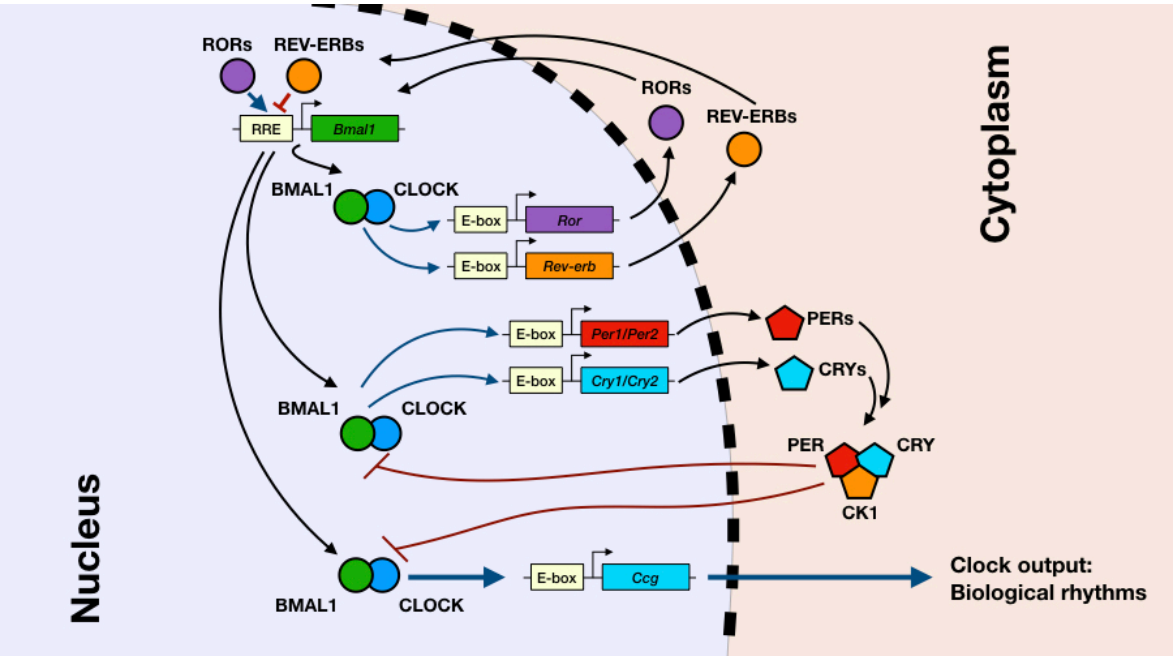

Figure 4. The core of the molecular clock mechanism is composed by two interacting loops. The core loop is formed by the positive elements CLOCK and BMAL, which heterodimerize and activate the transcription of the negative elements of the loop, the PER and CRY genes. Subsequently, PER and CRY proteins enter the nucleus as heterodimers and repress their own transcription by the inhibition of CLOCK-BMAL action. This mechanism is stabilized by a secondary loop, in which the CLOCK-BMAL complex induces the expression of REV-ERBs and RORs, regulating in this way the transcription of the BMAL gene.

Animals have evolved specialized photoreceptors in the retina and in extraocular tissues that allow them to measure light changes in their environment. In mammals, the retina is the main structure that detects light and relays this information to the brain. The classical photoreceptors, rods and cones, are responsible for vision through activation of rhodopsin and cone opsins. Melanopsin (OPN4) is expressed in a small subset of retinal ganglion cells (RGCs) in the mammalian retina, where it mediates non-image forming functions such as circadian photoentrainment and sleep (Provencio et al., 2002; Hattar et al., 2002). While mammals have a single melanopsin gene, zebrafish have evolved a sophisticated melanopsin system with distinct patterns of gene expression in multiple neuronal cell types in the retina, as well as in the brain and somites. As in mammals, perception of light by melanopsin

may involve a subset of RGCs in zebrafish, but additional melanopsin have an expanded role in information processing in the developing retina of fish. Zebrafish retinal cells also have the capacity to regulate OPN4 expression based on the length of the photoperiod (Matos-Cruz et al., 2011). Compared to zebrafish, the blind Somalian cavefish *P. andruzzii*, has a drastic circadian phenotypes and it has completely lost the ability to synchronize with the light-dark (LD) cycle. *P. andruzzii* has mutations in circadian photoreceptors such as TMT-opsin and melanopsin, which are normally light inducible in sighted fish species such as the zebrafish (Cavallari et al., 2011). Furthermore, previous findings by our research group showed the loss of function of the CRY1a and PER2 clock genes in *P. andruzzii* (Ceinos et al., 2018), bringing to our knowledge the idea of general loss of expression of neither gene inducible by light. Interestingly, the cavefish *A. mexicanus* have the capacity to generate molecular oscillation including the clock repressor PER2 (Beale et., al 2013).

The rotation of the Earth provides a predictably changing environment in which all life has evolved. Changes between night and day result in an enormous variation in environmental conditions and, as a result, dramatic differences in physiological and behavioral requirements. The ability to anticipate these environmental changes rather than passively responding to them confers a clear selective advantage, enabling internal time to be coordinated with the external timing cycle (Hughes et al., 2015).

2.1.3 - Phototaxis

The ability to make decisions and take the appropriate actions is critical for the survival and welfare of the animals. The choice of behavior depends on experience and has been widely observed in the animal kingdom. Phototaxis involves the movement of the whole organism in response to light. There are two types of phototactic behavior: photophilic, in which the movement is towards the light, and photophobic, in which the movement is in the opposite direction (Diehn et al., 1977). It is thought that phototaxis is involved in many biological phenomena, such as reproduction, diet and escape from predators. Avoid predators is one of the most important factors in phototaxis (Forward, 1988; Stich and Lampert, 1981). Behavioral responses to light / dark preference are easy to observe and quantify from an observer. Thorndike (1911) was the first to propose this method in Actinopterygii, in order to develop motivational and learning studies. In the last twenty years, the light / dark preference protocol (in the presence of full light spectra “white source” and/or monochromatic lights source) has been established for species such as the zebrafish (Maximino et al., 2007; Serra et al., 1999), the perch *Lepomis macrochirus*, the carps *Carassius langsdorfii* and *Carassius auratus* (Yoshida et al., 2005), the guppy *Poecilia reticulata*, the tilapia *Oreochromis niloticus*, the lambari *Astyanax altiparanae*, the cardinal fish *Paracheirodon axelrodi* and the swordfish *Gymnotus carapo* (Maximino et al., 2007). In these species, it has been noted the use of the dark portion of the tank rather than the illuminated portion, hence a photophobic behavior to polychromatic light. Because of these results, a scototaxy protocol has been developed in fish, a behavioral model validated to estimate the anxiolytic effect of pharmacological agents and effects of toxic substances. The main advantage of this method is the presence of a clear conflict situation for fish, and it allows to evaluate the genetic bases of innate behaviors such as anxiety and fear (Maximino et al., 2010). In the zebrafish, the differential employment of neural sensory pathways involved in scototaxy behavior is a known mechanism. The neurobiological substrates of the brain that underlie the choice of a decision during light-sensory perception have been partly understood through the mapping of neural activities (Figure 5). Through the study of the innate scototaxy behavior it has been detected the use of distinct regions in the brain, including the medial area of the dorsal telencephalic region (Dm), and the

dorsal nuclei of the ventral telencephalic area (Vd), respectively, the anatomical homologues of the amygdala and of the striatum of mammals. A particular model has been reported in which Dm and Vd are activated differently between control animals that avoid light and treated animals that do not avoid it, while the brain nuclei involved in visual processes are similarly activated between these two groups of animals. Since Vd is probably downstream of Dm, it has been suggested that the Dm operate as a brain center, whose activity discriminates the outcome of this behavior of choice (Lau et al., 2011). Some results indicate that preference for the dark environment of the zebrafish depends on age (Miklósi and Andews, 2006), which is probably an effect of the maturation of the melanophores (McClure, 1999; Langsdale, 1993). Thus, in zebrafish larvae, which did not show pigmentation, a preference for the light environment was observed (Watkins et al., 2004; Bjerke, 2002), while for the zebrafish adults a preference for the dark environment (Maximino et al., 2007; Serra et al., 1999). Given that melanophores are important for the ontogenesis of defensive behavior in fish (Fuiman and Magurran, 1994), these differences in development are an important consideration.

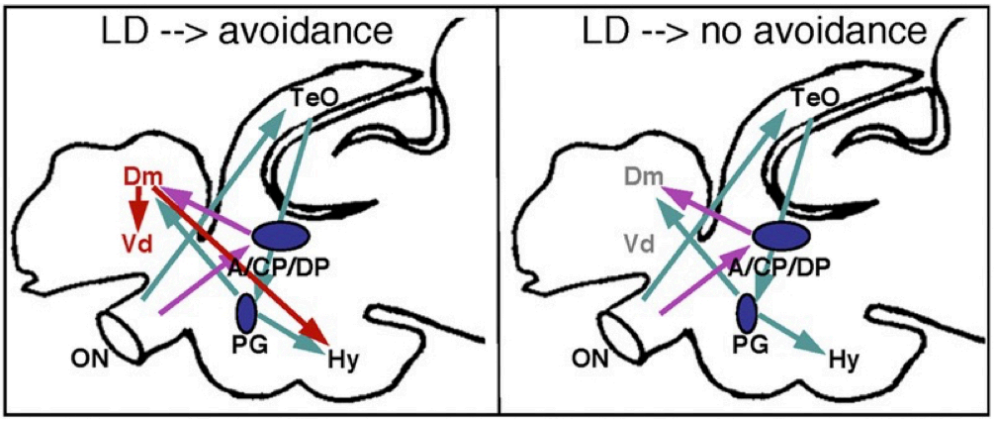

Figure 5. Scheme of a core neural circuitry underlying the light / dark choice behavior. Details are presented in the text. Image from Lau et al., 2011.

However, some species do not have a preference for both light / dark environments. This is the case of mosquitofish *Gambusia holbrooki*, which conversely to other Poeciliidae as guppy (*Poecilia reticulata*) and swordtail (*Xiphophorus helleri*), do not have a preference for the dark environment (Maximino et al., 2010). In another species of Poeciliidae (*Gambusia affinis*) which has two phenotypes, one epigeal and the other hypogeal, it has been shown that the

surface population presents a photophilic behavior, while the cave population presents a photophobic behavior (Camassa et al., 2001).

A recent study on 5-7 dpf zebrafish have shown that larvae swim toward visible light (blue and red spectrum) stimuli and away from UV-A stimulus in a closed loop split field paradigm. This preference is expressed mainly via turning direction of larvae with no discernible changes in other swimming parameters as a function of the stimulus. They found that UV avoidance behavior interacts negatively but not cooperatively with phototaxis, and relies on the visual system, and the UV cone in particular, to function. Finally, phototaxis to visible stimuli seems to be a shallow function of contrast while UV avoidance shows a sharp change (Guggiana-Nilo and Engert et al., 2016).

The regression of the visual system and the depigmentation of fish species that have evolved in the subterranean environment, induces ethological research to the spectral sensitivity of light. This in order to understand the biology and behavior of these forms, and at the same time to investigate the morphological and physiological adaptation of these animals to the completely dark environment. In the hypogean species *P. andruzzii*, the phototactic behavior was evaluated using four monochromatic lights (blue, green, orange and red) (Ercolini and Berti, 1975). This species has a photophobic behavior that varies from blue to red and depend on the intensity of light. The increase in the tendency to photophobia under blue light is an interesting consideration. These fish seem to be able to perceive not only the presence of light energy but are also able to discriminate between various types of electromagnetic irradiations (Tarttelin et al., 2012). They identified two *P. andruzzii* photopigments, orthologues of ROD opsin and EXO-ROD opsin. *In vitro*, both opsins serve as light-absorbing photopigments with λ_{max} around 500 nm when reconstituted with an A_1 chromophore. When they next explored the involvement of both opsins in the negative phototaxis reported for this species. A comparison of the spectral sensitivity of the photophobic response with the putative A_2 absorbance spectra corrected for skin/skull absorbance indicates that the A_2 versions of either or both of these pigments could explain the observed behavioral spectral sensitivity (Tarttelin et al., 2012). This scenario is consistent with the hypothesis that encephalic photoreceptors are the basis for phototactic response in *P. andruzzii*. The surface ancestors of the predominantly troglobial species derive from forms already predisposed to live in the darkness. Escaping from the light

showed a strong photophobic behavior, preferring mostly the way of life in a dark environment. This was also observed in the Mexican surface catfish *Rhamdia laticauda* (Wilkens, 2001; Langecker, 1992a). Photophobic behavior has long been considered as a prerequisite of surface species for the colonization of caves, as well as an adaptation of cave species to prevent them from leaving the dark environment. However, *R. zongolicensis* and *R. reddelli*, two cave sister species originate from the surface species *R. laticauda*, reveal a less strong photophobia and show a higher inter-individual variability. However, photosensitivity is probably still functioning because the pineal organ contains photoreceptors (Eilertsen et al., 2014; Langecker, 1992a). This may imply that photophobic behavior has lost its biological function in these cave species and is a regressive feature in the underground system, probably because fish are rarely in contact with the surface environment. Comparing the phototactic behavior between the surface- and cavefish *Astyanax mexicanus*, the visual orientation was experimentally excluded by the complete removal of the surface fish eye. In these conditions, the intensity of the photophobic reaction of the surface fish increase if compared to the untreated surface fish, and is very accentuated at low light intensity, and above all it is much stronger than in the cave phenotype. While, after removal of the pineal organ, the phototactic reaction of surface fish is almost neutral, and equal to that of untreated fish (Langecker, 1992a; 1992b). The slight photophobic behavior observed in the cave phenotype after the removal of the pineal gland could be based mainly on the existence of ipRGCs (Lucas et al., 2014). This suggests that the general low degree of photophobia of *A. mexicanus* populations from the Pachòn cave compared with surface individuals is not due to the morphological degeneration of structures that perceive light, but is caused by the regression of photophobic behavior (Langecker, 1992a). This is also confirmed by phylogenetic studies on cave fish *A. mexicanus* of the Tinaja cave, which shows a neutral phototactic behavior. By crossing surface phenotypes with cave ones, it was revealed that the F1 hybrid generation shows a strong photophobic behavior comparable to surface fish, while for the F2 generation the distribution is bimodal (Kowalko et al., 2013b). From this it can be interpreted that a polygenic system exhibits an epistatic effect responsible for the phototactic behavior.

2.2 - Aim

The objective of the investigation reported in this chapter is to verify in our model species the ability of UV-A light on driving behavioral responses. For this purposes we have studied two different behavioral assays, the entrainment of the rhythms of locomotor activity and the phototactic behavior to UV-A light. Is the UV-A light alone capable to photoentrain the behavioral locomotor activity of the zebrafish? The UV-A photoreception in sighted fish depends mostly from the retina that involve SWS opsin photoreceptors family. The cavefishes *P. andruzzii* and *A. mexicanus* have lost this opsin family during the evolution due to the eyes degeneration. Is this ability of UV-A to photoentrain still conserved in the two blind cavefishes influenced by different evolutionary history? Otherwise, does these cavefish preserve extra-ocular photoreceptors in order to respond with phototaxia to UV-A? Though the use of these models species that strongly differ for the pathways involved in photoreceptions, we gain a deeper understanding on influence and processing of UV-A light in teleost fish and how this is evolved in the perpetual dark of the cave environment.

2.3 - Material and Methods

2.3.1 - Entrainment of circadian clock

In order to assess whether the UV-A λ_{peak}=395 nm (Figure S1) light could mediate the synchronization of biological clock in our species, we used the same set-up published by Cavallari and colleagues (2011). The fish were kept in the fish-house in monospecific groups, under own naturally cycles: the constant darkness for the cavefish species and the 12:12h LD cycle for the zebrafish (see paragraph S1.1). Animals were transferred from the fish-house to the specific room used for experimentation "the clock-room" provided of aquariums for the recording of the locomotor activity. To achieve our data we used three aquariums (56 x 31 x 32.5 cm) provided of heater to preserve the constant temperature of 27 ± 0.5 °C and filter with sponge and activated carbon to ensure a continuous flow of clean water. The animals locomotor activity were recorded through the use of infrared photocells (E3S-AD62, Omron; J), positioned at 10 cm from the water level of each aquarium. Only for the specie *D. rerio* we used aquariums half filled with the photocell positioned at the same distance from the water level. We recorded every 10 minutes the number of fish-transitions across the infrared ray of the photocells. Before starting each experimentation animals were monitored daily in order to ensure the desynchronization of the behavioral circadian rhythms coming from the fish-house. The experimental protocol involved two consecutively cycles. In the first period of 7 days the animals were exposed to light-dark (LD) cycle consisting of 12 hours of light and 12 hours of dark. During the second period of 7 days the animals were maintained in constant darkness (DD), 24 hours of dark in free-running. Recordings of locomotor activities were biologically replicate 3 times for each species investigated, *D. rerio*, *P. andruzzii* and *A. mexicanus*. The number of individual tested for each biological replicate were n=6 per species. We exposed animals to UV-A light in LD cycle (UV-A lamp with λ_{max} = 395 nm) and as control the full light-spectrum LD cycle (White LED lamp "450 nm<λ<700 nm" (Figure S1).

2.3.2 - Phototactic behaviour

In order to record the phototaxy in zebrafish we developed a set-up assembled with six parallel tanks of the same dimensions (30x12x12 cm). The size of the set-up was designed according with the ecology of the species (Spence et al., 2008) due to the fact that the zebrafish in natural condition inhabit fresh water at low level (see paragraph S1.1). Each tanks were half-covered of black plastic materials maintaining one zone in constant darkness and the other one of possible light-exposition at the switch-on. These two areas was connected by 2-cm-high gap left above the bottom of the tanks. This gap allowed the test fish to move from one compartment to the other. The set-up was placed on a table backlit with infrared light (λ_{max} = 850 nm; Noldus, NL) which is not perceived by the fish and allow video-recording (Dekens et al., 2017). Filming were performed through higher resolution video camera (Monochrome GigE camera; Resolution: 1280 x 1024 Blaser, D) and the recording of locomotor activity were carry out with a frequency of 25 frame per second (fps). Analyses of the video-records were conducted using the software EthoVision XT 11.5 (Noldus, NL).

Concerning the cave species *P. andruzzii* and *A. mexicanus* it was used another set-up recently published in Tarttelin and colleagues (2012) this reflect more the ecology of the species that in cave environment swim along the vertical column of the water. The measures of the test tank were 40 x 40 x 48 cm, one half of the set-up was covered by black plastic foil and remained in constant darkness while the other half was not covered, the light exposition zone. A black PVC partition was used to divide the aquarium into two halves in through a small 5-cm-high gap left above the bottom of the tank. The tank was equipped with infrared lights and filming was carried out with an infrared video camera (Logitech HD 270). The video-recording were acquired at 15 fps through the software Multiviewer (University of Murcia, SP) and subsequently were converted at 1 fps by the software VirtualDub 1.9.11. Finally, video data were analyzed on a PC.

The experiments were conducted in a experimental dark-room at 27 ± 0.5 °C. Animals were tested at different times in the set-ups described above. Each specimens were subjected to independent photic-stimulation in separates experiment by the two monochromatic UV-A light sources (UV-A 365 nm with λ_{max} = 365 and UV-A 395 nm with λ_{max} = 395 nm, Figure S1) and one polychromatic light

source (White LED lamp “450 nm < λ < 700 nm”) (Figure S1). The three photic-stimulations of 30 minutes each one were preceded by 30 minutes of recording which the fish were maintained in the dark. Before all experimental sessions, in order to ensure acclimation of the animals they were placed for 24 hours in constant darkness into the appropriate set-up. For each lighting conditions were tested: *n*=18 individuals divided into 3 groups each one of *n*=6 for the zebrafish, and *n*=10 individuals for both cavefish *P. andruzzii* and *A. mexicanus* individually tested in the set-up.

2.3.3 - Statistical analysis

Regarding the analyses of the behavioral circadian rhythms, data were automatically achieved by the system in a text files (.txt format). Actograms, mean waves and periodograms were built using the software ‘‘El Temps’’ (version 1.249, University of Barcelona). The temporal series were analyzed using the Lomb–Scargle periodogram technique. Analyses were performed for each group of animals and the power spectrum of the circadian components was used for comparisons between species.

The analysis of the phototactic behavioral responses was performed using the GraphPad software (Prism Hallogram, USA). The results were expressed as Mean ± SD of time periods in the dark and in the light periods. For all the species and lighting conditions it was performed the D'agostino & Pearson normality test, in order to assess how much the data differ from the expected value of the Gaussian distribution. In all cases the normality test were significative, so it was decided to perform a paired t-Student tests between the dark and the respective light periods of time. The Mean ± SD values in the graphs were plotted using Δ (%) values, subtracting the time spent in light period from the previous time spent in the dark period.

2.4 - Results

2.4.1 - Entrainment of the behavioral locomotor activity

Concerning the UV-A analysis on zebrafish the results reported in the actogram show that during the 7 days in LD cycle the individuals concentred the behavioral locomotor activity during the light phase (Figure 6A). The mean wave analysis of this LD cycle highlights an increase in activity during the light phase and a subsequently decrease in activity during the dark phase (Figure 6B). In order to confirm these results we performed a periodogram analysis showing that the significative entrainment was obtained in the LD cycle having a periodicity of about 24 h (Figure 6C). During the 7 days in DD zebrafish assume a rhythmic pattern with residual activity derived from the previous LD cycle (Figure 6A). Particularly the actogram relative to the DD condition report an activity with the period shorter than 24 h. The mean wave and periodogram analyses of the DD confirm the circadian pattern (Figure 6B-C).

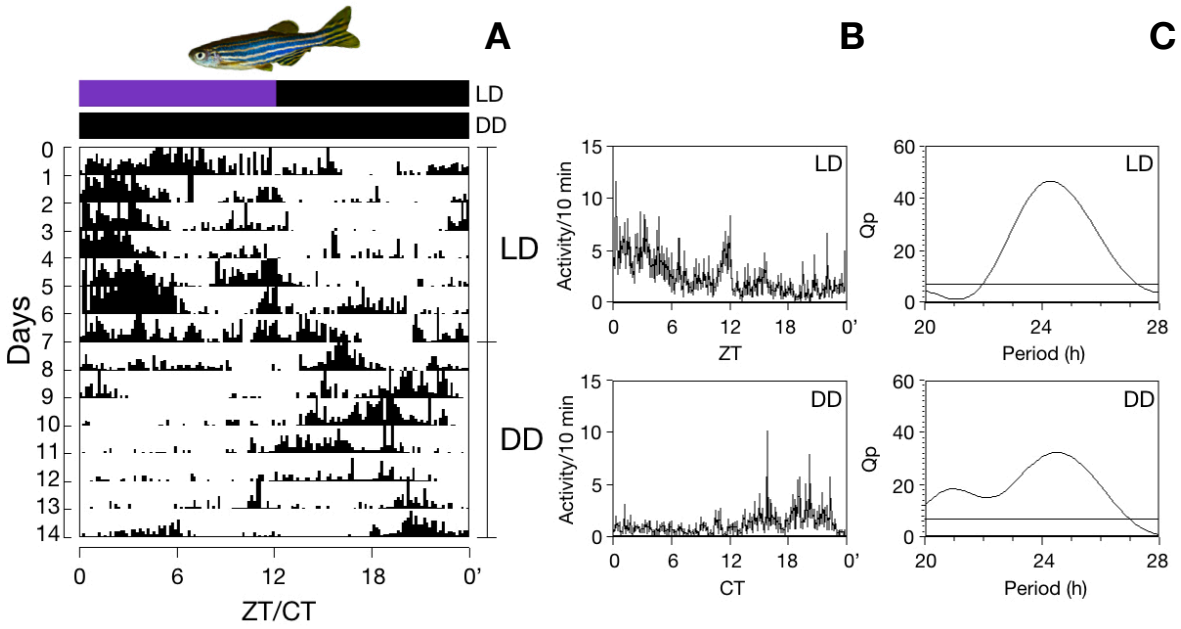

Figure 6. (**A**) Representative actograms under UV-A light condition of zebrafish maintained in LD cycle and subsequently shifted in DD. Records are single plotted on 24 h time scale. Mean and SD of the waveforms (**B**) and Lomb-Scargle periodogram (**C**) of the behavioral locomotor activity of the LD cycle and DD. The periodogram indicates the quantitative periods (Qp) of the rhythm plotted for each analyzed period within a range of 20–28 h; the lines represent the threshold of significance, set at p=0.05.

Differently the UV-A light did not entrain the blind cavefish *P. andruzzii* locomotor activity. As consequence of this asynchrony the individuals analyzed were striking arhythmic during the DD also (Figure 7A). The mean wave and periodogram analyses of both LD and DD cycles indicate that the locomotor activity did not have any pattern (Figure 7B-C).

As control we investigate the photoentrainment of circadian clock using the white/polychromatic lamp. This is provided by full light spectrum without the UV-A band (Figure S1). As previously reported in the work of our colleagues (Cavallari et al., 2011) zebrafish show clear diurnal and rhythmic locomotor activity pattern that contrast with the arrhythmic patter of *P. andruzzii* (Figure S2-S3).

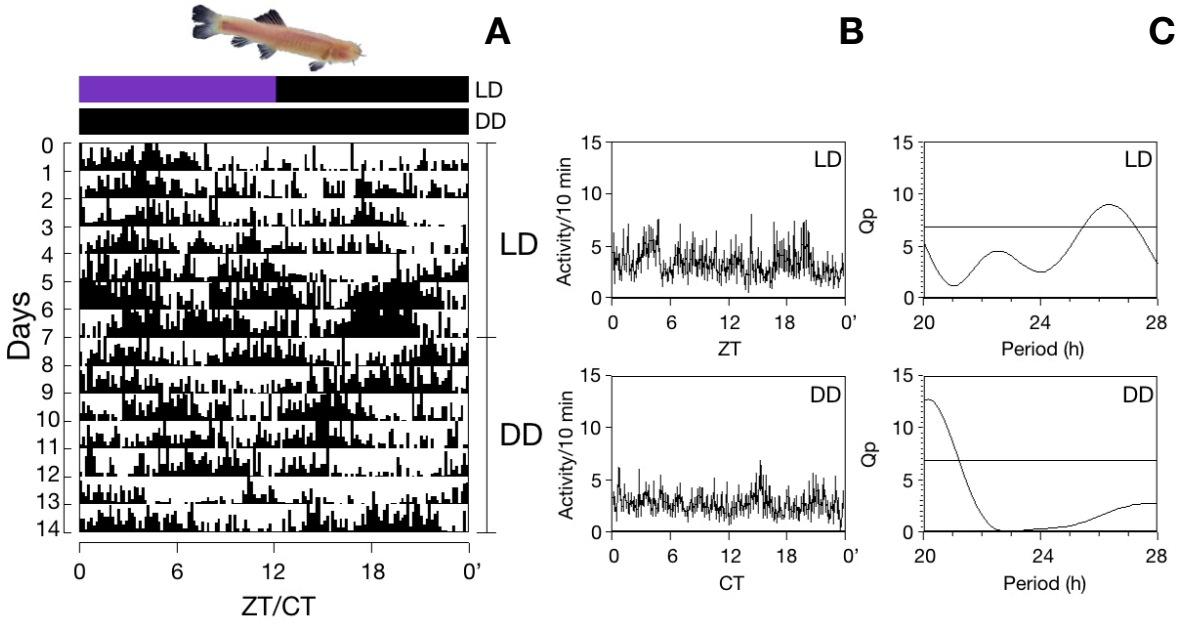

Figure 7. (**A**) Representative actograms under UV-A light condition of blind cavefish *P. andruzzii* maintained in LD cycle and subsequently shifted in DD. Records are single plotted on 24 h time scale. Mean and SD of the waveforms (**B**) and Lomb-Scargle periodogram (**C**) of the behavioral locomotor activity of the LD cycle and DD. The periodogram indicates the quantitative periods (Qp) of the rhythm plotted for each analyzed period within a range of 20–28 h; the lines represent the threshold of significance, set at p=0.05.

Analyzing the UV-A light effect on the circadian locomotor activity of blind cavefish *A. mexicanus* we report the powerful of this wavelength to entrain the biological rhythms during the LD cycle (Figure 8A). The actogram relative to the LD cycle confirm that this cavefish conserved the ability to synchronize own rhythms through the use of UV-A light. The mean wave analysis relative to this LD cycle confirm this entrainment with a particular increase in activity before the light phase (Figure 8B). Our periodogram analysis rise the capacity of this cavefish to assume a period of about 24 h during the LD cycle (Figure 8C). Making focus on the second period in DD cycle, the actogram identify a strong influence of the activity from the previous LD cycles (Figure 8A). The mean wave and periodogram analyses of the DD cycle show the locomotor activity mediated by UV-A in the subsequently constant darkness period (Figure 8B-C). Using the control white/polychromatic lamp, we provide further evidence of the retained circadian rhythms of this cavefish species (Figure S4), as was showed in the previous work of Beale and colleagues (2013).

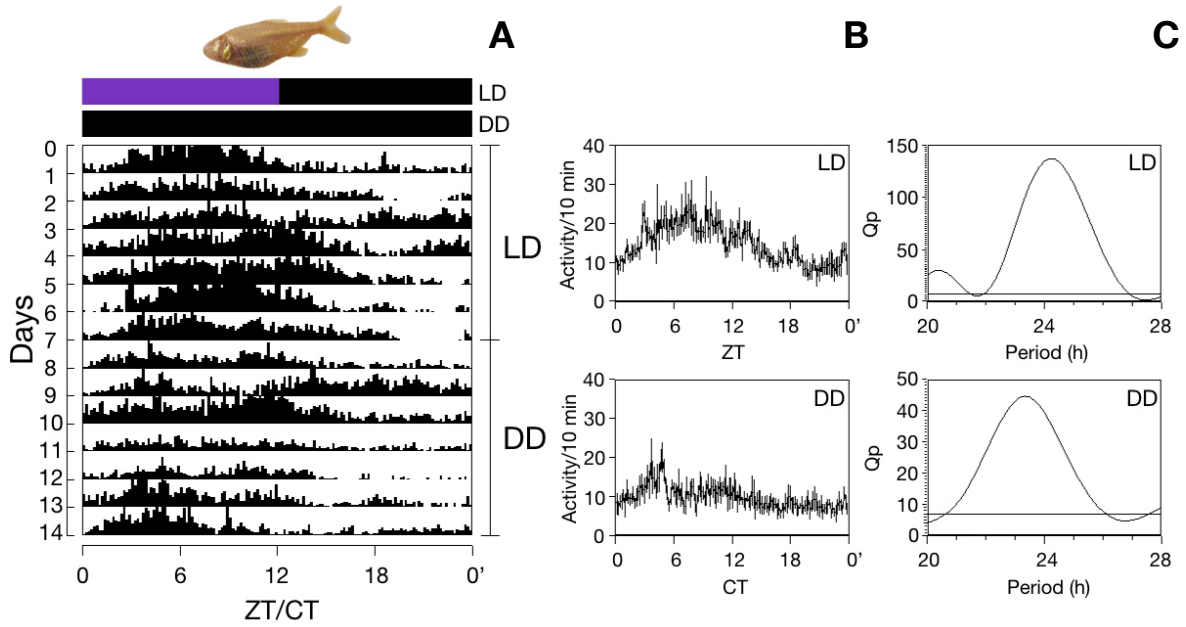

Figure 8. (**A**) Representative actograms under UV-A light condition of blind cavefish *A. mexicanus* maintained in LD cycle and subsequently shifted in DD. Records are single plotted on 24 h time scale. Mean and SD of the waveforms (**B**) and Lomb-Scargle periodogram (**C**) of the behavioral locomotor activity of the LD cycle and DD. The periodogram indicates the quantitative periods (Qp) of the rhythm plotted for each analyzed period within a range of 20–28 h; the lines represent the threshold of significance, set at p=0.05.

2.4.2 - Behavioural phototactic response

Through our set-up designed for the ecological characteristics of zebrafish we had the opportunity to evaluate the phototactic behavioral response to UV-A wavelengths. The zebrafish shown scototaxis only to the UV-A light source with λ_{max} 395 nm. Exposure to the 365nm UV-A lamp did not induce any significant response in zebrafish (Figure 9 left panel and Table S1). The mean of the time percentages (Table S1) spent in the data acquisition area of the system for the UV-A 365 nm light pulse were almost identical (Dark: Mean 56.93 ± SD 11.51; UV-A 365 nm: Mean 51.04 ± SD 18.88). While exposure to 395 nm UV-A lamp induces a statistically significant photophobic response (Figure 9 left panel and Table S1). The mean of the time percentages (Table S1) spent in the data acquisition area of the system for the UV-A 395 nm was reduced of 22,26% (Dark: 61.57 ± 18.03; UV-A 395 nm: 39.31 ± 20.11). As previously reviewed in the protocol of Maximino et al. (2010), under the white lighting condition *D. rerio* shown clear scototaxy (Figure S5 left panel). Coherently the exposure to the white lamp in our experiment induces a statistically significant photophobic response (Figure S5 left panel and Table S1) with the reduction of 15.57% of the time spent in illuminated area.

In our aquarium system designed for assaying negative phototactic behavior in cavefish (Tarttelin et al., 2012), the species *P. andruzzii* exhibited a photophobic behavior to both lamps type (UV-A 365 nm and UV-A 395 nm). The exposure to the UV-A 365 nm lamp induces the lower significant photophobic response (Figure 9 central panel and Table S1). The comparison between the percentage of time spent in the dark and the subsequently in the illuminated period at UV-A 365 nm highlights a reduction to 29.47% of time spent in the illuminated area (Dark: 61.24 ± 20.62; UV-A-365 nm: 31.77 ± 28.16). Analyzing the UV-A 395 nm light pulse it was noted an induction of more significant photophobic response (Figure 9 central panel and Table S1). The difference between the percentage of time in the dark and in the subsequently illuminated period at UV-A 365 nm highlights a reduction of 34.97% of the time spent in the light exposed area (Dark: 57.68 ± 23.85; UV-A-395 nm: 22.71 ± 24.63). How showed the previous work of our colleagues (Tarttelin et al., 2012) tested monochromatic lights, the species *P. andruzzii* have clear photophobic behavior. The exposure to our full spectrum white lamp induces a statistically significant photophobic response with a decrease of 24.32% of the

time spent in the illuminated area (Figure S5 central panel and Table S1), confirming the involvement of extra-ocular photoreceptors in the photophobic response.

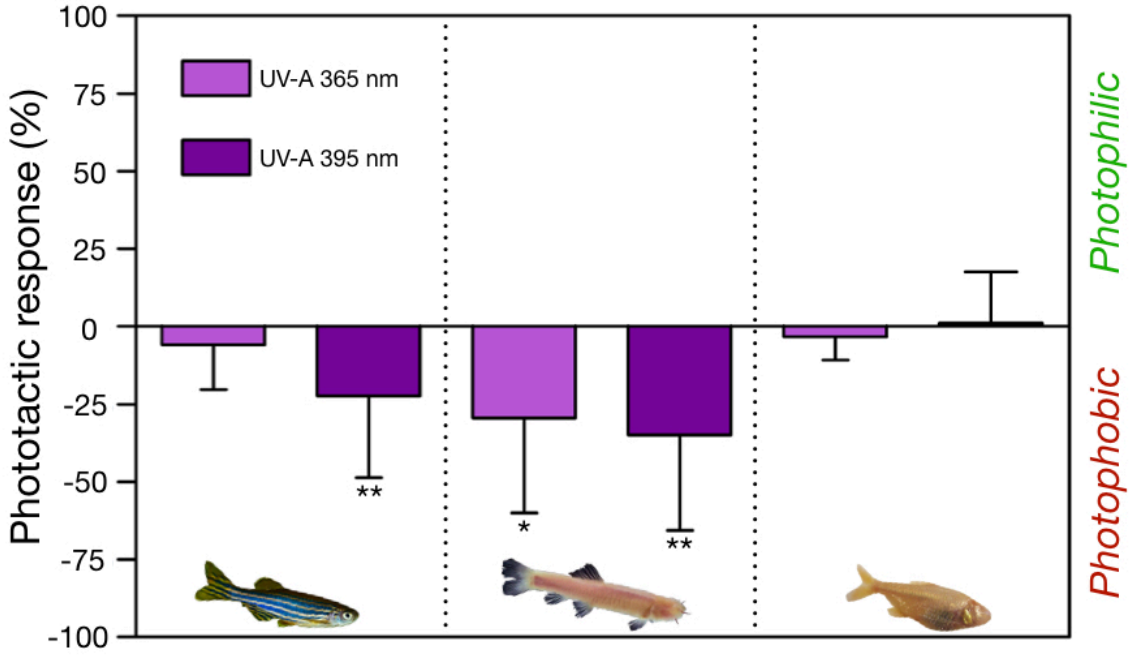

Figure 9. Behavioral phototactic response to UV-A light in our model species. Mean and SD of the percentage of time spent in the dark zone of zebrafish *D. rerio* (left panel), Somalian blind cavefish *P. andruzzii* (central panel) and Mexican blind cavefish *A. mexicanus* Pachón (right panel). Each fish was tested separately at UV-A λ_{max} = 365 nm, UV-A λ_{max} = 395 nm. Irradiances values are showed in the (Figure S1). Student's t-test for paired data are reported in Table S1, significant differences are indicated by asterisks (*** $p<0.001$, ** $p<0.01$, * $p<0.05$).

Unlikely *P. andruzzii*, the cavefish *A. mexicanus* showed neutral phototactic response to both UV-A lamps (Figure 9 right panel). The mean of the time percentages (Table S1) spent in the light exposed area for the UV-A 365 nm were almost identical (Dark: 59.80 ± 15.31; UV-A 365 nm: 56.41 ± 16.28). *A. mexicanus* uses the available space identically for the UV-A 395 nm also (Dark: 50.32 ± 10.53; UV-A 395 nm: 51.37 ± 24.15) confirming the irrelevance of UV-A light to lead choice in this paradigm. As reported the author Langecker (1992b), under the white lighting condition *A. mexicanus* Pachòn shown clear photophobic response. Consistently our results demonstrated that the exposure to the white lamp induces a statistically significant photophobic response (Figure S5 right panel and Table S1) with the reduction to 17.63% of the time spent in the illuminated area.

2.5 - Discussion

In the early development of life on our planet, the emerging photosynthesizing organisms that were exposed to sunlight faced several major problems owing to the alternation between day and night. They had to have access to energy throughout the day and night, and they had to protect themselves against damage by UV, which was not filtered by the earth's atmosphere around 3-4 billion years ago when early life emerged (Dvornyk et al., 2003; Pittendrigh, 1993).

Relatively few studies have explored the informative properties of UV-A light spectrum. A recent study on circadian activity reported how *Drosophila* entrain own biological rhythms through a LD cycle mediated by UV-A. The powerful of this wavelengh is also in shifting the LD cycle at an energy level seated below that of the visible spectrum (Negelspach et al., 2018). The data of this work establish that the UV-A light act as *zeitgeber*-time providing evidence to that the pacemaker might be capable of resetting to extremely low levels of UV-A light that exceed its sensitivity to visible light spectrum. This scenario maturing an idea of evolutionary convergences in the photoentrainment pathways of flies and mammals (Negelspach et al., 2018; Buhr et al., 2015) raising the possibility that UV-A from sunlight plays an equally important synchronizing role for the human circadian system. The investigations that we have conducted during this work allowed us to increase knowledge on the effects of UV radiation on the behavior of Teleostea. Given what has been published for zebrafish (Cavallari et al., 2011) regarding the attempts to synchronize the biological clock by white light. Our results obtained using a LD cycle in the presence of UV-A light shown the ability of the UV-A light spectrum to photoentrain the behavioral locomotor activity without the presence of the full light spectrum. Furthermore, it has been shown that the degree of development and the conditions of different monochromatic lights influence the expression of clock genes and the synchronization of circadian rhythms (Burton et al., 2017; Di Rosa et al., 2015). In zebrafish adults the temperature and the UV-B radiation interact causing the production of Reactive Oxygen Species (ROS), the reduction of the locomotor activity at temperatures above 26 °C and the selection of the thermal areas. In particular, zebrafish exposed chronically for a few weeks to UV-B avoid areas with extreme temperatures in order to maximize the efficiency of antioxidant enzymes (Seebacher et al., 2016). Previous research has highlighted

that zebrafish larvae swim away (via turning direction) from UV-A stimulus projected in the retina and this avoidance behavior involve the UV cone. We know also that they prefer swim in the visible spectrum (>400 nm) (Guggiana-Nilo and Engert et al., 2016). Given these harmful effects and changes in swimming performance (Seebacher et al., 2016), climate changes that cause a significant increase in the penetration of UV into ecosystems are a potential hazard to be avoided. It has been shown that high doses of UV produce harmful effects on the development of zebrafish embryos: UV-A and UV-B may induce negative effects on hatching percentage, increase mortality and malformations (Dong et al., 2007). From the literature, in a paradigm similar to ours, it emerges that zebrafish exposed to white light after a period of adaptation in the dark shown a natural photophobic behavior (Serra et al., 1999). This result has been confirmed for another 5 species of Teleostei (Maximino et al., 2010) and is probably an anxiogenic effect caused by the white light pulse. From our results on phototactic behavior to UV-A sources in zebrafish, it has been shown a neutral phototactic response to UV-A light with λ_{max} = 365 nm but significant photophobic behavior to UV-A light with λ_{max} = 395 nm. From a behavioral and physiological point of view, this different behavioral response could be given by the fact that the peak at 395 nm wavelength is closest to the spectrum of the visible violet light (400-430 nm). This lead our interpretation of a maximal absorption of the UV-A cones at the peak at 395 nm despite 365 nm, here we can speculate that lighting differential response may sustain zebrafish in the habitat selection. Both behavioral responses in zebrafish could be determined by the perception of the light source at the retina level or at the extra-ocular photoreceptors level. Recently, Buhr and co-workers (2015) showed that the mouse corneal circadian rhythm is also photoentrainable ex vivo, and this photoentrainment likewise requires neuropsin OPN5. Retinas lacking OPN5 fail to photoentrain, even though other visual functions appear largely normal. The molecular circadian clocks in the mammalian retina are locally synchronized by environmental light cycles independent of the SCN in the brain. Unexpectedly this entrainment does not require rods, cones, or melanopsin OPN4, suggesting the crucial involvement of neuropsin OPN5. It has been shown that the ex vivo mouse retinal rhythm is most sensitive to short-wavelength light but that this photoentrainment requires neither the short-wavelength-sensitive cone pigment

(S-pigment) nor encephalopsin (OPN3). However, retinas lacking neuropsin (OPN5) fail to photoentrain.

More recently, in a study focused primarily on behavioral analysis of circadian locomotor activity of various mutant mice, demonstrated impaired photoentrainment to UV-A light in OPN5-null mice (Ota et al., 2018). Surprising, mice that lack melanopsin and rod-cone photoreceptors, but still posses OPN5, failed to photoentrain to LD cycles of both white and UV-A light. This means that OPN5 is required for maximum UV-A sensitivity, but it alone is not sufficient for entrainment to UV-A LD cycle. We currently know nothing about the OPN5-expressing cell type or the nature of OPN5 signaling in the cornea of zebrafish, although may work properly like OPN5 signaling in mammalian. OPN4 was initially identified by virtue of its role in entrainment of the SCN clock, but it is now known to be involved in a broad range of functions, including pupillary light reflex, SCN photoentrainment, visual irradiance coding, retinal vascular development, and negative phototaxis during mammalian development (Lucas, 2013). By the same token, OPN5 may have other functions besides circadian photoentrainment of the retina and cornea of fish (Sato et al., 2016). A detailed molecular study on zebrafish has found that retinal and extra-retinal photoreceptors are present. The results of this work has reported the expression of 10 visual photopigments and 32 non-visual opsins, representing the largest number of photoreceptors identified in the vertebrate world (Davies et al., 2015). Our results in zebrafish revealed that SWS visual-opsin family as well as neuropsin OPN5 could have mediated the photoentrain of biological clock and the photophobic response. Although insects, reptiles, amphibians, fishes and birds have long been known to use extra-ocular photoreceptors, this photosensitivity via OPN5 remain poor evaluated.

In this work we decided to use the hypogean model *P. andruzzii* that present extreme phenotype in order to evaluate whether the photoreception of UV-A light may show an extra-ocular pathway in the blind cavefish. Considering our cavefish species we showed that UV-A does not affect the regulation of circadian rhythm. This founding has been published for cavefish (Cavallari et al., 2011) regarding the fail to synchronize the biological clock by white light.

Our unpublished data revealed that neuropsin OPN5 sequence of *P. andruzzii* share the 87,50 of Identity (%) compared to zebrafish. Here we can speculate about the

fact that cavefish have this conserved domain but do not preserve the function as in *Drosophila*, mammals and presumably rest of Teleost. Regarding the phototactic behavior in *P. andruzzii* we observed for both the UV-A light pulses (365 nm and 395 nm) a behavioral photophobic response, with higher significance for the UV-A light pulse with λ_{max} = 395 nm. As in zebrafish, even in *P. andruzzii* we can compute the same hypotheses on the evaluated behaviors. The greatest photophobia on the second light pulse could be given the 30 nm increasing of the λ_{max}. Despite the complete anophthalmia (Berti et al., 2001), *P. andruzzii* shows a clear photophobic behavior. This behavior has been studied under red, green and blue lighting conditions. The comparison between molecular and behavioral information has been shown that the negative phototaxy at these wavelengths are mediated by both the photopigments rodopsin and exorodopsin (Tarttelin et al., 2012). However, it is not possible to exclude the possibility that further encephalic photopigments are involved in the phototactic behavioral responses UV-A light. As for the zebrafish, an opsin member of the neuropsin family recently identified in the brain of *P. andruzzii* could be responsible for this behavioral responses. This species colonized the phreatic environment of the Somalia desert about 5 million years ago, initially the populations maintained a certain level of gene flow with surface populations. This situation was maintained until about 2.5 million years ago, before the desertification event in Somalia leading the complete isolation in this hypogean environment (Calderoni et al., 2016).

As expected from the previous work of Beale and colleagues (2013) that use the white light in order to photoentrain the behavioral circadian activity in the blind cavefish *A. mexicanus*, using the UV-A wavelength this cavefish species retain the ability to synchronize own activity during the light phase. Surprising, our results showed that UV light does not affect the phototactic behavior of cavefish *A. mexicanus*. However, this behavior has been shown to be present in all populations of *A. mexicanus* in response to white light (Langecker, 1992a; 1992b). The effect of white light could be explained as in the sighted zebrafish that show a clear behavioral conflict of anxiety and fear under this lighting condition. Considering the behaviors mediated by the two UV-A long wave, it is possible explain the neutral phototactic response as result of distinct ecology of the species and different time of divergence from the surface population. The biogeography of *A. mexicanus*

pinpoint the hypogean forms of this species in a series of isolated populations in the karstic environment of the east-Mexico. Through the global decline in sea level and the rivers that flowed beneath the limestone mountains, a series of underground environments were created isolating the populations. Trapped individuals began an evolutionary process in this new environment. However, during the flood periods, a certain entry of surface population within the cave system was maintained ensured the gene flow from the outside environment (Foulkes et al., 2016; Bradic et al., 2012). From one recent study of Fumey and colleagues (2018) that reanalyzed the geographic distribution of mitochondrial and nuclear DNA polymorphisms it has been established a very recent origin (< 20.000 years) of cave populations.

The preliminary results reported in this work highlight species-specific differences in behavioral responses to UV-A that could be the result of adaptation to the environment in which animals evolved. Furthermore, the use of hypogeal species has allowed us to conclude a potential use of extra-ocular photoreceptors in the perception of UV-A light in fish. Further experiments are needed to investigate the effects of UV-B radiation on behavioral rhythms and phototactic responses. Moreover, given the differences found in the variation of the λ_{max}, further tests with increasing or decreasing irradiations will be appropriate.

To better investigate the behavioral responses to UV-A light in cavefish and in zebrafish at physiological and molecular levels, we will use modern techniques of genetic engineering and the numerous mutants available to evaluate at molecular level our behavioral results on circadian clock and phototactic response. Animals selectively deprived of specific ocular or extra-ocular photoreceptors will be used in order to understand the molecular basis of these behaviors in cavefish and zebrafish.

Chapter 3

Evolution of DNA repair mechanism in Somalian cavefish

3.1 - Introduction

3.1.1 - Shine on DNA repair by photolyase

Cells from all living organisms are constantly being threatened by the action of environmental agents or endogenous cellular metabolism, which can interact and modify the DNA structure. These alterations in DNA can result in cellular dysfunctions, such as genetic instability, mutagenesis or cell death. Thus, the removal of lesions in this molecule is a vital process for every single cell. Therefore, DNA stability is a requisite of importance to preserve the normal cellular function. Among the various environmental factors that assault them, the UV from sun light is the most common and powerful that can alter the normal state of DNA by inducing mutagenic and cytotoxic lesions, such as cyclobutane-pyrimidine dimers (CPDs), 6-4 photoproducts (6-4PPs), cry-DASH (*Drosophila*, *Arabidopsis*, *Synechocystis*, *Homo* cryptochromes) and their Dewar valence isomers (Sancar, 2016; Essen and Klar, 2006; Sinha and Häder, 2002). Such forms of damage must be rapidly removed to ensure complete and accurate DNA replication and transcription and so organisms have developed a battery of repair mechanisms to counteract these DNA (Cline and Hanawalt, 2003).

Photolyase is a photon-powered nanomachine that uses blue light photons to repair thymine dimers that are induced in DNA by UV (Sancar, 1996; Kim et al., 1994). This light dependent reaction is catalyzed by photolyases which belong to the photolyase/cryptochrome superfamily. This is a diverse class of flavoproteins containing not one, but two blue light-absorbing cofactors, which are methenyltetrahydrofolate *MTHF* (folate) and two-electron reduced and deprotonated flavin adenine dinucleotide *FADH* (flavin) (Figure 10). As predicted from the biochemical experiments, the folate (that differs between photolyases and species) is like a solar panel, where it sits on the “roof” of the enzyme, absorbs light, and then transfers the light energy to the flavin cofactor within the core the enzyme so to carry out catalysis (Sancar, 2016). With this general structural view, then, the mechanism of photolyase was developed: photolyase binds DNA containing a CPD because the T<>T distorts the backbone of the DNA. Upon binding to damaged DNA, through ionic interactions between the positively charged groove on the photolyase surface and negatively charged DNA

phosphodiester backbone the enzyme pulls the T<>T out from within the helix and into the core of the enzyme so that the T<>T is within Van der Waals contact with FADH- (Figure 10-11). It makes a very staple complex, and nothing happens until folate absorbs a photon and transfers the excitation energy to the flavin cofactor. The excited-state flavin, FADH-*, repairs the T<>T by a cyclic redox reaction, and then the enzyme dissociates from the DNA to go on in search of other damage sites to carry out the repair reactions again (Zhong et al., 2015). Over the past decade it was determined the rates of energy transfer, electron transfer, bond breakage, bond forming and electron return, in real time and at picosecond resolution. The entire catalytic cycle is complete in 1.2 ns, and the enzyme repairs T<>T with a quantum yield of 0.9 (Figure 11) (Zhong et al., 2015; Liu et al 2011).

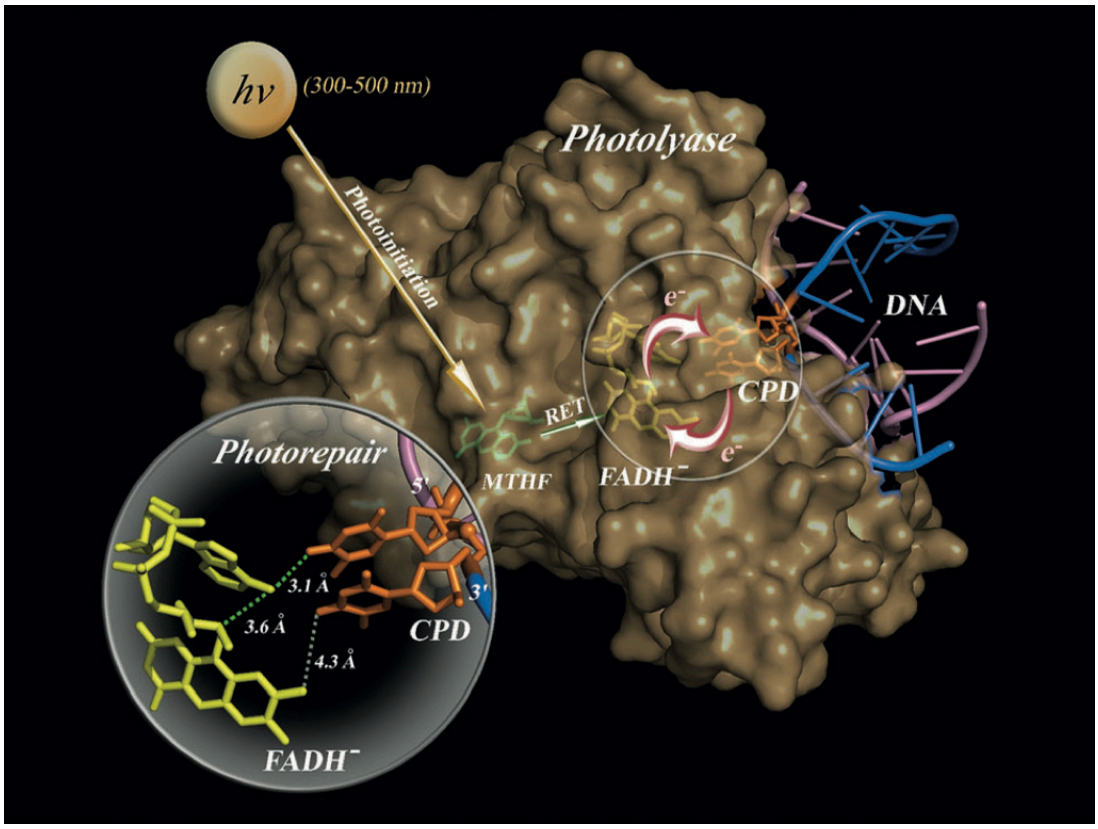

Figure 10. Reaction mechanism of photolyase. The enzyme makes ionic bonds with the phosphate residues of the damaged DNA strand and flips out the thymine dimer dinucleotide into the active site cavity so that the T<>T is within Van der Waals contact with $FADH^-$. The catalytic reaction is initiated by absorption of a photon (300–500 nm) by the folate (MTHF). The MTHF excited singlet state transfers the excitation energy to $FADH^-$ by Forster resonance energy transfer (FRET). The excited $FADH^{-*}$ splits the cyclobutane ring by cyclic redox reaction to convert T<>T to T–T, and the repaired DNA dissociates from the enzyme. Image from Sancar, 2016.

Photolyases and cryptochromes are evolutionarily related but perform distinct functions with photolyases repairing DNA damage, while cryptochromes serve as blue-light photoreceptors regulating growth and development in plants and as circadian clock components in animals (Selby and Sancar, 2006). Photolyases are subdivided into CPD photolyases and 6-4 photolyases based on their different substrates (UV-induced CPD and 6-4PP DNA lesions respectively) (Needham and Green, 1940), while cryptochrome-DASH, selectively repairs CPDs in single-stranded DNA and RNA (Chaves et al., 2011; Selby and Sancar, 2006; Daiyasu et al., 2004).

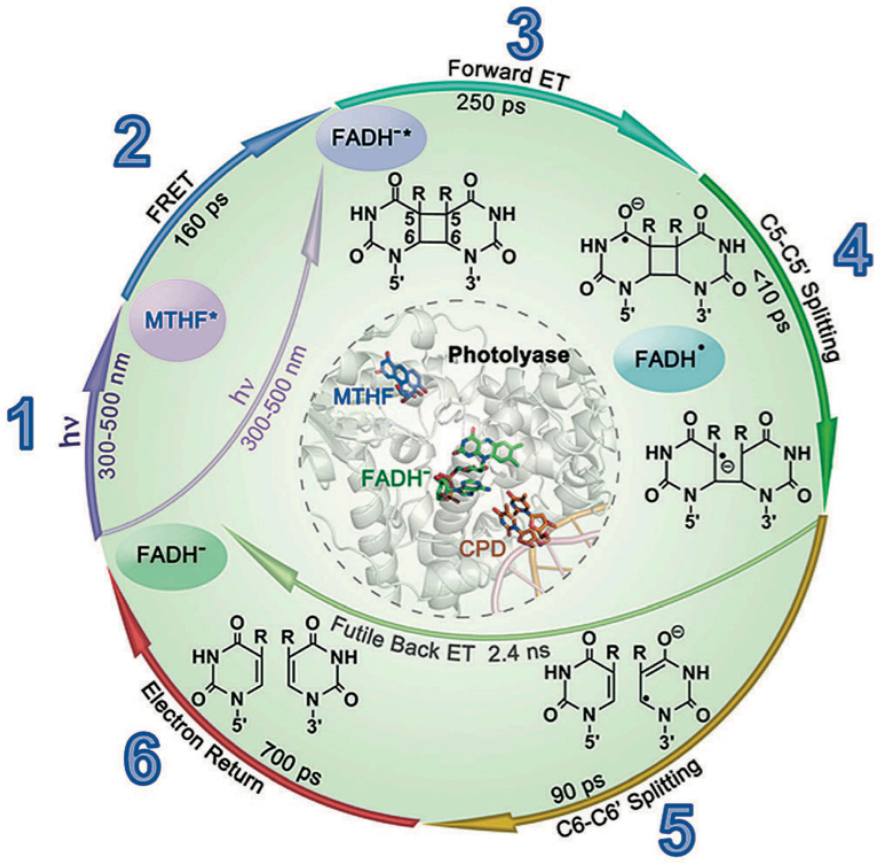

Figure 11. Microscopic rate constants for photolyase. The rate constants were determined by ultrafast time-resolved absorption and fluorescence up-conversion spectroscopy. The cleavage of the cylclobutane ring is by a concerted asynchronous mechanism which couples the cleavage of the C_5C_5 bond in less than 10 ps to cleavage of the C_6C_6 bond in 90 ps. The entire photochemical reaction is complete in 1.2 ns, with an overall quantum yield of about 0.9. The inner circle shows the relative locations of the photoantenna (MTHF), the catalyst (FADH) and the thymine dimer substrate (CPD). Image from Sancar, 2016.

It is hypothesized that an archaic enzyme evolved within primordial organisms featuring the photoentrainment of circadian clock and photoreactivation process mediated by DNA repair functionalities. Probably amplification of gene copies in the past had an elevated total repair capacities due to the heavy presence of the UV light in the environment. It is evaluated that the gene of this ancestral photolyase duplicated at least 4 times before the divergence between prokaryotes and eukaryotes, and gave thereby origin to a wide-spread protein family (Essen 2006; Cashmore 1999; Todo 1999). One of these copies evolved to become the class I CPD-photolyase in prokaryotes. Another copy became the class II CPD-photolyase in eukaryotes. Somehow, via lateral gene transfer the class I CPD-photolyase was later transmitted to eukaryotes and became functionally divergent. (6-4)-photolyase and cryptochrome genes derive from the latter. Finally, a third class of photolyase was discovered and described (Brudler et al., 2003; Hitomi and Okamoto, 2000). This is called DASH-photolyase also derives from the class I CPD-photolyase (Figure 12). Selby and Sancar (2006) supposed this protein catalyze the DNA repair of CPDs in single-strand DNA-specific photolyase activity. Most recently, it has been shown that DASH-photolyase has lost the ability to flip the CPD lesion out of the duplex DNA helix, and therefore can repair the latter only within loop structure regions (Pokorny et al. 2008). However, cryptochromes and photolyases are not ubiquitous within all species. These enzymes which attests to their fundamental role in protecting organisms from UV light appeared early in evolution, and are present in the three domains of life, Archaea, Bacteria and Eukarya. In vertebrates, photolyases are found in fish, amphibians, birds and mammals. Interestedly our ancestors seem to have lost this protection mechanism after the split of placental mammals and marsupials occurred approximately 170 million years ago (Kumar and Hedges, 1998). Therefore, photolyases are absent in placental mammals, including humans. Although orthologs of DASH have been identified in humans and only photoperception mechanisms was reported (Menck, 2002). Surprisingly, the CPD-specific photolyases have been found in marsupials (Chaves et al., 2011) and this relict in functionality was correlated mostly to the molecular clock. However no photorepair has been observed in placental mammals, including mouse and human (Menck, 2002). Recently, a published work asses the contribution of CPDs repair to the biological effects of UV light generating mice expressing a marsupial CPD photolyase transgene. Mice expressing the CPD

photolyase attain photoreactivation of CPDs drastically reduced the acute UV effects (Schul et al., 2002). This result indicate the significance of the core structure of the protein and that placental organisms still provide the necessary conditions for CPD-photolyase action.

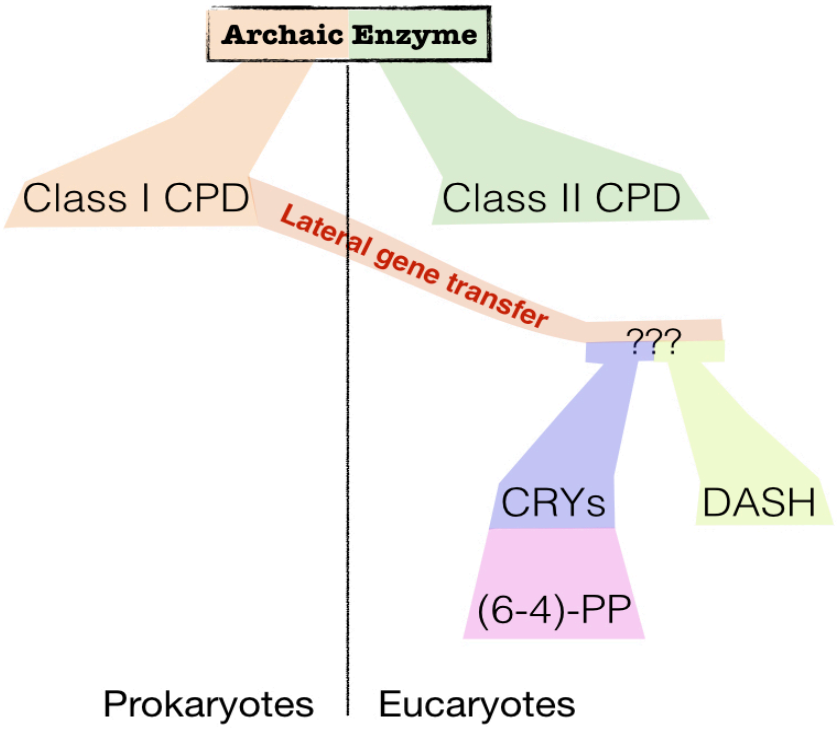

Figure 12. Schematic illustration of cryptochrome-photolyases evolution. Photoreactivation and photoentrainment is an archaic characteristic were evolved via lateral gene transfer from the prokaryotic CPD-photolyase into CRYs-cryptochromes, DASH-photolyases, and (6-4)-photolyases within eukaryotes.

Surprisingly, the CPD-specific photolyases have been found in marsupials (Chaves et al., 2011) and this relict in functionality was correlated mostly to the molecular clock. However no photorepair has been observed in placental mammals, including mouse and human (Menck, 2002). Recently, a published work asses the contribution of CPDs repair to the biological effects of UV light generating mice expressing a marsupial CPD photolyase transgene. Mice expressing the CPD photolyase attain photoreactivation of CPDs drastically reduced the acute UV effects (Schul et al., 2002). This result indicate the significance of the core structure of the protein and that placental organisms still provide the necessary conditions for CPD-photolyase action.

One of the main environmental conditions when organisms are exposed to its daily cycle is to evolve the internal or endogenous circadian clock influenced mostly by the lighting condition. Biological clock coordinate the timing and temporal information obtained from the light-dark cycle through activation of appropriate physiological processes. Light does not just have indirect effects on physiology via the entrainment of circadian clock but can affect physiology extending to many other aspects of cell biology closest to the circadian clock. This relationship between the molecular circadian clock and DNA repair has been subject of many studies, and suggest that the two systems are strictly linked (Uchida et al., 2010; Hirayama et al., 2009; Thompson and Sancar, 2002). In particular, the cross-talk between circadian clock and DNA repair is highlighted in the evolutionary relationship between cryptochromes blue-light photoreceptors, as core members of the circadian clock (see Chapter 2), and the photolyases system, as main DNA repair proteins pathway (Thompson and Sancar, 2002). Looking beyond the sequence similarity between cryptochromes and photolyases, they share the same signaling pathways that regulate their expression. In the zebrafish may include the MAPK pathway and signaling via reactive oxygen species (ROS) (Uchida et al., 2010; Hirayama et al., 2009). Photolyases also feature a “dark function”, it is conceivable that photolyases expressed in internal organs help the recognition of DNA-lesions and removing the internal and external physical or chemical genotoxic agents via binding to CPDs and thereby enhancing Nucleotide Excision Repair (NER) activity (Sancar, 2003; Ozer et al. 1995).

3.1.2 - Other DNA repair mechanisms

How appear clear, from its origin life has faced the fundamental problem that the form in which genetic information is stored is not chemically inert. DNA integrity is challenged by the damaging effect of numerous chemical and physical agents, compromising its function. To protect this weak point, an intricate network of DNA repair systems has evolved early in evolution. One of these is NER, a highly versatile and sophisticated DNA damage removal pathway that counteracts the deleterious effects of a multitude of DNA lesions, including major types of damage induced by environmental sources. NER recognizing and dealing with a variety of helix-distorting lesions, such as the UV-induced photoproducts cyclobutane pyrimidine

dimers (CPDs) and pyrimidine 6-4 pyrimidone photoproducts (6-4 PPs) (Costa et al., 2003). In addition, numerous bulky chemical adducts are eliminated by this process. Within the divergent spectrum of NER lesions, significant distortion of the DNA helix appears to be a common denominator. Defects in NER underlie the extreme photosensitivity and predisposition to skin cancer observed with the prototype repair syndrome xeroderma pigmentosum (XP). Seven XP complementation groups have been identified, representing distinct repair genes *XPA–G* (de Laat et al., 1999). In the last decade, all key NER factors have been cloned and the core of the 'cut-and-paste' reaction has been reconstituted in vitro from purified components. The excised oligomer is removed from the duplex, and the resulting gap is filled and ligated (Figure 12).

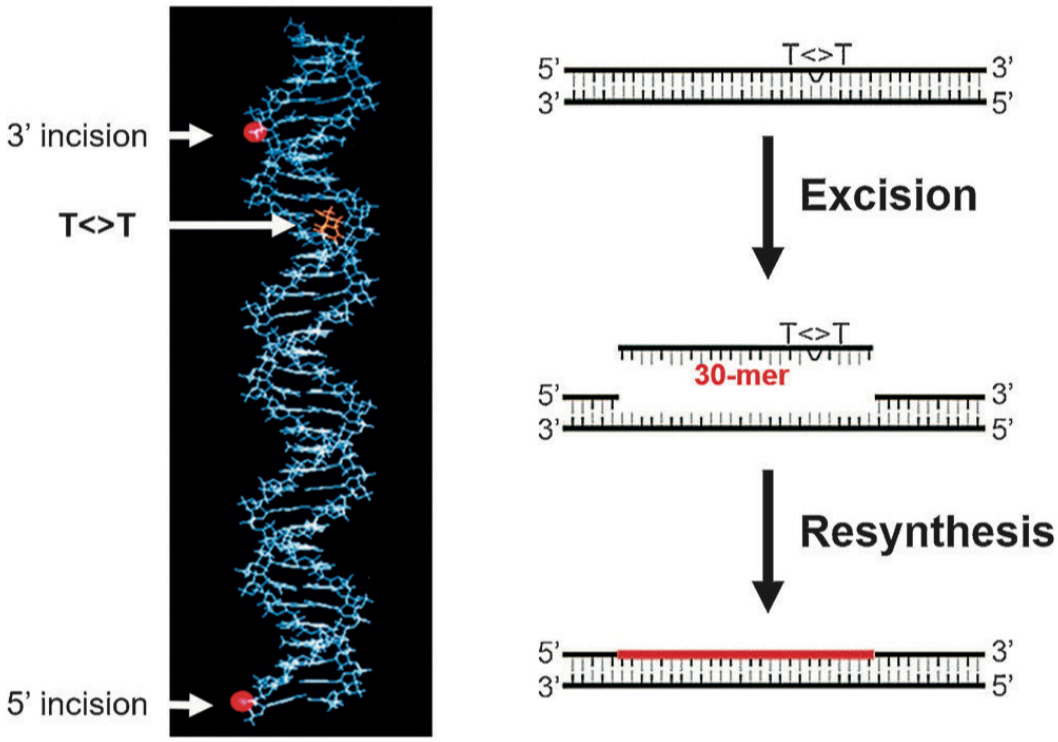

Figure 12. Excision by dual incisions in humans. In humans, thymine dimers (T<>T) and other bulky base adducts are removed by dual incisions located 20± 5 phosphodiester bonds 5' and 6 ±3 phosphodiester bonds 3' to the damage, which releases an oligonucleotide 24–32 nt in length (referred to as nominal 30-mers). Left: dual incision sites on a 3D representation of DNA. Right: schematic of human dual incisions followed by repair synthesis and ligation. Image from Sancar, 2016.

In human, 16 proteins in six repair factors (Mu et al., 1996; 1995) are necessary for making the dual incision. The human excision repair system incises the damaged strand 20–22 nucleotides 5’ and five nucleotides 3’ to the damage to release an excised oligomer of 27–30 nt in length (Huang et al., 1992). Finally, the damage is recognize in by RPA, XPA and XPC followed by recruitment of TFIIH, which contains the XPB and XPD helices that unwind the helix and recruit the XPG and XPF nuclease to make the 3’ and 5’ incision. The dual incision event is followed by the release of the 30- nucleotide excised oligomer, gap filling and ligation by DNA polymerase and ligase to produce a 30-nucleotide repair patch (Reardon et al., 1997). The Figure 13 summarizes the current model for the mechanism of human nucleotide excision repair. Most recently this work led us to study other cellular responses to DNA damage including the DNA damage checkpoints (Lindsey-Boltz et al., 2014; 2001).

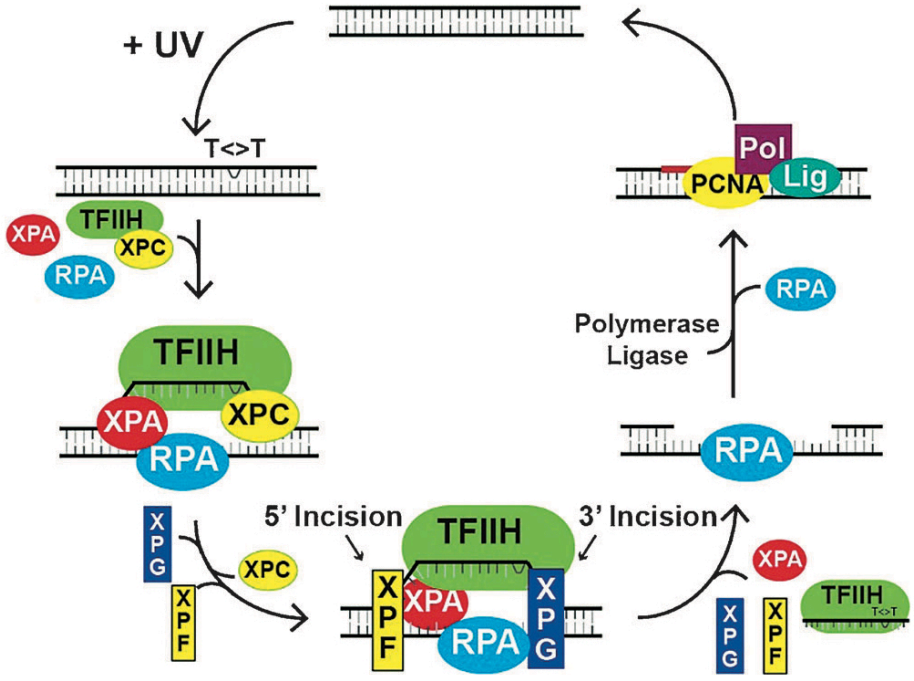

Figure 13. Reaction mechanism of the human excision nuclease system. The damage is recognized by cooperative interactions of RPA, XPA, and XPC followed by recruitment of TFIIH. The helicase activity of TFIIH provides the major specificity by kinetic proofreading and results in formation of a tight complex from which XPC is ejected. XPC plays an essential role in damage recognition leaving the complex to allow subsequent steps to proceed (molecular matchmaker). Concomitant with the dissociation of XPC, the XPG and XPF nucleases are recruited to make the 3’ and 5’ incisions in a concerted reaction. The excised “30-mer” is released in a tight complex with TFIIH. The excision gap is filled in by DNA polymerases and ligated to produce a 30 nt long repair patch. Image from Sancar, 2016.

The other DNA-repair mechanism is the Base Excision Repair (BER), these represents the predominant pathway repairing lesions arising from intracellular metabolites, oxygen radicals, ionizing radiation (IR) and, indirectly from UV radiation (*via* generation of ROS) (Robertson et al., 2009; Seeberg et al., 1995). These excision repair pathways remove DNA lesions by a sequential multistep process including damage recognition, opening of the DNA double helix at the damage site, and dual incisions on both sides of the lesion followed by resynthesis and ligation (Nouspikel, 2009; Costa et al., 2003). The lesion recognition, in the case of NER, is performed by a complex incorporating XPC and DDB2 (p48) while the DNA glycosylase Neil1, initiates this first step in BER. BER facilitates the repair of damaged DNA via two general pathways, short-patch and long-patch. The short-patch BER pathway leads to a repair tract of a single nucleotide. Alternatively, the long-patch BER path-way produces a repair tract of at least two nucleotides. The BER pathway is initiated by one of many DNA glycosylases, which recognize and catalyze the removal of damaged bases. The completion of the BER pathway is accomplished by the coordinated action of at least three additional enzymes. These downstream enzymes carry out strand incision, gap-filling and ligation (Robertson et al., 2009).

3.1.3 - Molecular adaptation of subterranean species

The rate of mutation is subjected to evolutionary change. This is showed by the different patterns of mutation rates among taxa, selection acts primarily to reduce the standard mutation rate allowing higher rates in specific circumstances (Britten et al., 1986). The fidelity of DNA replication depends on elaborate enzymatic machinery and mutational inactivation of any component can greatly elevate the mutation rate. Rate of spontaneous mutation in the genome vary strikingly among different groups of organisms and per replication and measure target by many orders of magnitude depending on the mutational target size. A mutation rate included all kinds of mutations in a mutational target such as base pair substitutions, base additions and deletions often producing frame-shifting in exons. Generally the order of these mutation rates is clearly correlate with the evolutionary history of the species under consideration. Among the mutations that affect a characteristic gene different kinds of pressure may influence differently.

Many mutations are deleterious and neutral, producing no effect strong enough to permit selection against. Obviously, some protein evolution are the results of positive mutations. The impact of each mutations is distinctive in different DNA sequences (Drake et al., 1998). Positive selection fixing advantageous mutations, while purifying selection act against deleterious mutation. The measurement of mutation rates at molecular level based on specific loci is a powerful tool to understand the evolutionary changes. The molecular evolution have been identified through the substitution ratios of non-synonymous (d_N) and synonymous (d_S) in protein-coding DNA sequences. A non-synonymous substation is a nucleotide substitution that changes the encoded amino acid, while the synonymous substitution does not change the encoding. Thus the ratio $\omega=d_N/d_S$ measures the difference between the two rates and it is easily to understood from a statistic point of view. If an amino acid changes is neutral it is fixed at the same rate as a synonymous mutation ($\omega=1$). When the amino acid changes have a positive selection it is fixed at higher rate compared to synonymous mutation ($\omega>1$). Otherwise in the case of purifying selection it is fixed at lower rate than a synonymous mutation ($\omega<1$). This kind of estimation using provide an efficacy tool to investigate the types of natural selection act on the protein molecule (Yang and Bielawski, 2000). The method described involve the following steps: counting synonyms (*S*) and non-synonymous (*N*) sites in the two sequences, estimated the differences and correcting for multiple substitutions at the same site. *S* and *N* are definite as the sequence length multiplied by the proportions of synonymous and non-synonymous change before selection on the protein (Yang and Nielsen, 2000). Different approaches can produce different estimates, even when the sequences are highly similar. Because all estimation procedures partition the total number of sites and differences into synonyms and non-synonymous categories, underestimation of one means overestimation of the other, thus resulting in large errors in the ω ration. For example the approach of New and Gojobori (1986) assume an equal rate for transitions (T — C and A — G) and transversions (T,C — A,G), as well as a uniform codon usage. Another approach is the maximum likelihood (ML) based on explicit models of codon substitution. Parameters in the model such as sequence divergence, transition/transversion ratio and d_N/d_S ratio are estimate from the data by ML (Yang and Nielsen, 2000). The major aspect of the method is that the model is formulated at the level of instantaneous rates,

without the possibility of multiple changes. Then in one step it is possible estimate mutational parameters, correcting for multiple hits and weighting pathways of change between codons.

Photoreactivation is one of the first DNA repair pathways to evolve. This mechanism is catalyzed by photolyases in a light depended manner in order to direct repair lesions caused by UV irradiation (Eisen and Hanawalt, 1999). Despite their obvious beneficial effects of photoreactivation, several organisms such as placental mammals lost this capacity of photorepair. In a work of the last decade it has been performed an extensive phylogenomic analysis of the photolyase / cryptocrome family in order to asses which species lack each kind of photolyase gene. Through the estimation of the d_N/d_S substitution rates in several group of photolyase genes, it has been evaluated the power of purifying natural selection in shape evolution of some organisms (Lucas-Lled´o and Lynch et al., 2009). They propose that the loss of photolyase genes in eukaryotic species may be due to weak natural selection and may result in a deleterious increase of their genomic mutation rates. While, in contrast to this domain, the loss of photolyase genes in prokaryotes may not cause an increase in the mutation rate and be neutral in most cases. The loss of photolyase gens in eubacterial species that are not exposed to UV radiation may not results in an increase of their genomic mutation rate at all. Thus, this is an evidence that the composition of the DNA repair and replication machineries must affect the spontaneous mutation rate of a species.

Studies on the molecular evolution especially in regressive adaptation generally start from the identification of a regressive phenotypic trait. Connecting the trait to a specific environmental condition such as the completely absence of light and then test for relaxed selection on candidate genes may motived the role of particular pressure that shaped the evolution of particular organism. Obligate cave-dwelling fishes are a good examples of regressive evolution (Cavallari et al., 2011; Beale et al., 2013). Similar phenotypes often evolve repeatedly when independent lineages are exposed to similar ecological conditions but the likelihoods of convergent, parallel, and reverse evolution are thought to differ among traits and depends on their complexity and genetic basis (Losos, 2011; Schluter et al., 2004). In a work that studied the regressive evolution in the blind cavefish from North America (Amblyopsidae) it has been investigated whether the candidate gene rhodopsin showed evidence of relaxed selection. The authors demonstrated the

loss of function constraints caused parallel inactivation of this protein in different cave lineages, suggesting multiple indenting cave colonization events (Niemiller et al., 2013). A previous work of our colleagues (Calderoni et al., 2016), using our cavefish species model (*P. andruzzii*) and started from the results of comparative functional analysis of the circadian clock that proved mutation in melanopsin photoreceptor (Cavallari et al., 2011). It has been hypothesized that this protein is under neutral evolution most probably as a consequence of the loss of selective constraint on this photoreceptor in the dark environment. This conclusion could be obvious given that melanopsin is a pseudogene (Calderoni et al., 2016). To generalize this conclusion the authors tested for the presence of relaxed selective selection in the widely studied photoreceptors rhodopsin revealed this protein to be under purifying selection. This reinforce the conclusion that relaxed selection operates on light-responsive mechanisms in *P. andruzzii*.

A mutation individuated as deleterious or advantageous in a large population may be neutral in a small population. The connection between genome size variation and his evolution in eucaryotes remain poor evaluated. The effective size of populations is one of know parameter that underlying genome size evolution. In a recent work by Lefébure and collegues (2017) it has been shown this hypothesis using transcriptomes and low coverage genome of asellid isopods, which represent 11 pairs of surface and subterranean species influenced by independent habitat shifts from surface water to resource-poor groundwater. They motived that the habitat shift are associated with higher transcriptome-wide d_N/d_S. Through this estimation it was excluded the role of positive selection and pseudogenization. These transcriptome-wide d_N/d_S increases are the result of a reduction in selection efficacy imposed by the smaller effective population size of subterranean species. This reduction is paralleled by an important increase of 25% in genome size. They shown that the increases in genome size estimated in subterranean species are the consequence of increasing invasion rates by repeat elements, which are less efficiently removed by purifying selection (Lefébure et al., 2017).

3.1.4 - DNA repair in fish

In order to evaluate the direct effects of light in vertebrate cell biology, the light sensitivity of zebrafish, medaka and other teleosts provides a very good basis for investigation. The zebrafish contains nearly all the genes involved in DNA repair pathways in eukaryotes, including the photolyases and so represents an ideal model for gaining mechanistic insight into DNA repair systems (Pei and Strauss, 2013). In this model, light is able to induce the expression of genes that mediate stress responses and promote the DNA repair. Previous findings have revealed that following UV irradiation, exposure to a light/dark cycle enhances survival of zebrafish embryos (Tamai et al., 2004).

As explained in the first paragraph of this chapter, the UV radiation induces DNA damage by causing the formation of CPDs photoproducts which repairs by CPD photolyase and 6-4PPs photoproducts which repairs by 6-4 photolyase. Moreover it is know that DASH proteins have photolyase activity with high specificity for CPDs photoproducts. The powerful repair mechanisms of photoreactivation lead the light-dependent repair of the UV-induced photoproducts by exposure to blue light. Thus, today are know to exist three types of photorepair proteins: the CPD and 6-4PP photolyases and the cryptochrome-DASH (Sancar, 2016).

Small laboratory fish are suitable for the study of this light dependent mechanisms. A more recent work on medaka model and DNA repair established a mutant strain for these genes. In order to evaluate the lack of photoreactivation activity mediated by CPD, 6-4PP and DASH, cultured cell lines and its repair activity was examined *in vitro*. In wild-type cell the 80% of CPDs were removed by photoreactivation, whereas no CPD removal was delectable in the CPD mutant cells. A clear difference in repair of 6-4PPs was also observed between 6-4PP wild-type and mutant, respectively the 65% and the 25% of 6-4PPs removed. In addition, 6-4PPs were removed by the dark repair pathway more rapidly than CPDs, therefore the effect of the 6-4PP deficiency might have been too small. An explanation could be that genes related to dark repair pathways may have been induced (Ishikawa-Fujiwara et al., 2017).

It has been demonstrated that *Astyanax mexicanus* cavefish have a modified DNA repair pathway and core clock compared to surface populations of the same species. It is therefore highly likely that cavefish possess alterations in other closely

related aspects of light-regulated biology (Beale et al., 2013). They examined two DNA repair genes from populations of *A. mexicanus*: CPD photolyase involved in photoreactivation, and DDB2 part of the nucleotide excision repair pathway.

Similar to the induction of DNA repair proteins that have been shown in zebrafish to be transcriptionally activated by light (Weger et al., 2011; Gavriouchkina et al., 2010), in this cavefish *A. mexicanus* the DNA repair are also induced by light but with a lower magnitude, because were significantly raised basal expression in dark control samples. More recently, Frøland-Steindal and colleagues (2018) examined the core clock and DNA repair gene expression in early development of *Astyanax*. They have shown the differences in the development of the light response of surface and cave population. Similar to that reported in zebrafish, the surface population become light responsive during the first 5-8 h of development, while in contrast the cave population is slower to develop. Examining CPD photolyase expression of the cave population, it is clear that the expression closely resembles to the PER2a profile. Surprising in the case of CPD there are big amount of maternally deposited transcript in both strains, which remains raised in cave population for six hours longer.

This intriguing result shine the question: why and how is upregulated the DNA repair genes in the cave system? Is it a peculiar adaptive response to this extreme habitat to increase DNA repair activity? There are some direct influence of the environmental conditions of the cave on the expression of these genes beyond the absence of light?

3.2 - Aim

How the environment shapes the function and evolution of DNA repair systems is poorly understood. We study whether the Somalian blind cavefish, *Phreatichthys andruzzii* during evolution for millions of years in continuous darkness conserved the photoreactivation process in DNA repair system. We investigated whether the visible light and UV induced the expression of *P. andruzzii* DNA repair genes. In addition, we demonstrated whether is due to the loss of function mutations in pivotal DNA repair genes. Despite our results point to *P. andruzzii* being the only species described, apart from placental mammals, which lacks the highly evolutionary conserved photoreactivation function. We discussed that these species may have experienced a similar selective pressure during evolution linked with exposure to prolonged periods of darkness. Indeed, the ancestors of placental mammals are predicted to have adapted to an exclusively nocturnal or subterranean lifestyle as a strategy to avoid predation from dinosaurs.

3.3 - Material and Methods

3.3.1 - Embryo survival

In the embryo survival experiment, zebrafish and cavefish embryos were exposed to different doses of UV-C (Figure S1) at 3 days post fertilization (dpf), when both species showed a similar developmental stage (see paragraph S1.1) (Stemmer et al., 2015). We maintained zebrafish and cavefish embryos at 27°C in complete darkness and exposed embryos to different doses of UV-C (53 - 106 - 212 - 424 J/m^2) to induce DNA damage. Subsequently, they were transferred to white light/dark cycles (LD) or returned to constant darkness (DD) and over the following 5 days (Figure 15A, Figure S1). The proportion of survival animals was measured daily by lack of heat beat. Embryos were managed in a classical raising condition, daily feeding and regular water changing until 10 dpt and eventually malformation were recorded. Embryos were raised in 24-well plates and for each group condition we used *n*=48 embryos.

3.3.2 - Immunofluorescence assay in cell lines

Cells derived from zebrafish (PAC-2) and cavefish (EPA) embryos (see paragraph S1.2) were maintained at 27 °C in constant darkness for 48 hours (DD) and then exposed to UV-C (40 J/m^2) to induce DNA damage. Subsequently, one group was exposed to blue light (BL) (Figure S1) and another returned to constant darkness (DD) and the sampling were carried out each hour until 5 hours. Another parallel group was treated in the same way but with the only difference of pre-exposition of 48 hours in constant lightness (LL) (Figure 16A, S1). The establishment of medaka fish mutant lines for CPD, 6-4PP and DASH photolyases were editing by Ishikawa-Fujiwara and collegues (2017). Using the CRISPR/Cas9 technique they generate mutants in wild type medaka. The six embryonic cell lines were maintained as reported in paragraph S1.2. The mutant cell lines were maintained at 27 °C in constant darkness for 48 hours (DD) and then exposed to hydrogen peroxide (H_2O_2, Sigma-Aldrich) at 100 - 200 - 400 µM to induce DNA damage. After 1 hour of treatment at different doses, the medium with H_2O_2 was replace with the fresh one in order to ensure 1 hour of recovery before sampling (Figure 22A).

Immunofluorescence assays were performed as previously described (Pagano et al., 2016; Muslimovic et al., 2012). Specifically, cells were seeded on glass slides (1×10^5 cells/well), fixed with 4% PFA at room temperature for 15 to 20 minutes and washed with PBST (1×PBS + 0.1% Tween). Cells were permeabilized by incubation with 0.2% Triton X-100 in PBS for 5 minutes. Pre-incubations were performed at room temperature for 1 hour in blocking solution (1×PBST + 1% BSA). Incubations with primary antibodies (γ-H2AX, Cell Signaling) were performed overnight at 4°C also in blocking solution. The goat anti-rabbit, Alexa Fluor 546 (Invitrogen) was used as the secondary fluorescent antibody in a 1 hour incubation step at room temperature. DAPI staining was used for visualization of nuclei. The samples were mounting on glass slides and acquired using a Confocal Microscope SPE (Leica) with a 20x objective. The experiment were biologically reproduced independently 3 times, for each time point it were evaluated at least *n*=300 cells. The quantification of the H2AX nuclear signals from image acquired was calculated using Fiji Software.

3.3.3 - Gene expression of blue-light inducible genes in embryo

Here we tested whether the CPD, 6-4PP and DASH photolyases and XPC involved in the excision repair are light inducible in zebrafish and cavefish. A groups of embryo were raised in DD at 27°C and then at 5 dpf when both species showed a complete developmental stage (Stemmer et al., 2015) were exposed for 10 hours to blue light (Figure S1). A control group were raised in DD without any light exposure. Embryos were sampled at 4 - 6 - 8 - 10 hours after blue light on to check for the inducibility of the genes by qPCR. The control group in DD were sampled at the same time points (Figure 19A). We used at least *n*=4 samples for each time point, *n*=15 embryos per sample.

After corresponding treatments, RNA extraction was conducted using Trizol Reagent (Invitrogen) added to each Eppendorf tubes and homogenized. Samples were stored at -80 °C for at least 24 hours before processing. After thawing and the addition of 100 µl of Chloroform, the samples were mixed and incubated at room temperature for 5 minutes, and centrifuged at 12000 rpm for 15 minutes at 4°C; the aqueous phases were transferred to a new tube and 500 µl of Isopropanol were added, RNA was then recovered by centrifugation at 12000 rpm for 10

minutes at 4°C; the RNA pellet was washed with 80% ethanol and dissolved in RNase free water and the concentration was determined using a NanoDrop Spectrophotometer (Themo Scientific). The quality of the extracted RNA samples was determined by electrophoresis on a 0.8% agarose gel to visualize the integrity of the ribosomal 28S, 18S and 5S RNA bands.

For each sample, 1 µg of total RNA was diluted in RNase free water to reach the total volume of 7 µl, 1 µl of RQ1 DNase 10×buffer, 1 µl of DNase (1 U/µl) and 1 µl of RNase inhibitor (40 U/µl) (Promega) were added to the reaction system, which was then incubated for 30 minutes at 37°C; after addition of 1 µl of DNase Stop solution (Promega), the sample was incubated for 10 minutes at 65 °C; after addition of 1 µl of random primers (Table S9) (200 ng/µl, Sigma Aldrich) and incubation for 5 minutes at 70 °C, the cDNA synthesis mix composed of 3 µl H_2O, 4 µl M-MLV RT 5×buffer (Thermo Scientific), 2 µl of 10 mM dNTPs (Sigma Aldrich) and 1 µl of M-MLV reverse transcriptase (200 U/µl, Thermo Scientific) was added and incubated for 10 minutes at 25 °C, followed by 60 minutes at 42 °C and 10 minutes at 70 °C; finally, the cDNA sample was diluted 10 times with RNase free water and stored at -20 °C. A control PCR with a standard reaction system and programme was performed to evaluate the quality of the cDNA synthesis. Specifically, we amplified *β-actin* using 4 µl of the diluted cDNA in 20 µl reaction with 0.25 µl GoldTaq polymerase (Promega), 0.5 µl of 10 mM dNTP (Sigma Aldrich) and 1 µl of zebrafish/cavefish *β-actin* forward and reverse primers (10 µM).

Real-time PCR was performed by using the StepOne Plus Real-Time qPCR machine with the standard reaction system and program according to the manufacturer's instructions. Relative mRNA expression levels were calculated by the $2^{-\Delta\Delta CT}$ method and normalized by zebrafish / cavefish *β-actin* mRNA expression.

3.3.4 - Estimation of synonymous and non-synonymous substitution rates

In order to analyze the selective constrains on photolyases (CPD, 6-4PP and DASH) estimating the non-synonymous/synonymous substitution ($\omega=d_N/d_S$) under different evolutionary models in a likelihood framework. For each genes under examination we analyzing the coding sequence of n=20 (CPD), n=17 (6-4PP) and n=37 (DASH) teleost fish including *P. andruzzii*. Orthologous sequences were collected using BLAST protein, we consider protein sequences with query cover

>90% and excluded isoforms and low quality proteins using default algorithm parameters of the database: non-redundant protein sequences in Teleostei organisms. As reported in the previous Chapter the photolyases of *P. andruzzii* are truncated, then the orthologous sequences of zebrafish were used as a query. The respective coding sequences were obtained from GeneBank and Ensembl, the aligned were performed using the MAFFT software using default parameters (Katoh and Standley, 2013). Taking advantage of the detailed knowledge of the photoreactivation mechanism, we ask whether the inefficiency of photolyases are correlated with the strength of purifying natural selection. We used the phylogenetic analysis by maximum likelihood to estimate ω between d_N and d_S changes across a fish phylogeny. The analyses were performed using the CODEML module of PAML package (Yang, 2007). We considered the Model 0 "M0" properly for the single ω estimated for the entire phylogeny, the Model 1 "M1" respectively for two ω estimated (ω cavefish and ω rest of the phylogenetic tree) which are used as a proxy for the strength of purifying selection. The likelihoods of different models were then compared by means of likelihood ratio tests (LRTs) of hypotheses through comparison of nested statistical models (M0 *vs* M1). The LRTs were calculated as twice the difference in the log-likelihoods values between models. The significance of the LRTs statistic were determined by using the χ^2 distribution where the degrees of freedom equal the difference between the number of estimated parameters in the two nested models.

3.3.5 - Statistical analysis

The statistical analyses were performed using the GraphPad software (Prism Hallogram, USA), the results were expressed as Mean ± SD. Regarding the embryos survival it were used two tests specifically for the survival rate: the Gehan-Breslow-Wilcoxon method that gives more weight to deaths at early time points, and the Log-rank (Mantel-Cox) method that gives equal weight to all time points. Concerning the gene expression and the immunofluorescence assays it were used 2-way ANOVA followed by Sidak's post-test.

3.4 - Results

3.4.1 - Loss of light-driven DNA repair in Somalian cavefish

Previous reports have revealed that following UV irradiation, exposure to a light/dark cycle enhances survival of zebrafish embryos (Tamai et al., 2004). Exposure of zebrafish cells to LD cycles also results in entrainment of the endogenous circadian clock (Vallone et al., 2004). Is this property conserved in a fish species that has evolved for millions of years in the complete absence of sunlight? Embryo mortality was then assessed daily under either light/dark cycle (LD) or constant darkness (DD) condition. Under the two lighting conditions, we observed a dose dependent increase in mortality in the embryos of both species (Figure 15B-E, Figure S6). However, all doses of UV tested resulted in a significantly lower cavefish embryo survival compared with the zebrafish (Table S2), indicating a clear species-specific difference in sensitivity to UV damage. Importantly, consistent with previous findings (Tamai et al., 2004), zebrafish embryos exposed to a LD cycle exhibited a significantly lower mortality compared to the DD group following UV exposure (Figure 15A-E, Figure S6 and Table S2). In contrast to the zebrafish embryos, the presence of a LD cycle did not significantly enhance cavefish survival (Figure 15A-E, Figure S6 and Table S2). In the case of *P. andruzzii* embryos, exposure to the lowest dose of UV (53 J/m^2) (Figure 15B) already led to approximately 50% mortality after 5 days, while 424 J/m^2 (Figure 15E) resulted in 100% mortality. Importantly, at all doses of UV tested, the presence of a LD cycle did not significantly enhance survival of the UV exposed *P. andruzzii* embryos compared with DD controls. These results point to a loss of the photoprotecting effect of LD cycles in *P. andruzzii*.

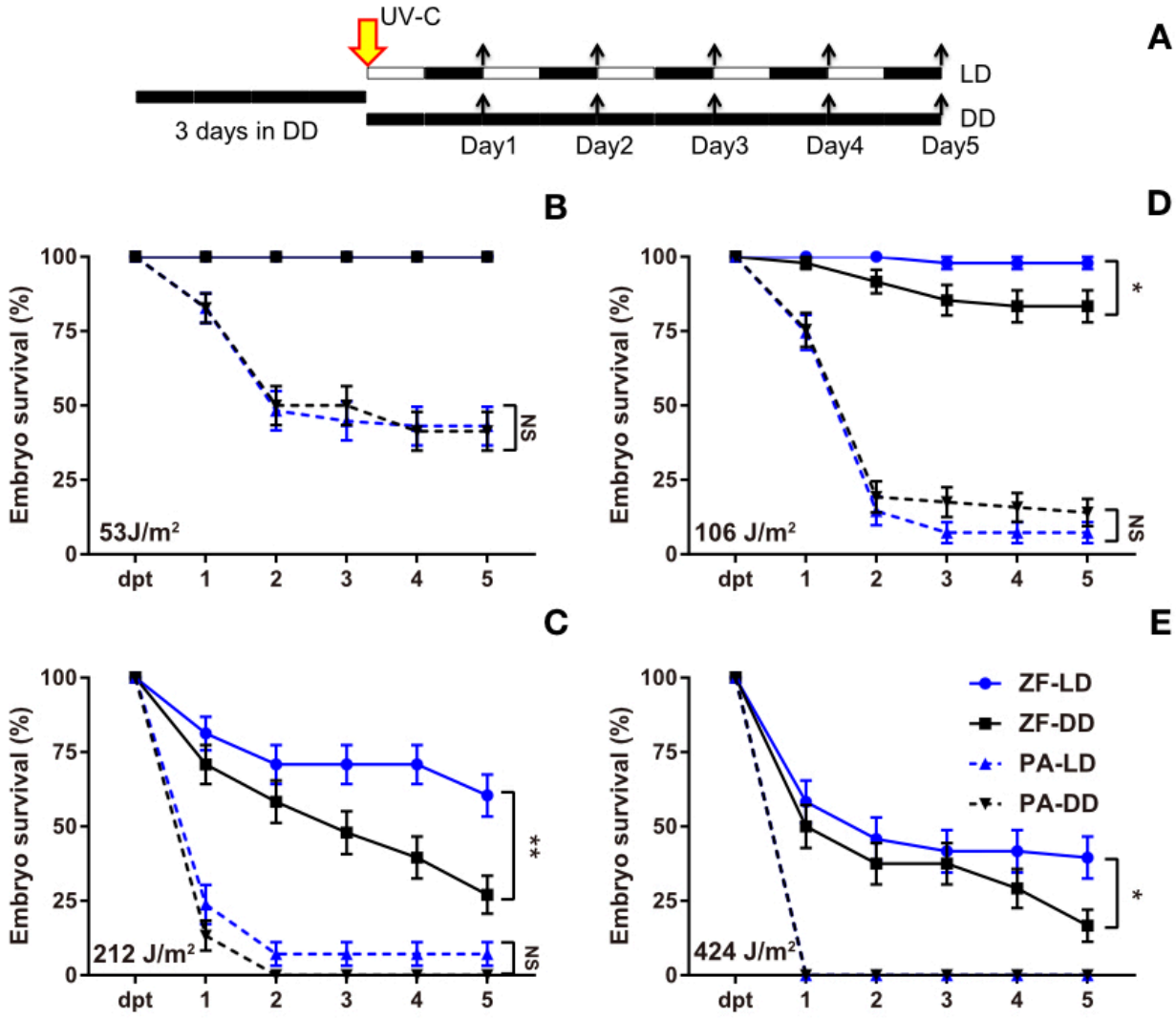

Figure 14. Light fails to protect cavefish *P. andruzzii* from UV-induced mortality. (**A**) Schematic representation of the experimental design. (**B**-**E**) Percentage survival of zebrafish (ZF) and cavefish *P. andruzzii* (PA) embryos irradiated with (**B**) 53 J/m^2, (**C**) 106 J/m^2, (**D**) 212 J/m^2 and (**E**) 424 J/m^2 UV-C radiation and subsequently transferred to light cycles (LD, blue traces) or constant darkness (DD, black traces) conditions. Survival rates of embryos (%) were then calculated daily during the following 5 days and plotted against time (dpt, days post-treatment). For each panel, Log-rank (Mantel Cox) and Gehan-Breslow-Wilcoxon tests, results are reported in Table S2. Significant differences are indicated by asterisks (*** p<0.001, **p<0.01, *p<0.05).

3.4.2 - Light fails to protect cavefish from UV-treatment

A characteristic marker for DNA damage events is the elevated phosphorylation of Histone H2AX at Ser 139 (γ-H2AX). This represents one of the first cellular responses to double-strand breaks (DSBs) (Sharma et al., 2012; Rogakou et al., 1998), where phosphorylated H2AX rapidly associates with other proteins to form a complex at the site of DSBs (Nakamura et al., 2010) and is also closely correlated with the level of cell death (Banáth et al., 2003).

Might the loss of the protective effect of light in this cavefish species reflect abnormalities in DNA repair systems? To address this question, we assessed the process of DNA repair in cavefish and zebrafish cells under pre-treatment of 48h in constant darkness (DD) or lightness (LL) conditions following UV exposure. Given the documented importance of blue light wavelengths in DNA repair system function (Weber, 2005), we chose to specifically test the effects of blue light exposure. We first performed a test for the formation of DNA strand breaks, which are generated during NER- and BER-based DNA repair, by measuring Histone H2AX phosphorylation at Ser 139 (γ-H2AX).

Consistent with our previous results, UV-induced H2AX phosphorylation, as measured by an immunofluorescence assay, was significantly reduced upon exposure to blue light in zebrafish but not in cavefish cells (Figure 16B-E, Figure 17 and Table S2). Specifically, zebrafish cells pre-treated in 48h LL of white light compared to the 48h DD, extremely reduced the levels of fragmented DNA following UV treatment in both recovery condition DD and BL (Figure 16B-C, Figure 17 and Table S2). In contrast, cavefish cells pre-treated with 48h LL of white light compared to the 48h DD, increased the levels of fragmented DNA following UV treatment in both recovery condition DD and BL (Figure 16D-E, Figure 17 and Table S2). Together, these results are consistent to explain that during evolution in the absence of sunlight, *P. andruzzii* has lost the capacity to harness light for enhancing the repair of DNA damage observed in zebrafish.

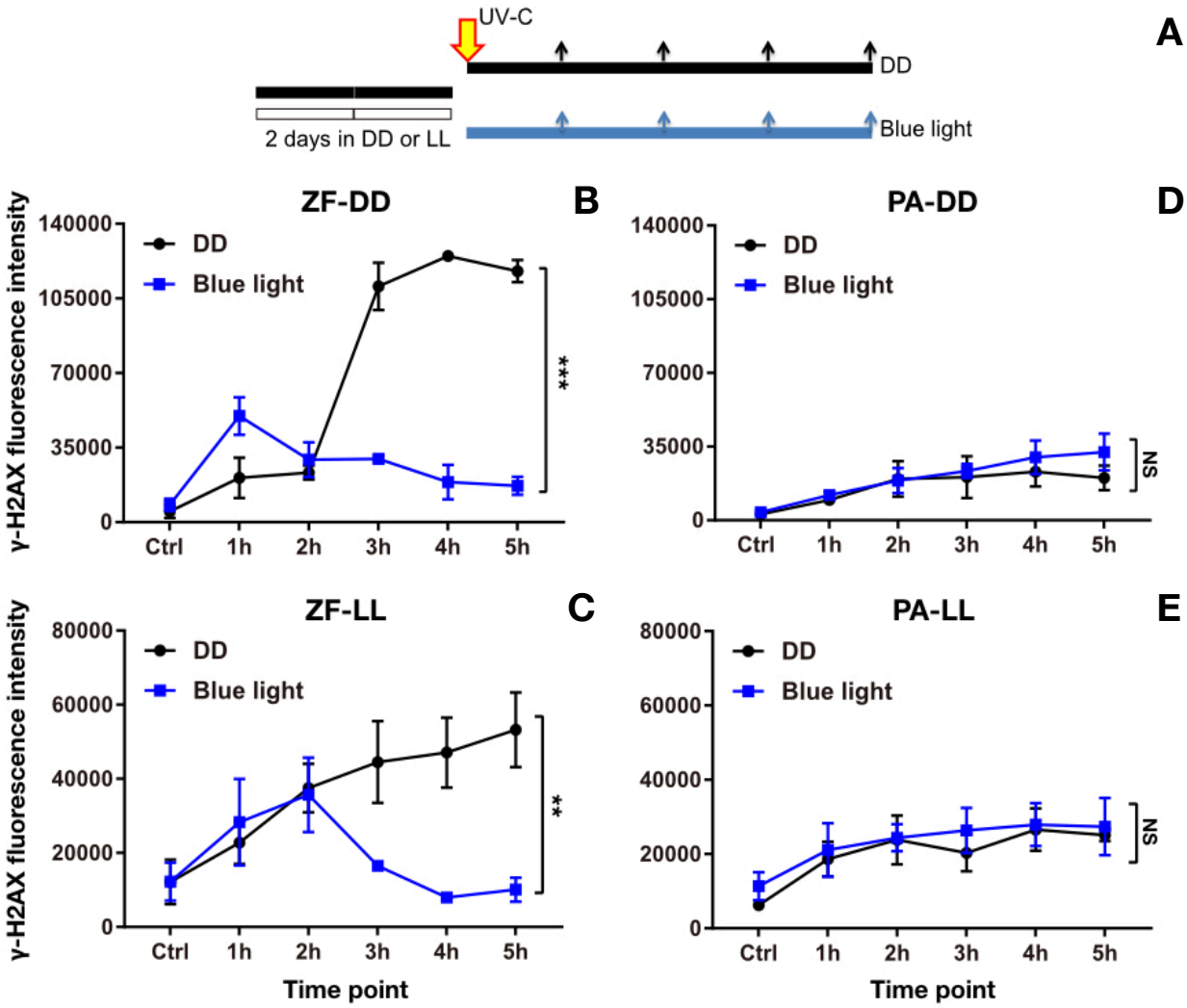

Figure 16. Effect of blue light on DNA repair. (**A**) Experimental design. Immunofluorescence analysis of γ-H2AX in (**B**-**C**) zebrafish (ZF) and (**D**-**E**) cavefish *P.andruzzii* (PA) cells treated as described in panel **A**. On the y-axes is indicated fluorescence intensity (n=3) ± SD, while time after treatment is indicated on the x-axes. Representative images of stained cells are also presented below in Figure 17. For each panel, Two-way ANOVA followed by Sidak's multiple comparisons test results are reported in Table S2. Each experiment was performed a minimum of three times. Significant thresholds are indicated by asterisks (*** $p<0.001$, ** $p<0.01$, * $p<0.05$).

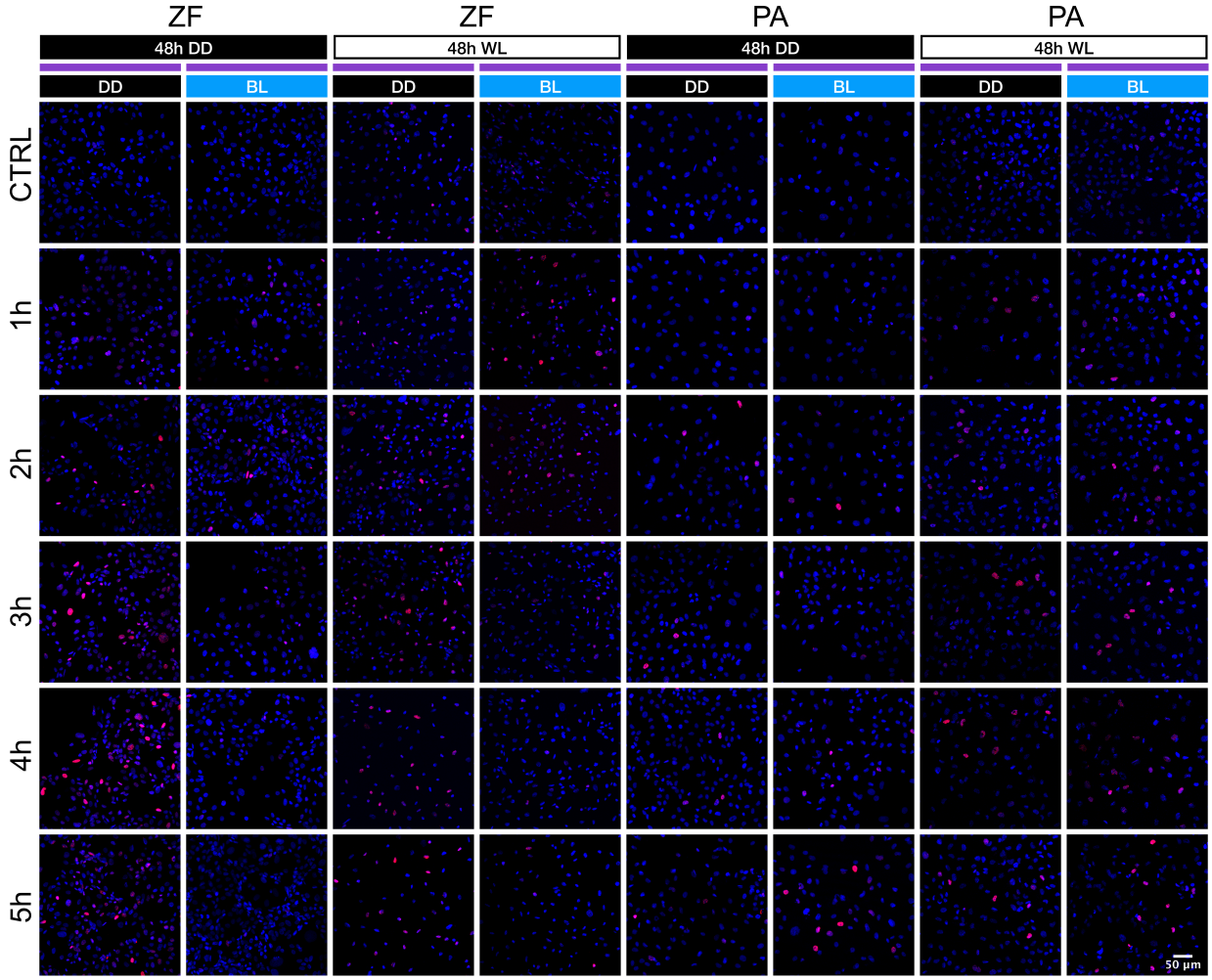

Figure 17. Representative images from the immunofluorescence assays of γ-H2AX levels upon exposure of zebrafish and cavefish *P. andruzzii* cells to a short UV-C pulse (40 J/m²). Merged images of nuclear staining (DAPI, Blue) and γ-H2AX staining (Red) are presented.

3.4.3 - Loss of function mutations in cavefish photolyase genes

It has been documented that light enhances DNA repair, both via photoreactivation and by inducing the transcription of many DNA repair genes. We wished to explore the contribution of these two functions to the observed loss of photoprotection in the blind cavefish. Photolyase catalysed light-dependent repair represents the principle mechanism underlying photoreactivation. Therefore, to tackle this question, in collaboration with Haiyu Zhao from the Foulkes group in Karlsruhe (KIT), Germany, we performed the following analyses. We searched the coding sequences of all three photolyase genes in the cavefish for evidence of loss of function mutations. Based on RNA-seq analysis and RT-PCR, we revealed that the coding sequences of two of the three cavefish *P. andruzzii* photolyases, pa 6-4 photolyase and pa DASH photolyase are disrupted by premature termination codons (PTCs) located within the vicinity of their FAD binding domains (Figure 18A). Specifically, in the case of pa 6-4 photolyase, cDNAs were characterized which encoded a full-length form (pa 6-4phr), sharing high homology over its entire length with the zebrafish (zf 6-4phr) ortholog, as well as two additional C-terminally truncated proteins (pa 6-4phr-MT1 and pa 6-4phr-MT2). In these mutants, PTCs are generated by base substitutions within the FAD binding domain (pa 6-4phr-MT1) or upstream within the photolyase domain (pa 6-4phr-MT2). In the case of DASH photolyase, only cDNAs encoding C-terminally truncated proteins lacking a major portion of the FAD binding domain were identified. In these two mutant forms, PTCs are incorporated either by inclusion of an unspliced intron (pa DASH-MT1) or an aberrantly spliced exon sequence (pa DASH-MT2). pa DASH-MT2 also carries an inframe deletion of the C-terminal portion of the photolyase domain as a result of alternative splicing. Interestingly, in contrast to the situation observed for these two cavefish photolyase genes, we only encountered cDNAs encoding a single form of *P. andruzzii* CPD photolyase (pa CPDphr) bearing high homology over its entire length with zf CPDphr and with all predicted functional domains intact (Figure 18A and Table S5).

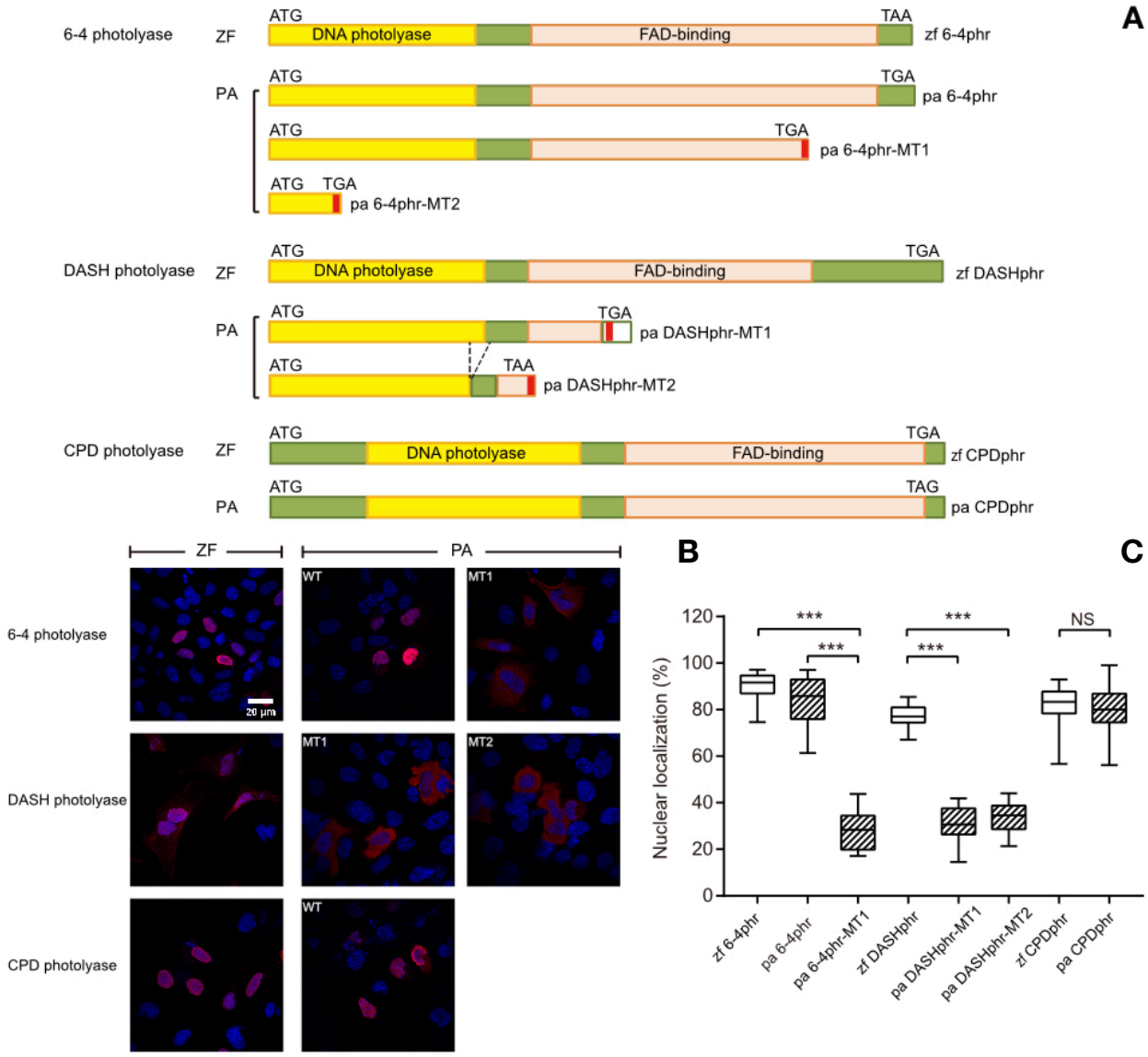

Figure 18. Cavefish photolyase characterization. (**A**) Predicted photolyase proteins from zebrafish (ZF) and *P.andruzzii* (CF). The conserved N-terminal photolyase domain (yellow) and C-terminal FAD binding domain (pink) are indicated. Premature stop codons are indicated in red. Dotted lines indicated the extent of the deletion of the DNA photolyase domain in pa DASHphr-MT2 relative to pa DASHphr-MT1. (**B**) Immunofluorescence images of myc-tagged *P. andruzzii* and zebrafish photolyase proteins (red signal) expressed in PAC-2 cells. Nuclei are stained with DAPI (blue signal). (**C**) Quantitative analysis of the data in panel B presented as box plots. The percentage of nuclear localization (n=30) for each construct is indicated on the y-axis. Boxes illustrate median as central line and 25th and 75th percentiles as outer lines. The percentage of nuclear localization for each construct is indicated on the y-axis. Boxes illustrate mean as central line and 25th and 75th percentiles as outer lines. Statistical differences of $p<0.05$, $p<0.01$, $p<0.001$ are represented by *, ** or ***, respectively. See Table S6 for detailed statistical analysis.

It has been previously shown that the integrity of the C-terminus of the closely related cryptochrome proteins is critical for their nuclear localization, predicting the presence of Nuclear Localization Signals (NLSs) within this region (Liu et al., 2015; Hirayama et al., 2003). Therefore, we tested the subcellular localization of Myc-tagged versions of the zebrafish and cavefish photolyase proteins, expressed in zebrafish PAC-2 (ZF) and *P. andruzzii* EPA (PA) cells. By immunofluorescent staining assay, we revealed that while the zebrafish zf 6-4phr, zf DASHphr and zf CPDphr, as well as the *P. andruzzii* pa 6-4phr and pa CPDphr forms are mainly nuclear proteins, all the truncated mutant forms of the cavefish photolyases are predominantly cytoplasmic (Figure 18B-C, Table S6). A bioinformatics analysis using the NLStradamus algorithm (www.moseslab.csb.utoronto.ca/NLStradamus) to search for candidate NLS sequences, revealed two C-terminal sequences (KKNILRMKAAYAKRSPEDKTINKGEKRKASPSIKEMFQKKAKR) and GPSSSKGRKGSSYTARQHKDR) in the zf 6-4phr and zf DASHphr proteins. These sequences are enriched in positively charged amino acids and thereby are predicted to serve as NLS sequences (Nguyen et al., 2009). Indeed, both sequences are deleted in the truncated pa 6-4phr and pa DASHphr proteins but are still retained in pa CPDphr. Since nuclear localization is a prerequisite for performing DNA repair, it is reasonable to predict that the cavefish 6-4PP and DASH photolyase truncated forms which are restricted to the cytoplasm are unable to contribute directly to photoreactivation function. Thus, the mutant cavefish photolyases which lack a significant portion of their light harvesting FAD binding domains, are also restricted to the cytoplasmic compartment and so are unlikely to contribute directly to nuclear photoreactivation function. Interestingly, *P. andruzzii* pa CPDphr, like its zebrafish ortholog, contains a predicted NLS sequence (PDSAGGKQPKLTGGKGRESGWLLKEVTKLRKAA) at the N-terminus of the protein and is localized predominantly in the nucleus (Figures 18B-C and Table S6).

3.4.4 - Loss of light-inducible DNA repair gene expression in cavefish

Many genes implicated in DNA repair, including the photolyase genes, have been shown in zebrafish to be transcriptionally activated by visible light. Without this light-dependent induction, animals appear to have reduced tolerance of environmental stress and increased mortality (Tamai et al., 2004). We reasoned that the loss of light enhanced DNA repair in *P. andruzzii*, during evolution under extreme aphotic conditions, might have also involved abnormalities in light inducible expression of DNA repair genes.

Real-time qPCR analysis of DNA repair gene expression in zebrafish embryos upon exposure to blue light reveals a strong induction of all photolyases and XPC gene. Particularly, it were revealed a significative up-regulation of photolyase genes after 4h and 6h of blue light exposure with a subsequently strong down-regulation at 8h and again increasing at 10h compared to constant darkness group. This results may suggest a correlation between biological clock and DNA repair system (Figure 19B-I and Table S7). Real-time qPCR analysis of DNA repair gene expression in cavefish embryos upon exposure to blue light reveals a low significative induction of CPD photolyase gene at 4h and 10h of blue light exposure, while 6-4PP and DASH photolyases do not shown any light induction compare to constant darkness group. Interesting we found a significative strong induction of XPC at 8h and 10h of blue light exposure. Taken together, these results on CPD and XPC may indicate an advance features in cavefish that inhabit harsh environment (Figure 19B-I and Table S7). In the case of CPD, although the amplitude of blue light induced expression was comparable to that in zebrafish. Thus, our results point to an impairment of the DNA repair gene expression response to blue light in *P. andruzzii*.

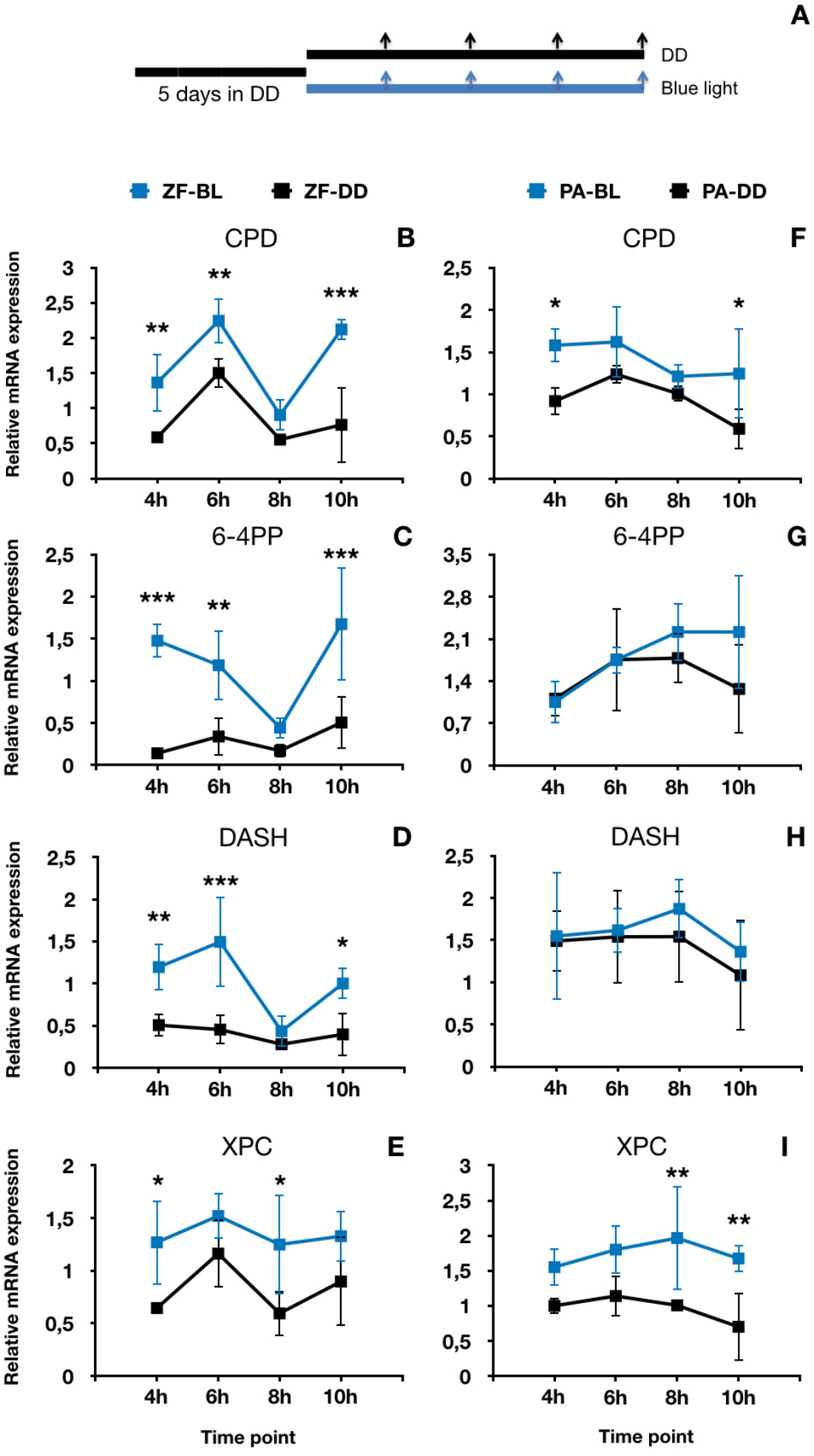
A
DD
Blue light
5 days in DD
ZF-BL
ZF-DD
PA-BL
PA-DD
CPD
B
F
6-4PP
C
G
DASH
D
H
XPC
E
I
Relative mRNA expression
4h
6h
8h
10h
Time point

Figure 19. Blue-light induced mRNA expression of DNA repair genes in zebrafish and cavefish embryos. (**A**) Schematic representation of the experimental design. qRT-PCR analysis of DNA repair gene mRNA expression in (**B**-**E**) zebrafish (ZF) and (**F**-**I**) cavefish (PA) during 10 hours of blue light exposure. In each panel, relative mRNA expression levels are plotted on the y-axes as means ± SD (n=4) and time point (hours) are plotted on the x-axes. For each panel, Two way ANOVA followed by Sidak's multiple comparisons test results are reported in Table S7. Each experiment was performed a minimum four times. Significant differences are indicated by asterisks (*** p<0.001, ** p<0.01, * p<0.05).

3.4.5 - Loss of D-box-regulated transcription in *P. andruzzii*

What is the origin of the loss of visible and UV light-induced expression of the DNA repair genes in cavefish? In collaboration with Haiyu Zhao from the Foulkes group, we cloned 4029 bp and 900 bp promoter regions of the zebrafish *6-4* and *CPD photolyase* genes, respectively into a luciferase reporter vector. Transfection of both reporter constructs into zebrafish PAC-2 cells followed by exposure to alternating periods of light and darkness, revealed a light-driven induction of bioluminescence. On the contrary, no response to light was observed after transfection of the same two constructs into *P. andruzzii* cells (Figures 20A-B). To pinpoint specifically which promoter region underlies the light responsiveness of the zf *6-4phr* promoter, we prepared a series of overlapping promoter deletion and subdeletion constructs (Figure 20C) which were transiently transfected into zebrafish PAC-2 cells and then tested for light-induced bioluminescence (Figure 20D-E). We identified a promoter region (termed SURE for SUnlight REsponsive region) that is sufficient to confer light-induced reporter gene expression. This region contains two palindromic D-boxes, two E-boxes and one AP1/CREB binding site (Figures 21A).

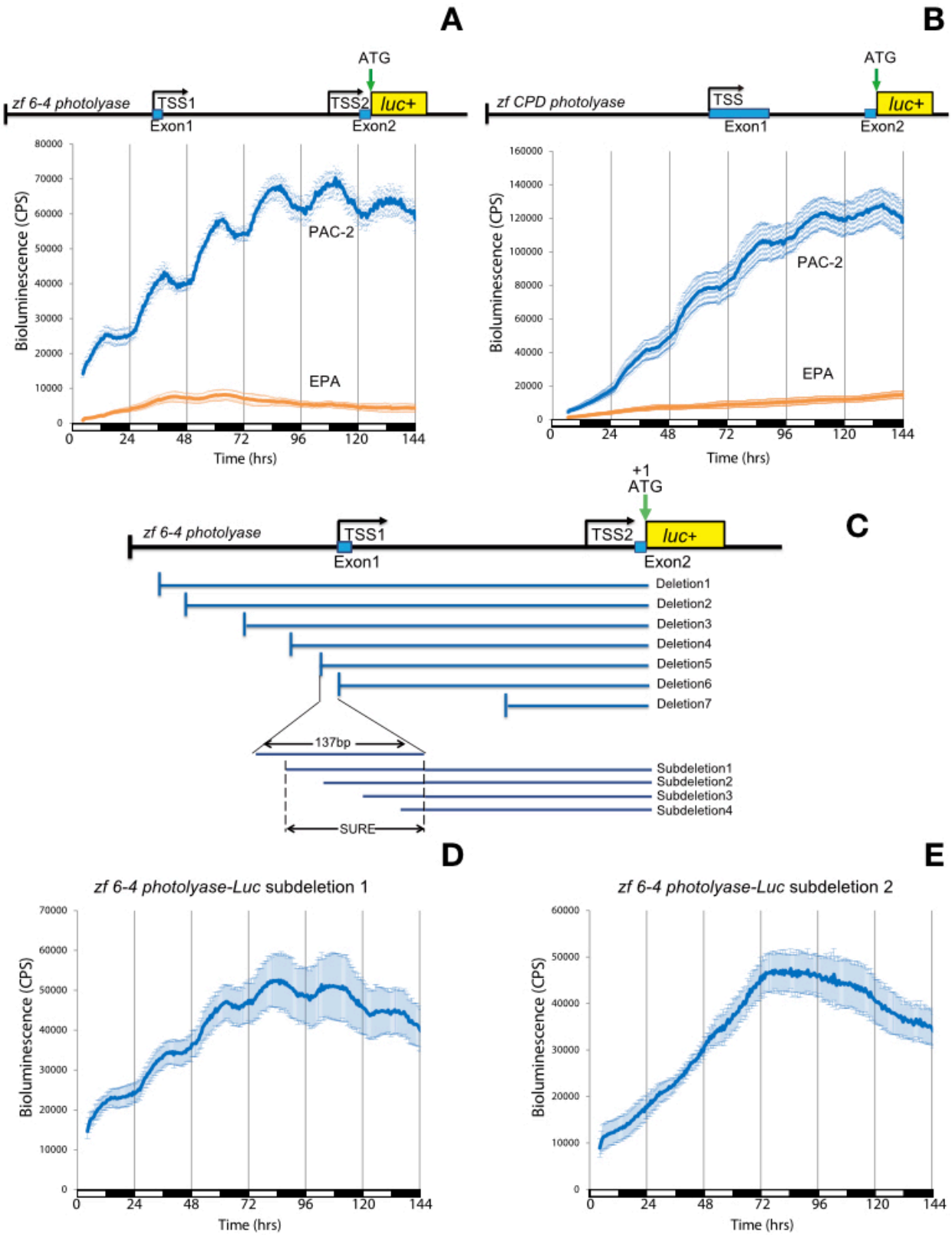

Figure 20. Identification of the light-responsive region of the zf 6-4phr promoter. (**A**-**B**) Upper sections, schematic representation of (**A**) the zf 6-4 photolyase-Luc and (**B**) zf CPD photolyase-Luc promoter reporter constructs. The positions of exons are indicated by blue rectangles. Transcription start sites are also indicated (TSS). The luciferase reporter gene (luc+) is shown by a yellow rectangle. Lower sections, Real-time bioluminescence assays in zebrafish PAC-2 (blue trace) or *P.*

andruzzii EPA cells (orange trace) transfected with the plasmids indicated above each panel. Bioluminescence is expressed as counts per second (cps) and is plotted against time (hours) on the x-axes. Black and white bars along the x-axes show periods of darkness and light, respectively. Each time-point represents the mean of n=8 ± SEM. (**C**) Schematic representation of the zf 6-4 photolyase-Luc together with the deletion 1 to 7 and subdeletion 1 to 4 constructs. The position of the 120bp zf 6-4phr SUnlight REsponsive region (SURE) is denoted by dotted lines and horizontal black arrows. (**D**-**E**) Comparable bioluminescence analysis of PAC-2 cells transfected with (**D**) zf 6-4 photolyase-Luc subdeletion 1 and (**E**) zf 6-4 photolyase-Luc subdeletion 2.

The SURE region was then subcloned upstream of a minimal promoter-luciferase reporter gene (*zf 6-4 photolyase SURE-Luc*) to assess its enhancer function and the contribution of each individual enhancer element within that region (Figure 20C). This reporter displayed robust light-inducible expression in zebrafish cells (Figure 20D-E) confirming its function as an enhancer region within the zebrafish *6-4phr* promoter. Systematic deletion of each individual element within the SURE region via site-directed mutagenesis (Figure 21A) revealed that the presence of the two palindromic D-box elements is crucial for the photic regulation of the zebrafish *6-4phr* gene (Figures 21B-C). Specifically, deletion of the two E-boxes together with the AP1/CREB binding site (Figure 21C) does not significantly affect the kinetics of the light-regulated SURE driven expression. On the contrary, deletion of both D-boxes (Figures 21B) results in a classical circadian clock-regulated pattern of expression, illustrated by the anticipation of induction in bioluminescence prior to the light onset. This clock-regulated behavior correlates with the presence of the E-box elements in the D-box-mutated SURE constructs. The importance of the D-box enhancer element in the light responsiveness of the zf *6-4phr* gene was confirmed by the loss of light-driven reporter expression upon mutation of both D-box elements in the context of the original full-length promoter reporter construct (*zf 6-4 photolyase (D-box mut)-Luc*).

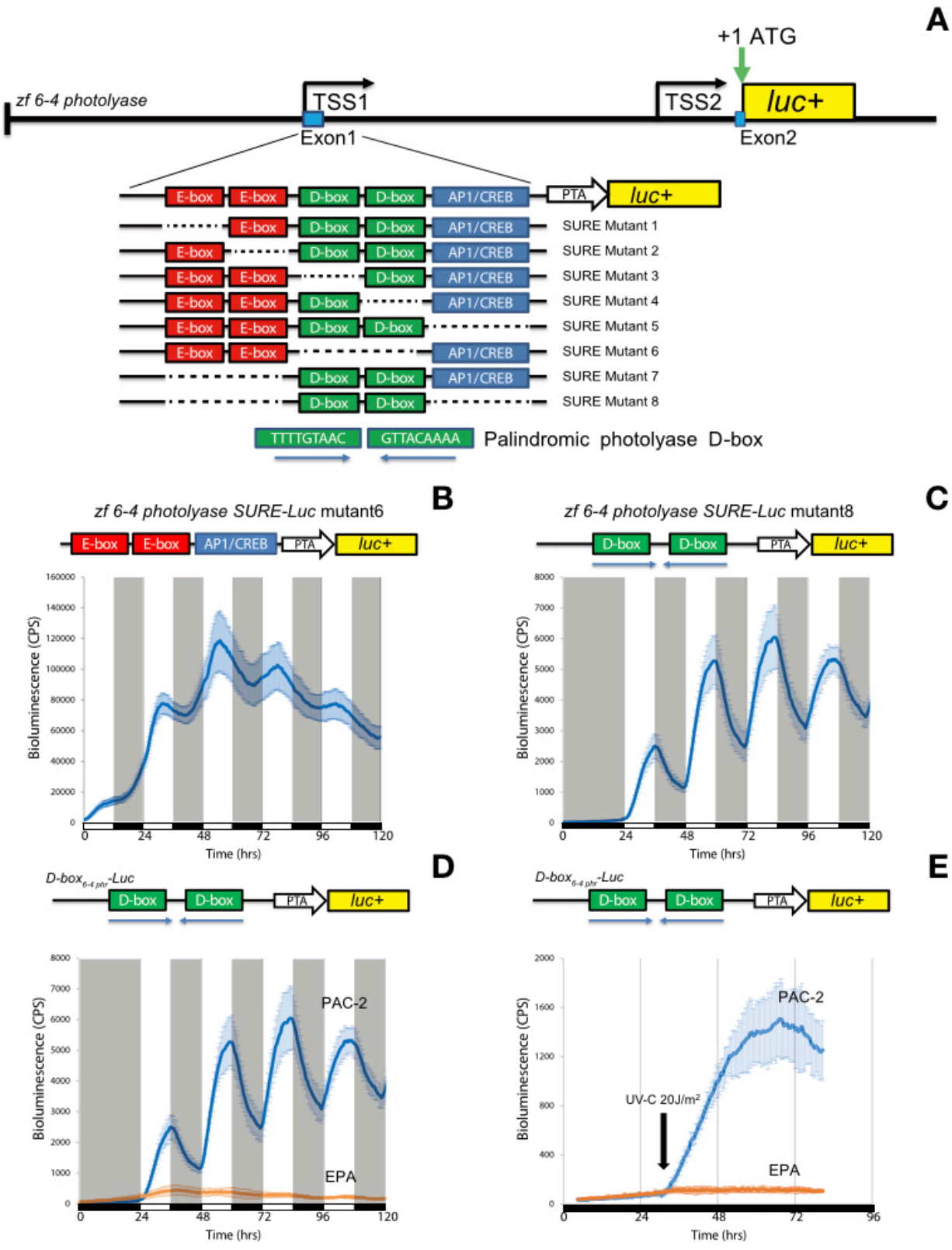

Figure 21. D-box enhancer elements are sufficient for light-induced transcription of the zf 6-4phr gene. (**A**) Schematic representation of SUnlight REsponsive region (SURE) and of the zf 6-4 photolyase SURE-Luc deletion constructs 1 to 8. The two E-boxes (red rectangles), the two palindromic D-boxes (green rectangles) and the AP1/CREB (blue rectangle) binding sites are indicated. (**B**-**C**) Representative real-time bioluminescence assays from PAC-2 cells transfected

with (**B**) zf 6-4 photolyase SURE-Luc mutant 6 (lacking D-box elements) and (**C**) zf 6-4 photolyase SURE-Luc mutant 8 (lacking E-boxes and AP1/CREB elements). (**D**-**E**), above, schematic representation of zf 6-4 photolyase SURE-Luc mutant 8 (renamed D-box$_{6\text{-}4phr}$-Luc); below, bioluminescence results from both PAC-2 (blue traces) and EPA (orange traces) cells transfected with the above reporter construct and exposed either (**D**) to alternating periods of light (white background) and dark (grey background) or (**E**) maintained in constant darkness (black bar below x-axis) following a short pulse of UV-C (black arrow, 20J/m^2). (**B**-**E**) Each time-point represents the mean of n=8 ± SEM. Bioluminescence is expressed as counts per second (cps) and is plotted against time (hours) on the x-axes.

Transfection of the *SURE* mutant 8 reporter construct retaining only the D-box enhancers of the SURE region (renamed as *D-box$_{6\text{-}4phr$-Luc*), into cavefish EPA cells showed no light responsiveness compared with the robust light-driven pattern observed in zebrafish cells (Figure 21D). Considering the complete conservation of D-box enhancer sequences between the zebrafish and *P. andruzzii 6-4phr* promoters, these results indicate that the absence of light-induced photolyase gene expression in cavefish is due to a loss-of-function of the light-regulated mechanisms which control transcription via the D-box enhancer. Expression of the *6-4phr* gene is induced in zebrafish by blue light and this inducibility is absent in *P. andruzzii* (Figure 19). Therefore, might the D-box enhancer represent a nuclear target for both types of light? To address this issue we studied the expression of the *D-box$_{6\text{-}4phr$-Luc* reporter in zebrafish PAC-2 and cavefish EPA cells upon exposure to a UV pulse. In zebrafish cells, our data showed that UV treatment induced bioluminescence with similar kinetics to those of the endogenous gene, revealing that the palindromic D-box elements in the SURE region are also sufficient for directing UV-induced expression (Figure 21E). Furthermore, in transfected EPA cells, UV-C treatment failed to activate expression of the *D-box$_{6\text{-}4phr$-Luc* reporter (Figure 21E). These results reveal that the D-box serves as the convergence point for the mechanisms mediating visible and UV light-induced gene expression and that this integrating function is absent in *P. andruzzii*.

3.4.6 - Molecular evolution of cavefish photolyases

As reported previously, photolyase genes and transcripts are not completely conserved in the Somalian cavefish *P. andruzzii*, they showed mutation that impair the photolyases protein function. Particularly in the case of 6-4PP and DASH photolyases, the genome show mutated alleles that do not code for full-functional proteins. This degeneration is mainly due to splicing errors. The 6-4PP and DASH photolyases are prematurely truncated, and thus lack nuclear localization and DNA-repair activity. Surprising, the CPD gene show one predicted isoforms and is full-length and therefore translocated into the nucleus. Here, due to a collaboration with Silvia Fuselli from the University of Ferrara, Italy, we reasoned whether is purifying selection still acting on the cavefish photolyase genes. Phylogenetic analysis by maximum likelihood to estimate whether ω changes across a fish phylogeny reveal that CPD, DASH and 6-4PP photolyases show ω values <1 as expected under selective constraint (Table S8). Despite the impaired photoreactivation activity showed in the previous result, our LRTs analyses on cavefish photolyases do not show signature of relaxation of natural selection compared to the rest of the lineages ($p>0.05$, Table S8). By means of interspecific analysis of molecular evolution and structure prediction we infer the evolutionary pattern of 6-4PP, DASH and CPD genes involved in the direct DNA photoprotection, testing the hypothesis that natural selection is no longer actively maintaining the photoreactivation pathway in this cave-dwelling organism.

3.4.7 - Dark function for CPD photolyase

Given the conserved sequence of CPD photolyase despite 6-4PP and DASH photolyases, we chose to test the effects of the three photolyases mutant in DNA repair system. Regressive evolution predicts that specific evolutionary events may trigger the loss of a specific function. Commonly, during the species evolution if some features are not used they are lost because are not required for sustaining life. Given the higher homology of CPD photolyase between cavefish and zebrafish/medaka, and our results regarding the loss of function of photolyase in cavefish. Here, we start to reasoned if the high conservation of CPD photolyase in cavefish is connected with a light-indipendent function. Inside the cave environment there are many stressors that elicit DNA damage, such as low concentration of oxygen in the water, slight acidic water, low availability of food, natural radioactive gas that induce double-strand breaks (DSBs) via generation of reactive oxygen species (ROS). Due to the fact that these factors may lead to an increase of intracellular oxidative stress, it is expected that cave organisms during the evolution have developed an efficient system that repair DNA. As reported previously the elevated phosphorylation of Histone H2AX at Ser 139 (γ-H2AX) represents one of the first cellular responses to DSBs. Might the loss of CPD photolyase reflect abnormalities in DNA repair systems? To address this question, we assessed the process of DNA repair in medaka photolyases mutant cell lines. Our immunofluorescence assay reveals a significative increase in H2AX phosphorylation of medaka CPD mutant cell line compared with wild type counterpart. While concerning the activity of 6-4PP and DASH we have not detected significative effect (Figure 22B-C and Table S4).

Here we found that the medaka CPD activity is light-independent and crucial to repair H_2O_2 DNA-damage. The fact that CPD photolyase is high conserved in both *P. andruzzii* and *A. mexicanus* (Beale et al., 2013) may reflect the evolution in extreme environment in order to gain high tolerance to stressor factors that dominate the subterranean habitat. Our result reveal that the cavefish *P. andruzzii* may have benefit to conserve CPD for enhancing the repair of DNA damage. This preliminary analysis is coherent to explain the adaptation in this harsh niche. However further biochemical and biomolecular assays will be applied in order to confirm this finding.

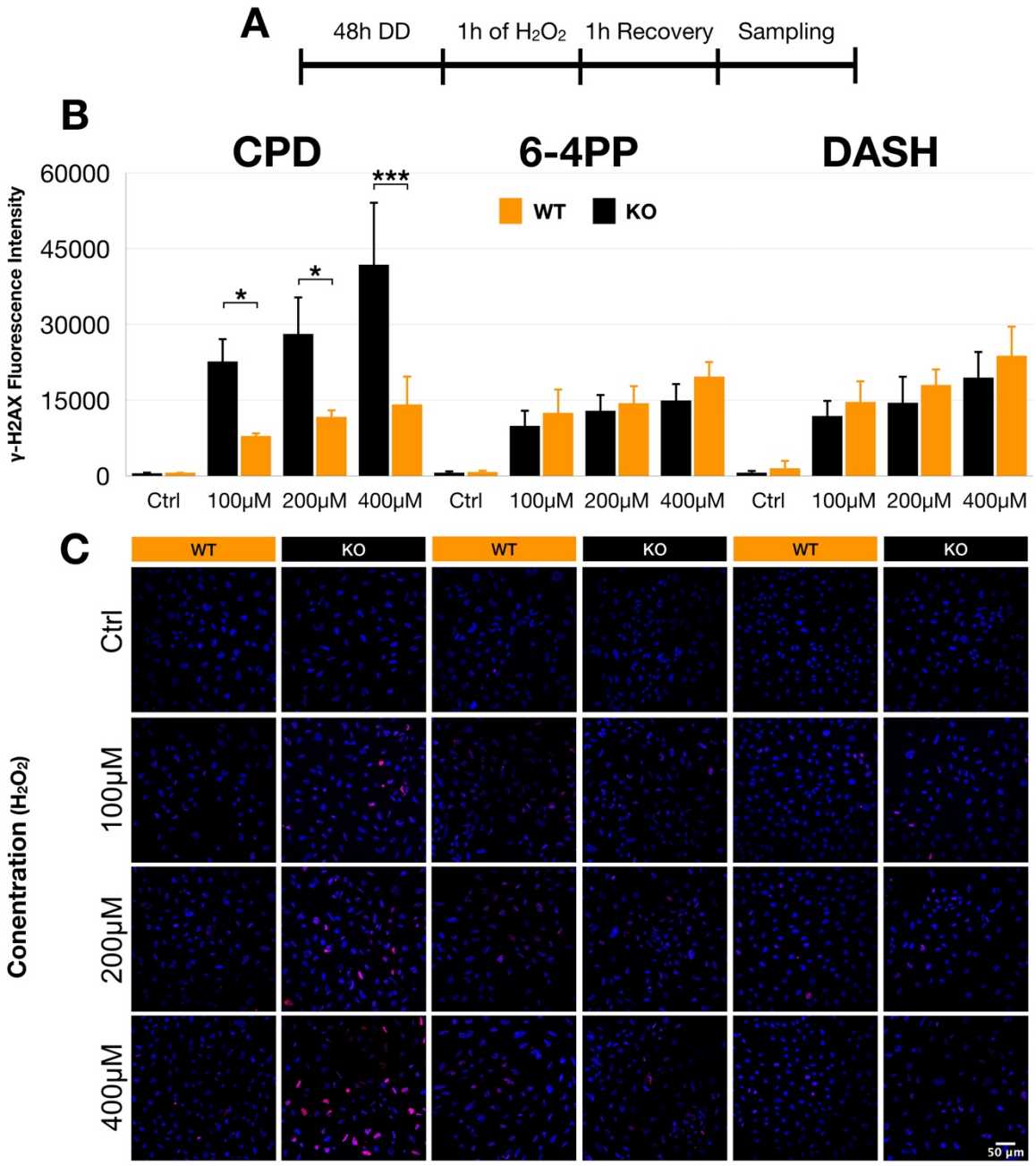

Figure 22. Effect of hydrogen peroxide on DNA repair. (**A**) Experimental design. (**B**) Immunofluorescence analysis of γ-H2AX in CPD, 6-4PP and DASH sibling cell lines treated as described in panel **A**. On the y-axes is indicated fluorescence intensity (n=3) ± SD, while different doses of treatment is indicated on the x-axes. (**C**) Representative images of stained cells are also presented as merged images of nuclear staining (DAPI, Blue) and γ-H2AX staining (Red). For each panel, Two-way ANOVA followed by Sidak's multiple comparisons test results are reported in Table S4. Each experiment was performed a minimum of three times. Significant thresholds are indicated by asterisks (*** $p<0.001$, ** $p<0.01$, * $p<0.05$).

3.5 - Discussion

Here, by comparing the blind cavefish *P. andruzzii* with the zebrafish, we have explored how sunlight shapes the evolution of DNA repair systems. We have revealed that both the integrity of photolyase genes, as well as transcriptional control mechanisms regulating the expression of DNA repair genes in response to sunlight, have been targeted by evolutionary mechanisms operating under extreme aphotic conditions. We have revealed the presence of point mutations in the 6-4PP and DASH photolyase genes which result in C-terminally truncated proteins. These truncated proteins lack a significant portion of the light harvesting FAD binding domain as well as showing a cytoplasmic localization and therefore are unable to perform DNA repair function. Only *P. andruzzii* CPD photolyase lacks such mutations and exhibits normal DNA repair function in our assay. However, we reveal a loss of light-induced photolyases expression associated with an impaired capacity of cavefish cells to perform light-driven repair of photoproducts. The conservation of CPD photolyase reflect the existence of a light-independent “dark” function that continues to be selected during evolution even in the complete absence of light. Although CPD photolyase requires light for photoreactivation catalysis, it has also been reported to bind to sites of DNA damage in the absence of light and subsequently, recruit DNA repair proteins to the damaged site (Thoma, 1999; Ozer et al., 1995). Recent studies have also shown that CPD photolyase, when ectopically expressed in mammalian cells, can interact directly with the CLOCK protein to reduce CLOCK/BMAL-dependent transactivation and thereby serve as a negative circadian clock element (Chaves et al, 2011). An alternative explanation for the apparent retention of CPD function in cavefish may simply be that an insufficient period of time has elapsed during evolution to observe mutations in this gene. In this scenario, all the photolyases perform an exclusively light dependent function and so even the CPD photolyase gene will eventually accumulate loss of function mutations or might even be lost as in placental mammals over a sufficient evolutionary time scale.

In *P. andruzzii*, we show that the lack of visible and UV light-induced DNA repair gene expression originates from a loss of light-responsive D-box enhancer function. Here and previous studies have also shown that the identified D-box enhancer element as being central for UV as well as visible light-induced

expression of clock and DNA repair genes in zebrafish (Mracek et al., 2012; Vatine et al., 2009). Zebrafish cells exposed to a short pulse of UV radiation, or sustained illumination with visible light, robustly up-regulate the transcription of a set of genes involved in photoreactivation, NER and BER. This observation may explain the previously reported, enhanced resistance to UV-induced DNA damage following exposure to UV or visible light (Tomicic et al., 2011; Dimova et al., 2008; Tamai et al., 2004). A similar interaction between a D-box and E-box enhancer has also been shown to be crucial for light-induced expression of the PER2 clock gene (Vatine et al., 2009). However, the D-box sequence in the PER2 promoter differs slightly from those identified here in the DNA repair gene promoters. Together, our results point to specific regulatory properties of these 5'- TTTTGTAAC -3' D-box elements being linked with DNA repair function. A family of six bZip/PAR factors as well as six E4BP4-related transcription factors can bind to D-box enhancer elements in homo and heterodimeric combinations (Ben-Moshe et al., 2010; Cowell, 2002). Differences in the consensus D-box sequence may therefore lead to differential binding of factors eliciting different transcriptional responses. Interestingly, previous evidence points to considerable plasticity in D-box function over the course of vertebrate evolution. While in fish the D-box serves as a light input pathway component for the entrainment of the circadian clock, in mammals the D-box is strictly clock regulated and acts within clock output pathways. Furthermore, in mammals the D-box is not light inducible and is targeted by a smaller family of three bZip/PAR and one E4BP4 factor. Taken together, our results point to the occurrence of major changes in D-box enhancer function during vertebrate evolution.

Starting from the results of comparative functional analysis of DNA repair that proved how specific loss of function mutation on photoreactivation caused the impairment of an important physiological and adaptive mechanism. We proved whether our finding on photolyases structure had a relationship between an event of pseudogenization and regressive phenotype began by relaxation of natural selection in the cave environment. *P. andruzzii* evolved in constant darkness, similarity to placental mammals, both habitat shift (i.e. cave colonization) and small population size may have affected the evolution of photolyases genes because weak purifying selection act in group with small effective population size (Lefébure et al., 2017). Recently, our colleagues have detected significant signature of

relaxation of natural selection at the mutated melanopsin photoreceptor gene responsible for the cavefish blind molecular clock (Calderoni et al., 2016). Transcription errors may represent the first step towards a complete regression of the photoreactivation pathway. An incomplete and ongoing non-functionalization of photolyases would explain why relaxation of natural selection is not yet detectable at these loci. Otherwise, this result may be masked possibly because statistical test may have less power if the change in selective regime is relatively recent evolution. The CODEML were originally designed to detect adaptive evolution by positive selection on a specific lineage (Yang, 1998), although it is very commonly used for cases of relaxed selection (Feng et al., 2014; Marková et al., 2014; Niemiller et al., 2013). While selective constraints on melanopsin photoreceptors were clearly relaxed, in the recent work conducted on PER2 that is involved in circadian clock, the coding region is conserved and included the C-terminal region which is absent in the prevalent mRNA isoform and thus could be regarded as a pseudogenic sequence. This observation would suggest that the truncated PER2 protein in cavefish play an additional role that are not exclusively linked with responsiveness to light and therefore may still be under selective pressure in the cave environment. Otherwise, one explanation is that change in the cavefish PER2 are at the first step of an ongoing relaxation of natural selection and are not yet detectable in the coding sequence (Ceinos et al., 2018). As observed for PER2 involved in the circadian clock, our results obtained using DNA repair genes may be well supported by the same reason. After the cave colonization, the change in selective constraint require a certain time to render genes non-functional and also require a certain time to enter in the population, this is strictly dependent on the population size and on the mutation rate. The integrity and functionality of certain genes may therefore persist for a long period before chance, unless selection favors degeneration. Subsequently, loss of function mutations might occur progressively. Here we can speculate that the loss of DNA repair expressions may represent a first step in this process followed by the appearance of ongoing mutations leading to complete pseudogenization of photolyases.

Do environmental factors, peculiar to subterranean aquatic environments, influence the evolution of DNA repair systems? Interestingly, in a previous study of the cavefish *A. mexicanus* (Beale et al., 2013), while no mutations were encountered in photolyase coding sequences, the levels of expression of both CPD photolyase

and DDB2 were significantly elevated in blind cave form compared with their surface dwelling, sighted relatives. It was speculated that this might reflect different types of DNA damage experienced in the cave environment and that elevated CPD photolyase and DDB2 expression levels may provide a selective advantage in repairing these types of damage. The conservation of CPD photolyase sequence and function in both *P. andruzzii* and *A. mexicanus,* as well as the upregulation of its expression would tend to further support the notion that this particular photolyase has a non-light dependent "dark" function that is selected for even in a perpetually dark environment. This may be exacerbated in certain caves in Mexico (e.g. *Cueva Chica and El Pachón*) which serve as roosting sites for large numbers of bats that bring organic materials (guano and dead bodies) into the water on a daily basis (Beale et al., 2013). Interestingly, an enhancement of DNA repair capacity has also been identified in the blind mole rat, *Spalax*, linked with its hypoxia tolerance (Domankevich et al., 2018). An additional feature of certain cave systems that might cause elevated DNA damage is the natural radioactive gas, radon ^{222}Rn (Jostes, 1996). High levels of this gas released from certain rocks and concentrated in caves constitute an important source of radioactivity and indeed have been linked with an increase in the rate of deletion of satellite DNA sequences at the whole genome level in *Dolichopoda* cave crickets (Allegrucci et al., 2015).

The difference in DNA repair phenotype between *P. andruzzii* and *A. mexicanus*, may be explained by two different factors. (*i*) Geological evidence suggests that *P. andruzzii* has been completely isolated from sunlit surface water for considerably longer than *A. mexicanus* (at least 3 million years and less than 1 million years, respectively) (Gross, 2012; Menck, 2002). Furthermore, as a result of the interconnected water systems in its cave habitat, many subpopulations of *A. mexicanus* are still able to contact surface dwelling forms. Therefore, *A. mexicanus* may be at a relatively early stage in terms of adapting its DNA repair systems to its environment. (*ii*) The cave systems inhabited by *A. mexicanus* also serve as roosting sites for bats which bring partially digested food material into the water, leading to a relatively low water quality. Instead, no bats roost beneath the Somalian desert and the water is actually constrained inside phreatic layers. Therefore, the habitats of these cavefish species differ considerably and they may face different genotoxic stressors. Photoreactivation is a highly conserved DNA repair mechanism encountered in most animal, plant and unicellular species with the curious and

unique exception of placental mammals (Menck, 2002). Based on the results of this study, we can now add the blind cavefish *P. andruzzii* to this small group of exceptions. Why placental mammals lost this DNA repair function remains a mystery. Taking into account palaeontological data, one theory that has been proposed is termed the “Nocturnal Bottleneck” (Maor et al., 2017; Gerkema et al., 2013). This predicts that the ancestors of modern mammals which lived during the dinosaurs’ domination of the Earth, avoided predation from dinosaurs by adopting an exclusively subterranean existence, only leaving their burrows at night to feed (Gerkema et al., 2013; Heesy et al., 2010). As a result of adapting to this ecological niche, many basic changes in light-dependent physiology occurred which may have included loss of photoreactivation DNA repair. Following the extinction of dinosaurs, mammals subsequently diversified and occupied new surface habitats, but still carrying relics of their dark-adapted past existence. Therefore, it is tempting to speculate that in the DNA repair systems of the blind cavefish *P. andruzzii*, we may be witnessing the first stages in a process that previously occurred in the ancestors of placental mammals during the Mesozoic era.

Supplementary Information

S1.1 - Fish rearing and ethical statements

Zebrafish (Tübingen strain) and cavefish *P. andruzzii* and *A. mexicanus* were crossed and raised according to standard methods. All husbandry and experimental procedures were performed in accordance with European Legislation for the Protection of Animals used for Scientific Purposes (Directive 2010/63/EU) and the Italian (D.lgs. 26/2014) animal protection standards. Research was approved by the University of Ferrara Institutional Animal Care and Use Committee and the Italian Ministry of Health (auth. num. 890/2016-PR). General license for fish maintenance and breeding: 47/2013-A for the University of Ferrara.

S1.2 – Zebrafish, medaka and cavefish *P. andruzzii* cell culture

The zebrafish PAC-2, the medaka (CPD, 6-4PP, DASH mutant and wild type) and the cavefish EPA embryonic cell lines, were cultured in L-15 (Leibovitz) medium (Gibco BRL) supplemented with 15% (zebrafish cells) or 20% (medaka and cavefish cells) fetal Calf Serum (Sigma Aldrich), 100 units/ml penicillin, 100 µg/ml streptomycin and 50 µg/ml gentamicin (Gibco BRL). Cells were maintained in the atmospheric CO_2, non-humidified cell culture incubator at 26°C.

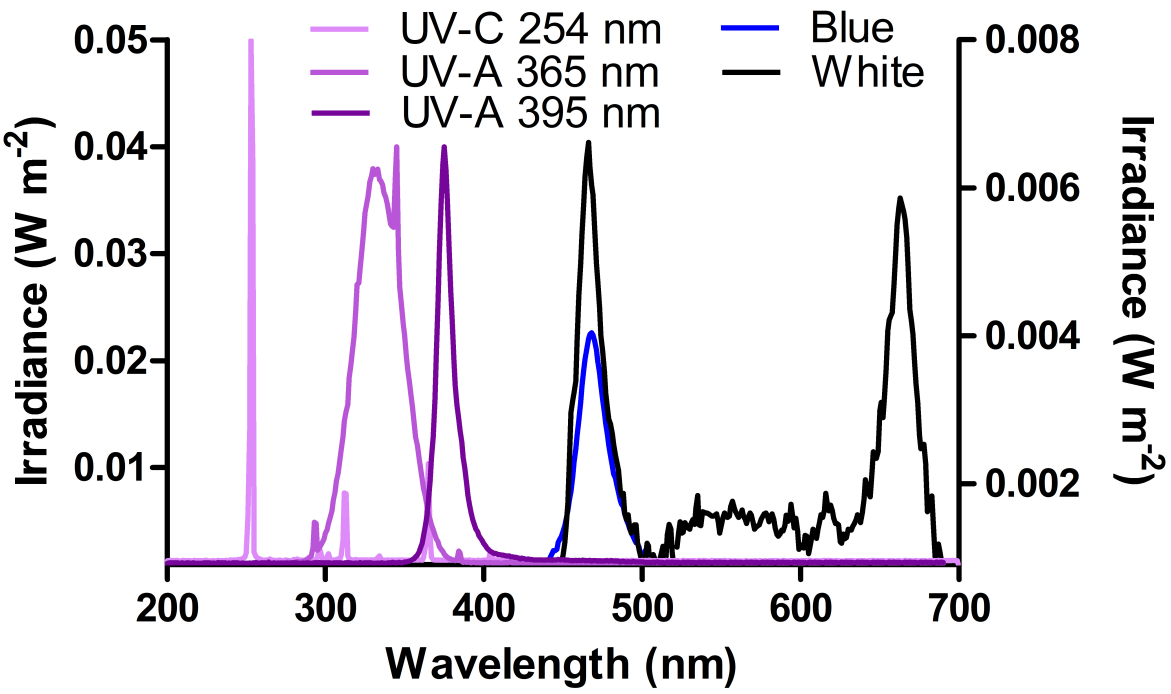

Figure S1. Irradiance curves for different monochromatic light sources. Light-emitting diode sources were used to produce white light (450 nm<λ<700 nm), monochromatic blue light (λ_{peak} =468 nm), UV-A (λ_{peak} = 365 and 395 nm) and UV-C (λ_{peak} = 254 nm) in the regions of the spectrum. Wavelengths are plotted on the x-axis, the irradiance for the white light is plotted on the right hand y-axis while the others are plotted on left hand y-axis. The total irradiance delivered from each light source were 0.80 W/m^2 for UV-C, 1.95 W/m^2 for UV-A 365 nm, 1.12 W/m^2 for UV-A 395 nm, 0.67 W/m^2 for blue and 0.54 W/m^2 for white light.

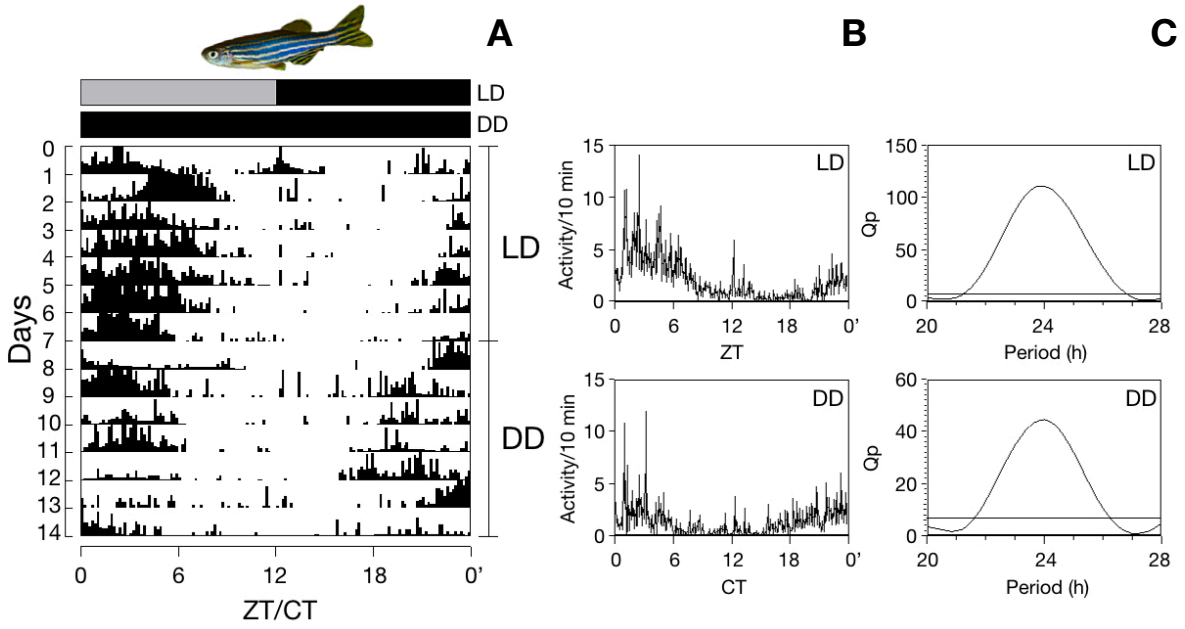

Figure S2. (**A**) Representative actograms under white light condition of zebrafish *D. rerio* maintained in LD cycle and subsequently shifted in DD. Records are single plotted on 24 h time scale. Mean and SD of the waveforms (**B**) and Lomb-Scargle periodogram (**C**) of the behavioral locomotor activity of the LD cycle and DD. The periodogram indicates the quantitative periods (Qp) of the rhythm plotted for each analyzed period within a range of 20–28 h; the lines represent the threshold of significance, set at p=0.05.

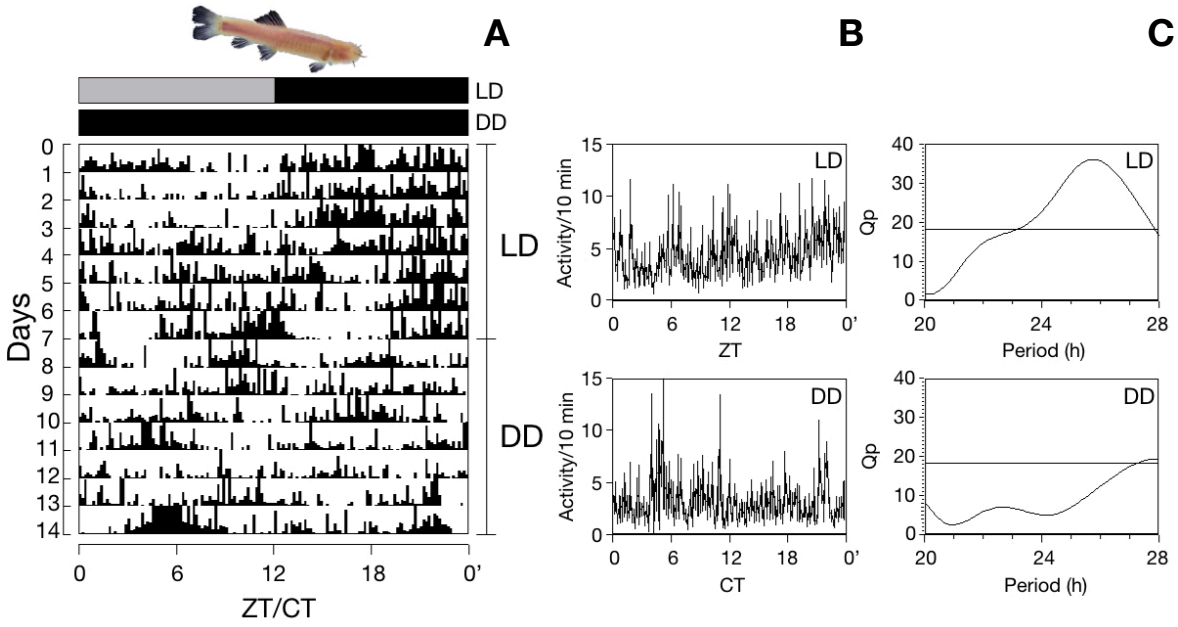

Figure S3. (**A**) Representative actograms under UV-A light condition of Somalian blind cavefish *P. andruzzii* maintained in LD cycle and subsequently shifted in DD. Records are single plotted on 24 h time scale. Mean and SD of the waveforms (**B**) and Lomb-Scargle periodogram (**C**) of the behavioral locomotor activity of the LD cycle and DD. The periodogram indicates the quantitative periods (Qp) of the rhythm plotted for each analyzed period within a range of 20–28 h; the lines represent the threshold of significance, set at p=0.05.

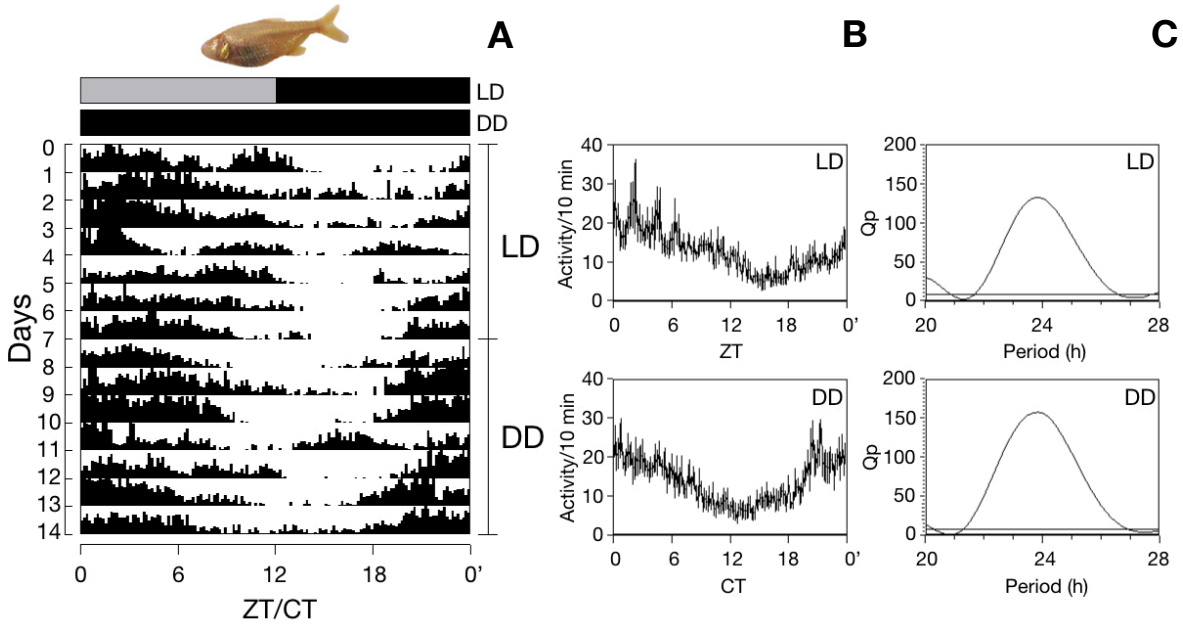

Figure S4. (**A**) Representative actograms under UV-A light condition of Mexican blind cavefish *A. mexicanus* maintained in LD cycle and subsequently shifted in DD. Records are single plotted on 24 h time scale. Mean and SD of the waveforms (**B**) and Lomb-Scargle periodogram (**C**) of the behavioral locomotor activity of the LD cycle and DD. The periodogram indicates the quantitative periods (Qp) of the rhythm plotted for each analyzed period within a range of 20–28 h; the lines represent the threshold of significance, set at p=0.05.

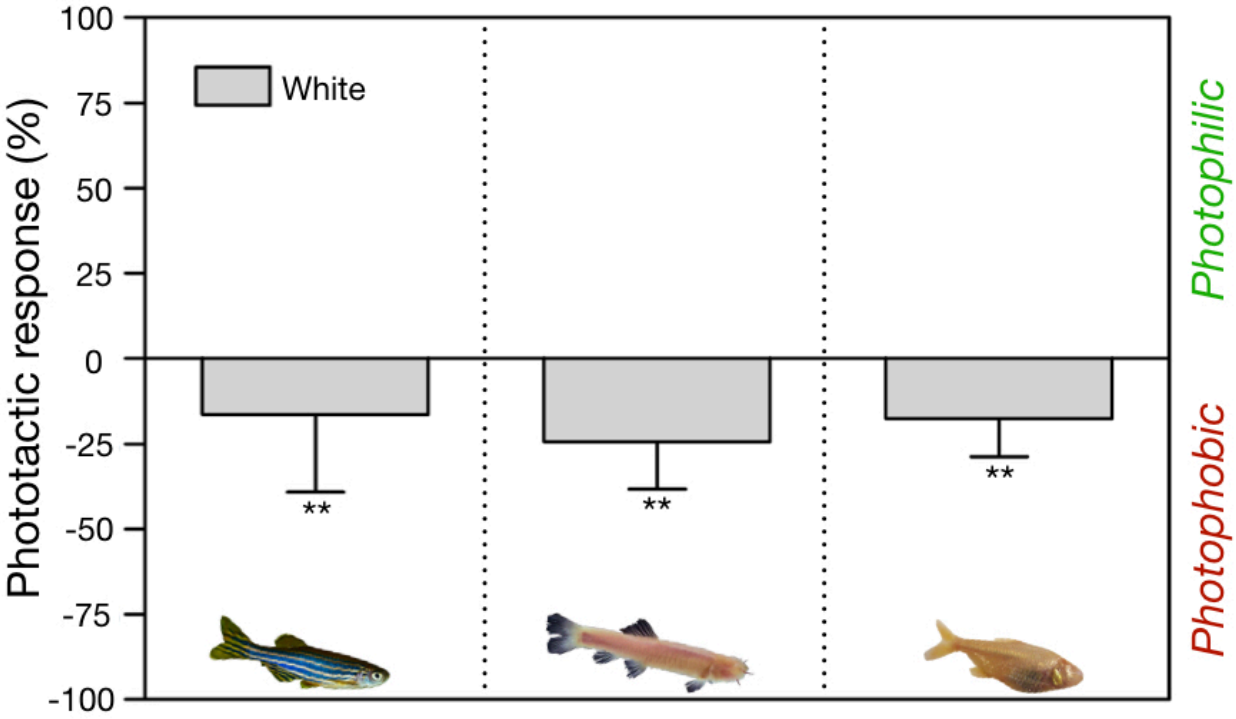

Figure S5. Behavioral phototactic response to white light (450 nm<λ<700 nm) in our model species. Mean and SD of the percentage of time spent in the dark zone of zebrafish (left panel), Somalian blind cavefish *P. andruzzii* (central panel) and Mexican blind cavefish *A. mexicanus* Pachón (right panel). Each fish was tested separately at the irradiances values are showed in the Figure S1. Student's t test for paired data are reported in Table S1. Significant differences are indicated by asterisks (*** $p<0.001$, ** $p<0.01$, * $p<0.05$).

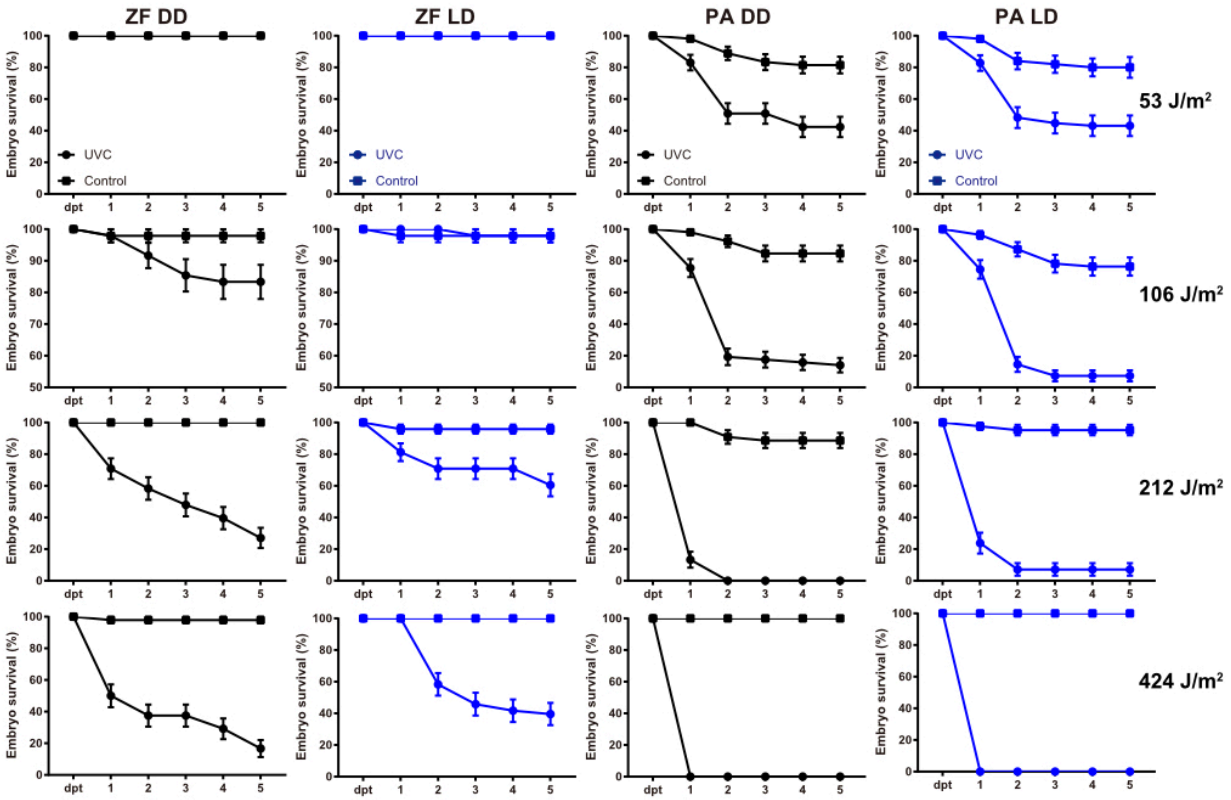

Figure S6. Survival of Zebrafish (ZF) and *P. andruzzii* (PA) embryos with and without exposure to different doses of UV-C irradiation and subsequent transfer to light cycles (LD) or constant darkness (DD). Survival rates (%) were calculated daily during the following 5 days and plotted against time (dpt, days post-treatment).

	Dark (Time %)		Light (Time %)		Δ (%)		*Paired t-test*	
D. rerio	Mean	SD±	Mean	SD±	Mean	SD±	*p*	*n*
White	75,31	21,09	58,92	11,85	-15,57	22,42	0,007 **	18
UV-A 365 nm	56,93	11,51	51,04	18,88	-6,30	14,07	0,099 ns	18
UV-A 395 nm	61,57	18,03	39,31	20,11	-22,26	26,44	0,004 **	16
P. andruzzii	Mean	SD±	Mean	SD±	Mean	SD±	*p*	*n*
White	67,90	8,39	43,58	13,26	-24,32	14,05	0,003 **	7
UV-A 365 nm	61,24	20,62	31,77	28,16	-29,47	30,52	0,013 *	10
UV-A 395 nm	57,68	23,85	22,71	24,63	-34,97	30,60	0,005 **	10
A. mexicanus	Mean	SD±	Mean	SD±	Mean	SD±	*p*	*n*
White	72,67	7,86	55,04	6,85	-17,63	11,19	0,003 **	8
UV-A 365 nm	59,80	15,31	56,41	16,28	-3,38	7,38	0,206 ns	9
UV-A 395 nm	50,32	10,53	51,37	24,15	1,05	16,52	0,853 ns	9

Table S1. Percentages of time spent in the recording area by our species studied at the different lighting conditions. Student's t-test for paired data (two tailed) are reported in Figure 9-S5. Significant thresholds are indicated by asterisks (*** $p<0.001$, ** $p<0.01$, * $p<0.05$).

	ZF - LD vs. DD		PA - LD vs. DD		
UV-C (J/m^2)	Log-rank (Mantel Cox)	Gehan-Breslow-Wilcoxon	Log-rank (Mantel Cox)	Gehan-Breslow-Wilcoxon	*n*
53	*p*				
	0,99 ns	0,99 ns	0,92 ns	0,98 ns	48
106	*p*				
	0,01 *	0,01 *	0,38 ns	0,59 ns	48
212	*p*				
	0,001 **	0,005 **	0,08 ns	0,17 ns	48
424	*p*				
	0,04 *	0,04 *	0,99 ns	0,99 ns	48

Table S2. Statistical analyses of the survival embryos of both species in examination (Figure 17) subjected to different doses of UV-C treatment (53 - 106 - 212 - 424 J/m^2) and recovered under LD or DD cycles. Significant thresholds are indicated by asterisks (*** $p<0.001$, ** $p<0.01$, * $p<0.05$).

ZF (48h DD)			*n*
BL vs. DD	2-way ANOVA	F=122.4; $p<0.001$ ***	3
Ctrl	Sidak's post-test	$p>0.99$ ns	3
1h		$p=0.04$ *	3
2h		$p=0.98$ ns	3
3h		$p<0.001$ ***	3
4h		$p<0.001$ ***	3
5h		$p<0.001$ ***	3
PA (48h DD)			*n*
BL vs. DD	2-way ANOVA	F=1.26; $p=0.27$ ns	3
Ctrl	Sidak's post-test	$p>0.99$ ns	3
1h		$p>0.99$ ns	3
2h		$p>0.99$ ns	3
3h		$p=0.99$ ns	3
4h		$p=0.96$ ns	3
5h		$p=0.68$ ns	3
ZF (48h LL)			*n*
BL vs. DD	2-way ANOVA	F=3.98; $p=0.009$ **	3
Ctrl	Sidak's post-test	$p>0.99$ ns	3
1h		$p>0.99$ ns	3
2h		$p>0.99$ ns	3
3h		$p>0.09$ ns	3
4h		$p=0.008$ **	3
5h		$p=0.003$ **	3
PA (48h LL)			*n*
BL vs. DD	2-way ANOVA	F=0.0827; $p=0.9943$ ns	3
Ctrl	Sidak's post-test	$p=0.98$ ns	3
1h		$p>0.99$ ns	3
2h		$p>0.99$ ns	3
3h		$p=0.96$ ns	3
4h		$p>0.99$ ns	3
5h		$p>0.99$ ns	3

Table S3. Statistical analyses of the γ-H2AX immunofluorescence assay of both species in examination (Figure 18) subjected to 48h of constant darkness (DD) or white lightness (LL) pre-treatments, followed by UV-C treatment (40 J/m^2) and recovered under BL or DD cycles. Significant thresholds are indicated by asterisks (*** $p<0.001$, ** $p<0.01$, * $p<0.05$).

CPD			*n*
WT vs. KO	2-way ANOVA	F=38.6; $p<0.001$ ***	3
Ctrl	Sidak's post-test	$p>0.99$ ns	3
100 µM		$p=0.03$ *	3
200 µM		$p=0.01$ *	3
400 µM		$p<0.001$ ***	3
6-4PP			*n*
WT vs. KO	2-way ANOVA	F=3.3; $p=0.10$ ns	3
Ctrl	Sidak's post-test	$p>0.99$ ns	3
100 µM		$p=0.80$ ns	3
200 µM		$p=0.97$ ns	3
400 µM		$p=0.30$ ns	3
DASH			*n*
WT vs. KO	2-way ANOVA	F=2.96; $p=0.10$ ns	3
Ctrl	Sidak's post-test	$p>0.99$ ns	3
100 µM		$p=0.88$ ns	3
200 µM		$p=0.77$ ns	3
400 µM		$p=0.62$ ns	3

Table S4. Statistical analyses of the γ-H2AX immunofluorescence assay of each medaka phototolyase mutant (KO) and sibling wild type (WT) in examination (Figure 22). Cells were subjected to 48h of constant darkness (DD) followed by Hydrogen peroxide treatment (from 100 to 400 µM) and recovered for one hour in constant darkness. Significant thresholds are indicated by asterisks (*** $p<0.001$, ** $p<0.01$, * $p<0.05$).

cDNAs	Accession numbers		% of amino acid similarity with *D. rerio* homolog
pa 6-4phr	6-4 photolyase complete CDS	MG566087	88.80
pa 6-4phr-MT1	6-4 photolyase transcript variant X1	MG566088	89.15
pa 6-4phr-MT2	6-4 photolyase transcript variant X2	MG566089	62.96
pa DASHphr-MT1	DASH photolyase transcript variant X1	MG566090	86.82
pa DASHphr-MT2	DASH photolyase transcript variant X2	MG566091	72.73
pa CPDphr	CPD photolyase complete CDS	MG566092	84.50

Table S5. Genbank accession numbers for *P. andruzzii* photolyase cDNAs.

Subcellular localization	Unpaired t-test	*n*
zf 6-4phr vs. pa 6-4phr-MT1	*p*<0,001 ***	30
pa 6-4phr vs. pa 6-4phr-MT1	*p*<0,001 ***	30
zf DASHphr vs. pa DASHphr-MT1	*p*<0,001 ***	30
zf DASHphr vs. pa DASHphr-MT2	*p*<0,001 ***	30
zf CPDphr vs. pa CPDphr	*p*=0,40 ns	30

Table S6. Statistical analysis of predicted Nuclear Localization Signals (NLSs). Student's t-test for unpaired data (two tailed) reported in Figure 20D-B. Significant thresholds are indicated by asterisks (*** $p<0.001$, ** $p<0.01$, * $p<0.05$).

	ZF (BL vs. DD)	PA (BL vs. DD)	
	2-way ANOVA		*n*
CPD	F=60.16 $p<0.0001$ ***	F=22.74; $p<0.0001$ ***	4
	Sidak's post-test		*n*
4h	$p<0.01$ **	$p<0.05$ *	4
6h	$p<0.01$ **	$p>0.05$ ns	4
8h	$p>0.05$ ns	$p>0.05$ ns	4
10h	$p<0.001$ ***	$p<0.05$ *	4
	2-way ANOVA		*n*
6-4PP	F=62.68 $p<0.0001$ ***	F=2.412; $p=0.1341$ ns	4
	Sidak's post-test		*n*
4h	$p<0.001$ ***	$p>0.05$ ns	4
6h	$p<0.001$ **	$p>0.05$ ns	4
8h	$p>0.05$ ns	$p>0.05$ ns	4
10h	$p>0.001$ ***	$p>0.05$ ns	4
	2-way ANOVA		*n*
DASH	F=45.13 $p<0001$ ***	F=1.061; $p=3132$ ns	4
	Sidak's post-test		*n*
4h	$p<0.01$ **	$p>0.05$ ns	4
6h	$p<0.001$ ***	$p>0.05$ ns	4
8h	$p>0.05$ ns	$p>0.05$ ns	4
10h	$p<0.05$ *	$p>0.05$ ns	4
	2-way ANOVA		*n*
XPC	F=20.67 $p=0.0001$ ***	F=35.12; $p=0.0001$ ***	4
	Sidak's post-test		*n*
4h	$p<0.05$ *	$p>0.05$ ns	4
6h	$p>0.05$ ns	$p>0.05$ ns	4
8h	$p<0.05$ *	$p<0.01$ **	4
10h	$p>0.05$ ns	$p<0.01$ **	4

Table S7. Statistical analysis of gene expression of blue-light inducible genes in embryo reported in Figure 21. Significant thresholds are indicated by asterisks (*** $p<0.001$, ** $p<0.01$, * $p<0.05$.

		CPD *n*=20	**6-4PP** *n*=17	**DASH** *n*=37
Model 0	ω tree	0.10	0.12	0.09
Model 1	ω cavefish	0.12	0.11	0.13
Model 1	ω rest of the tree	0.10	0.14	0.09
LRTs M0 vs M1	*p* values	0.72	0.53	0.25

Table S8. Analysis by maximum likelihood using PAML to estimate ω between d_N and d_S changes under our Models which are used as a proxy for the strength of purifying selection.

Gene	Zebrafish	Cavefish
β-actin	F: GATGAGGAAATCGCTGCCCT	F: GATGAGGAAATCGCTGCCCT
	R: GTCCTTCTGTCCCATGCCAA	R: GTCCTTCTGTCCCATGCCAA
6-4PP	F: AATGGCAAGACTCCCATGAC	F: CTGCAGAGGTCCTTCCAAAG
	R: GTGGCCCTAAGGATGACGTA	R: GCTTTCCGTTGTTCTCTTCG
	F: CAAGGGGCTGCGTTTGCATGAT	-
	R: GAACAGGGGGTAGATGTGTCT	-
CPD	F: GAGTTCAGGGCATCACGTC	F: GCTGCTGAAGGAAGTGACC
	R: GCACTGATCGTCGACTTCA	R: CAGTAGAGGACCCCATCAG
	F: AGGGATGCGAGTTCAACAA	F: AGGGATGCGAGTTCAACAA
	R: TTCTCAGCCAAAGCCAGC	R: TTCTCAGCCAAAGCCAGC
	F: GCTGGCTTTGGCTGAGAA	F: GCTGGCTTTGGCTGAGAA
	R: ACATTATGTGCATCAACCTG	R: ACATTATGTGCATCAACCTG
	F: GCATGTACTGGGCAAAGA	F: GCATGTACTGGGCAAAGA
	R: AGACAAACGGTCATTCAGAT	R: AGACAAACGGTCATTCAGAT
DASH	F: ATCTGCGGCTGCATGATAA	F: ATTGGGCTCAGAGGAATGCC
	R: AGTACAGCGGTATTATGTGCTCT	R: GAAAGGGACCGGTCTTAGG
xpc	F: GCCAACATCCGTCTCAGAAT	F: GTGGACTCGACTGAACTAGC
	R: GAACGGTTGGAAAAACCAAG	R: CAGGTCAGACTCACAGCAC

Table S9. Primer sequences for qRT-PCR analysis.

References

Allegrucci G., Sbordoni V., Cesaroni D. (2015). Is radon emission in caves causing deletions in satellite DNA sequences of cave-dwelling crickets? *PLoS One,* 10: e0122456.

Allison W.T., Dann S.G., Helvik J.V., Bradley C., Moyer H.D., Hawryshyn C.W. (2003). Ontogeny of ultraviolet-sensitive cones in the retina of rainbow trout (*Oncorhynchus mykiss*). *Journal of Comparative Neurology*, 461: 294-306.

Ankley G.T., Diamond S.A., Tietge J.E., Holcombe G.W., Jensen K.M., Defoe D.L, Peterson R. (2002). Assessment of the risk of solar ultraviolet radiation to amphibians. Dose-dependent induction of hindlimb malformations in the northern leopard frog (*Rana pipiens*). *Environmental Science and Technology*, 36: 2853-2858.

Aschoff J., Daan S., Groos G.A. (1982). Vertebrate circadian rhythms: structure and physiology. *Vertebrate Circadian System (Structure and Physiology)*, pp.13-24.

Asher G. and Sassone-Corsi P. (2015). Time for food: the intimate interplay between nutrition, metabolism, and the circadian clock. *Cell*, 161(1): 84e92.

Avery J.A., Bowmaker J.K., Djamgoz M.B.A., Downing J.E.G. (1983). Ultraviolet receptors in a freshwater fish. *Journal of Physiology*, 334(23).

Banáth J.P. and Olive P.L. (2003). Expression of phosphorylated histone H2AX as a surrogate of cell killing by drugs that create DNA double-strand breaks. *Cancer Res*earch, 63: 4347-4350.

Beale A., Guibal C., Tamai T.K, Klotz L., Cowen S., Peyric E., Reynoso V.H., Yamamoto Y., Whitmore D. (2013). Circadian rhythms in Mexican blind cavefish *Astyanax mexicanus* in the lab and in the field. *Nature Communications*, 4: 2769.

Bellingham J., Chaurasia S.S., Melyan Z., Liu C., Cameron M.A., Tarttelin E.E., Luvone P.M., Hankins M.W., Tosini G., Lucas J.R. (2006). Evolution of melanopsin photoreceptors: discovery and characterization of a new melanopsin in nonmammalian vertebrates. *PLoS Biology*, 4: e254.

Bellingham J., Whitmore D., Philp A.R., Wells D.J., Foster R.G. (2002). Zebrafish melanopsin: isolation, tissue localisation and phylogenetic position. *Brain Research. Molecular Brain Research,* 107: 128-136.

Ben-Moshe Z., Vatine G., Alon S., Tovin A., Mracek P., Foulkes N.S., Gothilf Y. (2010). Multiple PAR and E4BP4 bZIP transcription factors in zebrafish: diverse spatial and temporal expression patterns. *Chronobiology International*, 27: 1509-1531.

Bennett A.T.D., Cuthill I.C., Partrige J.C., Maier E.J. (1996). Ultraviolet vision and mate choice in zebra finches. *Nature*, 380: 433-435.

Berti R., Durand J.P., Becchi S., Brizzi R., Keller N., Ruffat G. (2001). Eye degeneration in the blindcave-dwelling fish *Phreatichthys andruzzii*. *Canadian Journal of Zoology*. 79: 1278-1285.

Berti R., Messana G. (2010). Subterranean fishes of Africa. *In: Trajano E, Bichuette ME, Kapoor BG (eds), Biology of Subterranean Fishes. Science Publishers: Enfield, NH*, pp. 357-395.

Bertolucci C. and Foà A. (2004). Extraocular photoreception and circadian entrainment in nonmammalian vertebrates. *Chronobiology International,* 21: 501-519.

Bjerke S. (2002). Developing behavioral assays to study dopamine-related disorders in zebrafish (*Danio rerio*). *PhD thesis, The University of Oslo, Oslo, Sweden*, pp. 104.

Bowmaker J.K. and Kunz Y.W. (1987). Ultraviolet receptors, tetrachromatic colour vision and retinal mosaics in the brown trout (*Salmo trutta*): age-dependent changes. *Vision Research*, 27: 2101-2108.

Bowmaker J.K., Thorpe A., Douglas R.H. (1991). Ultraviolet-sensitive cones in the goldfish. *Vision Research*, 31: 349-352.

Bradic M., Beerli P., García de Leon F.J., Esquivel-Bobadilla S., Borowsky R.L. (2012). Gene flow and population structure in the Mexican blind cavefish complex (*Astyanax mexicanus*). *BMC Evolutionary Biology*, 12: 1471-2148.

Branchek T. and Bremiller R. (1984). The development of photoreceptors in the zebrafish, *Brachydanio rerio*. *The Journal of Comparative Neurology*, 224: 107-115.

Bridges C.D.B. (1972). The rhodopsin-porphyropsin visual system. *Photochemistry of Vision: Handbook of Sensory Physiology*, 7: 471-480.

Britten R.J. (1986). Rates of DNA sequence evolution differ between taxonomic groups. *Science*, 231: 1393-1398.

Browman H.I. and Hawryshyn C.W. (1994). The developmental trajectory of ultraviolet photosensitivity in rainbow trout is altered by thyroxine. *Vision Research*, 34: 1397-1406.

Brudler R., Hitomi K., Daiyasu H., Toh H. (2003). Identification of a new cryptochrome class: structure, function, and evolution. *Molecular cell*, 11: 59-67.

Buhr E.D. and Gelder R.N.V. (2014). Local photic entrainment of the retinal circadian oscillator in the absence of rods, cones, and melanopsin. *Proceedings of the National Academy of Science U.S.A.,* 111: 8625-8630.

Buhr E.D., Yue W.W.S., Ren X., Jiang Z., Liao H.W.R, Mei X., Vemaraju S., Nguyen M.T., Reed R.R., Lang R.A. Yau K.W., Van Gelder R.N. (2015). Neuropsin (OPN5)-mediated photoentrainment of local circadian oscillators in mammalian retina and cornea. *Proceedings of the National Academy of Science U.S.A.,* 112: 13093-13098.

Burton C.E., Zhou Y., Bai Q., Burton E.A. (2017). Spectral properties of the zebrafish visual motor response. *Neuroscience Letters*, 646: 62-67.

Calderoni L., Rota-Stabelli O., Frigato E., Panziera A., Kirchner S., Foulkes N.S., Kruckenhauser L., Bertolucci C., Fuselli S. (2016). Relaxed selective constraints drove functional modifications in peripheral photoreception of the cavefish *P. andruzzii* and provide insight into the time of cave colonization. *Heredity (Edinb.)*, 117:383-392.

Camassa, M.M. (2001). Responses to light in epigean and hypogean populations of *Gambusia affinis* (Cyprinodontiformes: Poeciliidae). *Enviromental Biology of Fishes,* 62: 115-118.

Carleton K.L., Harosi F.I., Kocher T.D. (2000). Visual pigments of African cichlid fishes: evidence for ultraviolet vision from microspectrophotometry and DNA sequences. *Vision Research*, 40: 879-890.

Carveth C.J., Widmer, A.M., Bonar S.A. (2011). Comparison of upper thermal

tolerances of native and nonnative fish species in Arizona. *Transactions of the American Fisheries Society*, 135: 1433-1440.

Cashmore A.R. (1999). Cryptochromes: blue light receptors for plants and animals. *Science*, 284: 760-765.

Cavallari N., Frigato E., Vallone D., Fröhlich N., Lopez-Olmeda J.F., Foà A., Berti R., Sánchez- Vázquez F.J., Bertolucci C., Foulkes N.S. (2011). A blind circadian clock in cavefish reveals that opsins mediate peripheral clock photoreception. *PLOS Biology*, 9:e1001142.

Ceinos R.M., Frigato E., Pagano C., Fröhlich N., Negrini P., Cavallari N., Vallone D., Fuselli S., Bertolucci C., Foulkes N.S. (2018). Mutations in blind cavefish target the light-regulated circadian clock gene, period 2. *Scientific Reports,* 8: 8754.

Charron R.A., Fenwick J.C., Lean D.R., Moon T.W., (2000). Ultraviolet-B radiation effects on antioxidant status and survival in the zebrafish, *Brachydanio rerio*. *Photochemistry and Photobiology*, 72: 327-333.

Chaves I., Pokorny R., Byrdin M., Hoang N., Ritz T., Brettel K., Essen L.O., van der Horst G.T., Batschauer A., Ahmad M. (2011). The cryptochromes: blue light photoreceptors in plants and animals. *Annual Review of Plant Biology*, 62: 335-364.

Cline S.D. and Hanawalt P.C. (2003). Who's on first in the cellular response to DNA damage? *Nature Reviews Molecular Cell Biology,* 4, 361-72.

Colli L., Paglianti A., Berti R., Gandolfi G., Tagliavini J. (2009). Molecular phylogeny of the blind cavefish *Phreatichthys andruzzii* and *Garra barreimiae* within the family Cyprinidae. *Environmental Biology of Fishes*, 84: 95-107.

Conway B.R., Chatterjee S., Field G.D., Horwitz G.D., Johnson E.N., Koida K., Mancuso K. (2010). Advances in color science: from retina to behavior. *Journal of Neuroscience*, 30: 14955-14963.

Costa R.M.A., Chiganças V., Galhardo R.D.S., Carvalho H. and Menck C.F.M. (2003). The eukaryotic nucleotide excision repair pathway. *Biochimie,* 85: 1083-1099.

Cowell I.G. (2002). E4BP4/NFIL3, a PAR-related bZIP factor with many roles. *BioEssays*, 24: 1023-1029.

Cummings W.E., Rosenthal G.G., Ryan M.J. (2003). A private ultraviolet channel in visual communication. *Proceedings of the Royal Society London B*, 279: 897-904.

d'Anglemont de Tassigny X., Fagg L.A., Dixon J.P.C., Day K., Leitch H.G., Hendrick A.G., Zahn D., Franceschini I., Caraty A., Carlton M.B., Aparicio S.A., Colledge W.H. (2007). Hypogonadotropic hypogonadism in mice lacking a functional Kiss1 gene. *Proceedings of the National Academy of Science U.S.A.*, 104: 10714-10719.

Daiyasu H., Ishikawa T., Kuma K., Iwai S., Todo T., Toh H. (2004). Identification of cryptochrome DASH from vertebrates. *Genes to Cells,* 9: 479-495.

Davies W.I.L., Tamai T.K., Zheng L., Fu J.K., Rihel J., Foster R.G., Whitmore D., Hankins M.W. (2015). An extended family of novel vertebrate photopigments is widely expressed and displays a diversity of function. *Genome Research*, 25: 1666-1679.

de Laat W.L., Jaspers N.G., Hoeijmakers J.H. (1999). Molecular mechanism of nucleotide excision repair. *Genes and Development*, 13(7): 768-785.

Dekens M.P.S., Foulkes N.S., Tessmar-Raible K. (2017). Instrument design and protocol for the study of light controlled processes in aquatic organisms, and its application to examine the effect of infrared light on zebrafish. *PLoS One* 12(2): e0172038.

Di Rosa V., Frigato E., López-Olmeda J.F., Sánchez-Vázquez F.J. , Bertolucci C. (2015). The light wavelength affects the ontogeny of clock gene expression and activity rhythms in zebrafish larvae. *PLoS One*, 10: e0132235.

Diehn B., Feinleid M., Haupt W., Hildebrand E., Luci F., Nultsch W. (1977). Terminology of behavioral-responses of motile microorganisms. *Photochemistry and Photobiology,* 26 (6): 559-560.

Dimova E.G., Bryant P.E., Chankova S.G. (2008). " Adaptive response " - Some underlying mechanisms and open questions. *DNA Repair*, 408: 396-408.

Domankevich V., Eddini H., Odeh A., Shams I. (2018). Resistance to DNA damage and enhanced DNA repair capacity in the hypoxia-tolerant blind mole rat *Spalax carmeli*. *Journal of Experimental Biology*, 221: jeb174540.

Dong Q., Svoboda K., Tlersch T.R., Monroe W.T. (2007). Photobiological effects of UVA and UVB light in zebrafish embryos: evidence for a competent photorepair system. *Journal of Photochemistry and Photobiology B: Biology*, 88: 137-146.

Doyle S. and Menaker M. (2007). Circadian photoreception in vertebrates. *Cold Spring Harbor Symposia on Quantitative Biology*, 72(1): 499-508.

Drake J.W., Charlesworth B., Charlesworth D., Crow J.F. (1998). Rates of spontaneous mutation. *Genetics*, 148: 1667-1686.

Drivenes Ø., Søviknes A.M., Ebbesson L.O.E., Fjose A., Seo H.C., Helvik J.V. (2003). Isolation and characterization of two teleost melanopsin genes and their differential expression within the inner retina and brain. *Journal of Comparative Neurology*, 456: 84-93.

Dvornyk V., Vinogradova O., Nevo E. (2003). Origin and evolution of circadian clock genes in prokaryotes. *Proceedings of the National Academy of Science U.S.A.,* 100: 2495-2500.

Eilertsen M., Drivenes Ö., Edvardsen R.B., Bradley C.A., Ebbesson L.O., Helvik J.V. (2014). Exorhodopsin and melanopsin systems in the pineal complex and brain at early developmental stages of Atlantic Halibut (*Hippoglossus hippoglossus*). *Journal of Comparative Neurology,* 522(18): 4003-4022.

Eisen J.A., Hanawalt P.C. (1999). A phylogenomic study of DNA repair genes, proteins, and processes. *Mutation Research*, 435: 171-213.

Ercolini A. and Berti R. (1975). Light sensitivity experiments and morphology studies. *Monitore Zoologico Italiano* 6: 29-43.

Ercolini A. and Berti R. (1975). Light sensitivity experiments and morphology studies. *Monitore Zoologico Italiano* 6: 29-43.

Essen L.O. (2006). Photolyases and cryptochromes: common mechanisms of DNA repair and light-driven signaling? *Current Opinion in Structural Biology*, 16: 51-59.

Essen L.O. and Klar T. (2006). Light-driven DNA repair by photolyases. *Cellular and Molecular Life Sciences,* 63: 1266-1277.

Feng P., Zheng J., Rossiter S.J., Wang D., Zhao H. (2014). Massive losses of taste receptor genes in toothed and baleen whales. *Genome Biology and Evolution*, 6: 1254-1265.

Ferrari M. (1993). Colors for Survival: Mimicry and Camoufage in Nature. *Thomasson-Grant, Charlottesville, VA*.

Fischer R.M., Fontinha B.M., Kirchmaier S., Steger J., Bloch S., Inoue D., Panda S., Rumpel S., Tessmar-Raible K. (2013). Co-expression of VAL- and TMT-opsins uncovers ancient photosensory interneurons and motorneurons in the vertebrate brain. *PLoS Biol*ogy, 11: e1001585.

Forger N.G. (2009). Control of cell number in the sexually dimorphic brain and spinal cord. *Journal of Neuroendocrinology*. 21: 393-399.

Forward R.B. (1988). Diel vertical migration: Zooplankton photobiology and behavior. *Oceanography and Marine Biology,* 26: 361-393.

Foster R.G. and Hankins M.W. (2002). Non-rod, non-cone photoreception in the vertebrates. *Progress in retinal and eye research*, 21: 507-527.

Foulkes N.S., Whitmore D., Vallone D., Bertolucci C. (2016). Studying the evolution of the vertebrate circadian clock: the power of fish as comparative models. *Advances in Genetics*, 95: 1-30.

Fraenkel G.S., Gunn D.L. (1940). The orientation of animals. *Oxford*, pp. 352.

Frøland-Steindal I.A., Beale A.D., Yamamoto Y., Whitmore D. (2018). Development of the *Astyanax mexicanus* circadian clock and non-visual light responses. *Developmental Biology*, 441: 345-354.

Fuiman L.A. and Magurran A.E. (1994). Development of predator defenses in fishes. *Reviews in Fish Biology and Fisheries,* 4: 145-183.

Fumey J., Hinaux H., Noirot C., Thermes C., Rétaux S., Casane D. (2018). Evidence for late Pleistocene origin of *Astyanax mexicanus* cavefish. *BMC Evolutionary Biology*, 18: 1-19.

Gavriouchkina D., Fischer S., Ivacevic T., Stolte J., Benes V., Dekens M.P.S. (2010). Thyrotroph embryonic factor regulates light-induced transcription of repair genes in zebrafish embryonic cells. *PLoS One,* 5: e12542.

Gerkema M.P., Davies W.I.L., Foster R.G., Menaker M., Hut R.A. (2013). The nocturnal bottleneck and the evolution of activity patterns in mammals. *Proceedings of the Royal Society B*, 280: 20130508.

Goldsmith T.H. (1980). Hummingbirds see near ultraviolet light. *Science*, 207: 786-788.

Gross J.B. (2012). The complex origin of *Astyanax cavefish*. *BMC Evolutionary Biology*. 12: 105.

Guggiana-Nilo D.A. and Engert F. (2016). Properties of the visible light phototaxis and UV avoidance behaviors in the larval zebrafish. *Frontiers in Behavioral Neuroscience*, 10:160.

Häder D.P., Kumar H.D., Smith R.C., Worrest R.C. (2003). Aquatic ecosystems: effects of solar ultraviolet radiation and interactions with other climatic change factors. *Photochemical and Photobiological Sciences*, 2: 39-50.

Hattar S., Liao H.W., Takao M., Berson D.M., Yau K.W. (2002). Melanopsin- containing retinal ganglion cells: architecture, projections, and intrinsic photosensitivity. *Science*, 295: 1065-1070.

Hauzman E., Bonci D.M.O., Suàrez-Villota E.Y., Neitz M., Ventura D.F. (2017). Daily activity patterns influence retinal morphology, signatures of selection, and spectral tuning of opsin genes in colubrid snakes. *BMC Evolutionary Biology*, 17: 249.

Heesy C.P. and Hall M.I. (2010). The nocturnal bottleneck and the evolution of

mammalian vision. *Brain, Behavior and Evolution*, 75: 195-203.

Hiraki T., Nakasone K., Hosono K., Kawabata Y., Nagahama Y., Okubo K. (2013). Neuropeptide B is female-specifically expressed in the telencephalic and preoptic nuclei of the medaka brain. *Endocrinology*, 155: 1021-1032.

Hirayama J., Miyamura N., Uchida Y., Asaoka Y., Honda R., Sawanobori K., Todo T., Yamamoto T., Sassone-Corsi P., Nishina H. (2009). Common light signaling pathways controlling DNA repair and circadian clock entrainment in zebrafish. *Cell Cycle*, 8: 2794-2801.

Hirayama J., Nakamura H., Ishikawa T., Kobayashi Y., Todo T. (2003). Functional and structural analyses of cryptochrome. Vertebrate CRY regions responsible for interaction with the CLOCK:BMAL1 heterodimer and its nuclear localization. *Journal of Biological Chemistry*, 278: 35620-35628.

Hisatomi O., Satoh T., Tokunaga F. (1997). The primary structure and distribution of killifish visual pigments. *Vision Research*, 37: 3089-3096.

Hitomi K. and Okamoto K. (2000). Bacterial cryptochrome and photolyase: characterization of two photolyase-like genes of *Synechocystis* sp. PCC6803. *Nucleic Acids Research*, 28: 2353-2362.

Huang J.C., Svoboda D.L., Reardon J.T., Sancar A. (1992). Human nucleotide excision nuclease removes thymine dimers from DNA by incising the 22nd phosphodiester bond 5' and the 6th phosphodiester bond 3' to the photodimer. *Proceedings of the National Academy of Science U.S.A.,* 89: 3664-3668.

Hughes S., Jagannath A., Hankins M.W., Foster R.G., Peirson S.N. (2015). Photic regulation of clock systems. *Methods in Enzymology*, 552: 125-143.

Hunt D.M., Cowing J.A., Patel R., Appukuttan B., Bowmaker J.K., Mollon J.D. (1995). Sequence and evolution of the blue cone pigment gene in old and new world primates. *Genomics*, 27: 535-538.

Hunt D.M., Hankins M.W, Collin S.P., Marshall N.J. (2014). Evolution of visual and non-visual pigments. *Springer Series in Vision Research*.

Hunt D.M., Wilkie S.E., Bowmaker J.K., Poopalasundaram S. (2001). Vision in the ultraviolet. *Cellular and Molecular Life Sciences*, 58: 1583-1598.

Hunt S., Cuthill I.C., Bennett A.T., Griffiths R. (1999). Preferences for ultraviolet partners in the blue tit. *Animal Behaviour*, 58: 809-815.

Hut R.A. and Beersma D.G. (2011). Evolution of time-keeping mechanisms: early emergence and adaptation to photoperiod. *Philosophical Transactions of the Royal Society of London. Series B, Biological Sciences*, 366: 2141-2154.

Ishikawa-Fujiwara T., Shiraishi E., Fujikawa Y., Mori T., Tsujimura T., Todo T. (2017). Targeted inactivation of DNA photolyase genes in medaka fish (*Oryzias latipes*). *Photochemistry and Photobiology*, 93: 315-322.

Jacobs G.H. (1981). Comparative color vision. *New York: Academic Press*.

Jacobs G.H., Neitz J., Deegan J.F.I. (1991). Retinal receptors in rodents maximally sensitive to ultraviolet light. *Nature*, 353: 655-656.

Job S. and Bellwood D.R. (2006). Ultraviolet photosensitivity and feeding in larval and juvenile coral reef fishes. *Marine Biology*, 151: 495-503.

Jostes R.F. (1996). Genetic, cytogenetic, and carcinogenic effects of radon: a review. *Mutation Research*, 340: 125-139.

Kanda S., Akazome Y., Matsunaga T., Yamamoto N., Yamada S., Tsukamura H., Maeda K., Oka Y. (2008). Identification of KiSS-1 product kisspeptin and steroid-sensitive sexually dimorphic kisspeptin neurons in medaka (*Oryzias latipes*). *Endocrinology*, 149: 2467-2476.

Katoh K., Standley D.M. (2013). MAFFT multiple sequence alignment software version 7: improvements in performance and usability. *Molecular Biology and Evolution,* 30: 772-780.

Kawamura S. and Yokoyama S. (1998). Functional characterization of visual and nonvisual pigments of American chameleon (*Anolis carolinensis*). *Vision Research*, 38:

37-44.

Kelber A., Vorobyev M., Osorio D. (2003). Animal colour vision behavioural tests and physiological concepts. *Biological Reviews, Cambridge Philosophical Society*, 78: 81-118.

Kim S.T., Malhotra K., Smith C.A., Taylor J.S., Sancar A. (1994). Characterization of (6-4) photoproduct DNA photolyase. *Journal of Biological Chemistry,* 269: 8535-8540.

Kitahashi T., Ogawa S., Parhar I.S. (2009). Cloning and expression of kiss2 in the zebrafish and medaka. *Endocrinology*, 150: 821-831.

Ko C.H. and Takahashi J.S. (2006). Molecular components of the mammalian circadian clock. *Human Molecular Genetics,* 15(2): 271-277.

Kojima D., Mori S., Torii M., Wada A., Morishita R., Fukada Y. (2011). UV-sensitive photoreceptor protein OPN5 in humans and mice. *PloS One*, 6: e26388.

Kowalko J.E., Rohner N., Rompani S.B., Peterson B.K., Linden T.A., Yoshizawa M., Kay E.H., Weber J., Hoekstra H.E., Jeffery W.R., Borowsky R., Tabin C.J. (2013b). Loss of schooling behavior in cavefish through sight-independent and sight-dependent mechanisms. *Current Biology*, 23: 1874-1883.

Koyanagi M., Terakita A. (2014). Diversity of animal opsin-based pigments and their optogenetic potential. *Biochimica et Biophysica Acta BBA - Bioenergetics,* 1837: 710-716.

Kryger Z., Galli-Resta L., Jacobs G.H., Reese B.E. (1998). The topography of rod and cone photoreceptors in the retina of the ground squirrel. *Visual Neuroscience*, 15: 685-691.

Kumar S., and Hedges S.B. (1998). A molecular timescale for vertebrate evolution. *Nature*, 392: 917-920.

Langecker T.G. (1992a). Light sensitivity of cave vertebrates. Behavioral and morphological aspects. *In: Camacho AI (ed) The natural history of biospeleology, Monografias del Museo National de Ciencias Naturales. Graficas Mar-Car, Madrid*, pp.

295–326.

Langecker T.G. (1992b). Persistence of ultrastructurally well developed photoreceptor cells in the pineal organ of a phylogenetically old cave-dwelling population of *Astyanax fasciatus* Cuvier, 1819 (Teleostei, Characidae). *Journal of Zoological Systematics and Evolutionary Research,* 30: 287-296.

Langsdale J.R.M. (1993). Developmental changes in the opacity of larval herring, *Clupea harengus*, and their implications for vulnerability to predation. *Journal of Marine Biology,* 73: 225-232.

Lau B.Y., Mathur P., Gould G.G., Guo S. (2011). Identification of a brain center whose activity discriminates a choice behavior in zebrafish. *Proceedings of the National Academy of Science U.S.A.*, 108 (6): 2581-6.

Leech D.M., Boeing W.J., Cooke S.L., Williamson C.E., Torres L. (2009). UV-enhanced fish predation and the differential migration of zooplankton in response to UV radiation and fish. *Limnology and Oceanography*, 54: 1152-1161.

Lefébure T., Morvan C., Malard F., François C., Konecny-Dupré L., Guéguen L., Weiss-Gayet M., Seguin-Orlando A., Ermini L., Sarkissian C., Charrier N.P., Eme D., Mermillod-Blondin F., Duret L., Vieira C., Orlando L., Douady C.J. (2017). Less effective selection leads to larger genomes. *Genome Research*, 6: 1016-1028.

Lim C. and Allada R. (2013). Emerging roles for post-transcriptional regulation in circadian clocks. *Nature Neuroscience*, 16(11): 1544e1550.

Lindsey-Boltz L.A., Bermu-dez V.P., Hurwitz J., Sancar A. (2001). Purification and characterization of human DNA damage checkpoint Rad complexes. *Proceedings of the National Academy of Science U.S.A.,* 98: 11236-11241.

Lindsey-Boltz L.A., Kemp M.G., Reardon J.T., DeRocco V., Iyer R.R., Modrich P., Sancar A. (2014). Coupling of human DNA excision repair and the DNA damage checkpoint in a defined in vitro system. *Journal of Biological Chemistry*, 289: 5074-5082.

Liu C., Hu J., Qu C., Wang L., Huang G., Niu P., Zhong Z., Hong F., Wang G.,

Postlethwait J.H., Wang H. (2015). Molecular evolution and functional divergence of zebrafish (*Danio rerio*) cryptochrome genes. *Scientific Reports*, 5: 8113.

Liu Z., Tan C., Guo X., Kao Y.T., Li J., Wang L., Sancar A., Zhong D. (2011). Dynamics and mechanism of cyclobutane pyrimidine dimer repair by DNA photolyase. *Proceedings of the National Academy of Science U.S.A.*, 108: 14831-14836.

Loew E.R., and McFarland W.N. (1990). The underwater visual environment. *In Douglas R.H., and Djamgoz M.B.P. (Eds.), The visual system of fish,* pp. 1-43.

Losos J.B. (2011). Convergence, adaptation, and constraint. *Evolution,* 65: 1827-1840.

Lucas R.J. (2013). Mammalian inner retinal photoreception. *Curret Biology,* 23(3): 125-133.

Lucas R.J., Lall G.S., Allen A.E., Brown T.M. (2012). How rod, cone, and melanopsin photoreceptors come together to enlighten the mammalian circadian clock. *Progress in Brain Research*, 199: 1-18.

Lucas R.L., Peirson S.N., Berson D.M., Brown T.M., Cooper H.M., Czeisler C.A., Figueiro M.G., Gamlin P.D., Lockley S.W., O'Hagan J.B., Price L.L., Provencio I., Skene D.J., Brainard G.C. (2014). Measuring and using light in the melanopsin age. *Trends Neuroscience,* 37: 1-9.

Lucas-Lledó J.I. and Lynch M. (2009). Evolution of mutation rates: phylogenomic analysis of the photolyase/cryptochrome family. *Molecular Biology and Evolution,* 26: 1143-1153.

Maor R., Dayan T., Ferguson-Gow H., Jones K.E. (2017). Temporal niche expansion in mammals from a nocturnal ancestor after dinosaur extinction. *Nature Ecology and Evolution*, 1: 1889-1895.

Marková S., Searle J.B., Kotlík P. (2014). Relaxed functional constraints on triplicate α-globin gene in the bank vole suggest a different evolutionary history from other rodents. *Heredity (Edinb)*, 113: 64-73.

Marshall N.J., Vorobyev M. (2003). The design of color signals and color vision in fishes.

In: Collin SP, Marshall NJ, editors. Sensory processing in aquatic environments. New York: Springer, pp. 194–222.

Matos-Cruz V., Blasic J., Nickle B., Robinson P.R., Hattar S., Halpern M.E. (2011). Unexpected diversity and photoperiod dependence of the zebrafish melanopsin system. *PLoS One*, 6: e25111.

Maximino C., de Brito T.M., de Mattos Dias C.A.G., Gouveia Jr A., Morato S. (2010). Scototaxis as anxiety-like behavior in fish. *Nature Protocols,* 5: 209-216.

Maximino C., de Brito T.M., de Moraes F.D., de Oliveira F.V.C., Taccolini I.B., Pereira P.M., Colmanetti R., Lozano R., Gazolla R.A., Tenòrio R. (2007). A comparative analysis of the preference for dark environments in five teleosts. *International Journal of Comparative Psychology,* 20: 351-367.

McClure M. (1999). Development and evolution of melanophore patterns in fishes of the genus *Danio* (Teleostei: Cyprinidae). *Journal of Morphology,* 241: 83-105.

McFarland W.N. and Loew E.R. (1994). Ultraviolet visual pigments in marine fishes of the family Pomacentridae. *Vision Research*, 34: 1393-1396.

Meijkamp B., Aerts R., Van de Staaij J.W.M., Tosserams M., Ernst W.H.O., Rozema J. (1999). Stratospheric ozone depletion: the effects of enhanced UV-B radiation on terrestrial ecosystems. *Systems Ecology, Ecology and Plant Physiology*, pp 71-99.

Menaker M., Moreira L.F., Tosini G. (1997). Evolution of circadian organization in vertebrates. *Brazilian Journal of Medical and Biological Research*, 30(3): 305-313.

Menaker M., Takahashi J. S., Eskin, A. (1978). The physiology of circadian pacemakers. *Annual Review of Physiology*, 40: 501-526.

Menck C.F.M. (2002). Shining a light on photolyases. *Nature Genetics*, 32: 338-339.

Miklósi Á. and Andews R.J. (2006). The zebrafish as a model for behavioral studies. *Zebrafish,* 3: 227-234.

Mohawk J.A., Green C.B., Takahashi J.S. (2012). Central and peripheral circadian

clocks in mammals. *Annual Review of Neuroscience*, 35(1): 445-462.

Moutsaki P., Whitmore D., Bellingham J., Sakamoto K., David-Gray Z.K., Foster R.G. (2003). Teleost multiple tissue (tmt) opsin: a candidate photopigment regulating the peripheral clocks of zebrafish? *Brain Research. Molecular Brain Research,* 112: 135-145.

Mracek P., Santoriello C., Idda M.L., Pagano C., Ben-Moshe Z., Gothilf Y., Vallone D., Foulkes N.S. (2012). Regulation of per and cry genes reveals a central role for the D-Box enhancer in light-dependent gene expression. *PLoS One*, 7: e51278.

Mu D., Hsu D.S., Sancar A. (1996). Reaction mechanism of human DNA repair excision nuclease. *The Journal of Biological Chemistry*, 271: 8285-8294.

Mu D., Park C.H., Matsunaga T., Hsu D.S., Reardon J.T., Sancar A. (1995). Reconstitution of human DNA repair excision nuclease in a highly defined system. *The Journal of Biological Chemistry*, 270: 2415-2418.

Muslimovic A., Johansson P., Hammarsten O. (2012). Measurement of H2AX phosphorylation as a marker of ionizing radiation induced cell damage. *Current Topics in Ionizing Radiation Research*, 2-20.

Nakamura A.J., Rao V.A., Pommier Y., Bonner W.M. (2010). The complexity of phosphorylated H2AX foci formation and DNA repair assembly at DNA double-strand breaks. *Cell Cycle,* 9: 389-397.

Nakane Y., Ikegami K., Ono H., Yamamoto N., Yoshida S., Hirunagi K., Ebihara S., Kubo Y., Yoshimura T. (2010). A mammalian neural tissue opsin (Opsin 5) is a deep brain photoreceptor in birds. *Proceedings of the National Academy of Science U.S.A.*, 107: 15264-15268.

Nakane Y., Shimmura T., Abe H., Yoshimura T. (2014). Intrinsic photosensitivity of a deep brain photoreceptor. *Current Biology*, 24: 596-597.

Needham J. and Green D.E. (1940). Perspectives in Biochemistry. *The American Journal of the Medical Sciences,* 199: 281.

Negelspach D.C., Kaladchibachi S., Fernandez F. (2018). The circadian activity rhythm is reset by nanowatt pulses of ultraviolet light. *Proceedings of the Royal Society B*, 285: 20181288.

Nei M. and Gojobori T. (1986). Simple methods for estimating the numbers of synonymous and nonsynonymous nucleotide substitutions. *Molecular Biology and Evolution*, 3: 418-426.

Neumeyer C. (1992). Tetrachromatic color vision in goldfish: evidence from color mixture experiments. *Journal of Comparative Physiology A*, 171: 639-649.

Nguyen Ba A.N., Pogoutse A., Provart N., Moses A.M. (2009). NLStradamus: a simple Hidden Markov Model for nuclear localization signal prediction. *BMC Bioinformatics,* 10: 202.

Niemiller M.L., Fitzpatrick B.M., Shah P., Schmitz L., Near T.J. (2013). Evidence for repeated loss of selective constraint in rhodopsin of amblyopsid cavefishes (Teleostei: Amblyopsidae). *Evolution*, 67: 732-748.

Nigel D.P. and Dylan G.J. (2003). Ecological roles of solar UV radiation: towards an integrated approach. *Trends in Ecology and Evolution*, 18: 48-55.

Nouspikel T. (2009). Nucleotide excision repair: variations on versatility. *Cellular and Molecular Life Sciences,* 66: 994-1009.

Novales Flamarique I. (2000). The ontogeny of ultraviolet sensitivity, cone disappearance and regeneration in the sockeye salmon *Oncorhynchus nerka*. *Journal of Experimental Biology*, 203: 1161-1172.

Novales Flamarique I. (2016). Diminished foraging performance of a mutant zebrafish with reduced population of ultraviolet cones. *Proceedings of the Royal Society London B*, 283: 20160058.

Ohuchi H., Yamashita T., Tomonari S., Fujita-Yanagibayashi S., Sakai K., Noji S., Shichida Y. (2012). A Non-mammalian type opsin 5 functions dually in the photoreceptive and non-photoreceptive organs of birds. *PLoS ONE*, 7: e31534.

Okano T., Kojima D., Fukada Y., Shichida Y., Yoshizawa T. (1992). Primary structures of chicken cone visual pigments: vertebrate rhodopsins have evolved out of cone visual pigments. *Proceedings of the National Academy of Science U.S.A.*, 89: 5932-5936.

Ota W., Nakane Y., Hattar S., Yoshimura T. (2018). Impaired circadian photoentrainment in Opn5-null mice. *iScience*, 6: 299-305.

Ozer Z., Reardon J.T., Hsu D.S., Malhotra K., Sancar A. (1995). The other function of DNA photolyase: stimulation of excision repair of chemical damage to DNA. *Biochemistry*, 34: 15886-15889.

Pagano C., di Martino O., Ruggiero G., Guarino A.M., Mueller N., Siauciunaite R., Reischl M., Foulkes N.S., Vallone D., Calabrò V. (2016). The tumor-associated YB-1 protein: new player in the circadian control of cell proliferation. *Oncotarget*, 8: 6193-6205.

Parry J.W. and Bowmaker J.K. (2000). Visual pigment reconstitution in intact goldfish retina using synthetic retinaldehyde isomers. *Vision Research*, 40: 2241-2247.

Pasqualetti M., Bertolucci C., Ori M., Innocenti A., Magnone M.C., De Grip W.J., Nardi I., Foà A. (2003). Identification of circadian brain photoreceptors mediating photic entrainment of behavioural rhythms in lizards. *European Journal of Neuroscience*, 18: 364-372.

Pei D.S. and Strauss P.R. (2013). Zebrafish as a model system to study DNA damage and repair. *Mutation Research*, 743-744: 151-159.

Philp A.R., Garcia-Fernandez J.M., Soni B.G., Lucas R.J., Bellingham J., Foster R. G. (2000b). Vertebrate ancient (VA) opsin and extraretinal photoreception in the Atlantic salmon (*Salmo salar*). *Journal of Experimental Biology*, 203: 1925-1936.

Pichaud F., Briscoe A., Desplan C. (1999). Evolution of color vision. *Current Opinion in Neurobiology*, 9: 622-627.

Pittendrigh C.S. (1993). Temporal organisation: reflections of a Darwinian clock-watcher. *Annual Review of Physiology*, 55: 17-54.

Pokorny R., Klar T., Hennecke U., Carell T., Batschauer A., Essen, L.O. (2008). Recognition and repair of UV lesions in loop structures of duplex DNA by DASH-type cryptochrome. *Proceedings of the National Academy of Science U.S.A.*, 105: 21023–21027.

Preitner N., Damiola F., Lopez-Molina L., Zakany J., Duboule D., Albrecht U., Schibler U. (2002). The orphan nuclear receptor REV-ERBalpha controls circadian transcription within the positive limb of the mammalian circadian oscillator. *Cell*, 110(2): 251e260.

Proudlove G.S. (2010). Biodiversity and distribution of the subterranean fishes of the world. *In: Trajano E, Bicuette ME, Kapoor BG (eds) Biology of subterranean fishes. Science Publishers, New Hampshire,* pp. 65-80.

Provencio I., Jiang G., De Grip W.J., Hayes W.P., Rollag M.D. (1998). Melanopsin: an opsin in melanophores, brain, and eye. *Proceedings of the National Academy of Sciences of the U.S.A.,* 95: 340-345.

Provencio I., Rollag M.D., Castrucci A.M. (2002). Photoreceptive net in the mammalian retina. This mesh of cells may explain how some blind mice can still tell day from night. *Nature*, 415(6871): 493.

Raymond P.A., Barthel L.K., Rounsifer M.E., Sullivan S.A., Knight J.K. (1993). Expression of rod and cone visual pigments in goldfish and zebrafish: a rhodopsin-like gene is expressed in cones. *Neuron,* 10: 1161-1174.

Raymond P.A., Colvin S.M., Jabeen Z., Nagashima M., Barthel L.K., Hadidjojo J., Popova L., Pejaver V.R., Lubensky D.K. (2014). Patterning the cone mosaic array in zebrafish retina requires specification of ultraviolet-sensitive cones. *PLoS ONE*, 9(1): e85325.

Reardon J.T., Thompson L.H., Sancar A. (1997). Rodent UV-sensitive mutant cell lines in complementation groups 6-10 have normal general excision repair activity. *Nucleic Acids Research*, 25: 1015-1021.

Reppert S.M. and Weaver D.R. (2001). Molecular analysis of mammalian circadian rhythms. *Annual Review of Physiology*, 63(1): 647e676.

Rick I. P., Bloemker D., Bakker T.C.M. (2012). Spectral composition and visual foraging in the three-spined stickleback (Gasterosteidae: *Gasterosteus acuelatus L.*): elucidating the role of ultraviolet wavelengths. *Biological Journal of the Linnean Society*, 105: 359-368.

Risner M.L., Lemerise E., Vukmanic E.V., Moore A. (2006). Behavioral spectral sensitivity of the zebrafish (*Danio rerio*). *Vision Research*, 46: 2625-2635.

Robertson A.B., Klungland A., Rognes T., Leiros I. (2009). Base excision repair: the long and short of it. *Cellular and Molecular Life Sciences,* 66: 981-993.

Robinson J., Schmitt E.A., Hárosi F.I., Reece R.J., Dowling J.E. (1993). Zebrafish ultraviolet visual pigment: absorption spectrum, sequence, and localization. *Proceedings of the National Academy of Science U.S.A.*, 90: 6009-6012.

Roenneberg T., Daan S. and Merrow M. (2003). The art of entrainment. *Journal of Biological Rhythms*, 18(3): 183-194.

Roenneberg T., Foster R.G. (1997). Twilight times: light and the circadian system. *Photochemistry and Photobiology*, 66: 549-561.

Rogakou E.P., Pilch D.R., Orr A.H., Ivanova V.S., Bonner W.M. (1998). Double-stranded brekas induce histone H2AX phosphorylation on serine 139. *The Journal of Biological Chemistry*, 273: 5858-5868.

Sancar A. (1996). No “End of History” for photolyases. *Science*, *272*: 48-49.

Sancar A. (2003). Structure and function of DNA photolyase and cryptochrome blue-light photoreceptors. *Chemical Reviews*, 103: 2203-37.

Sancar A. (2016). Mechanisms of DNA repair by photolyase and excision nuclease (Nobel Lecture). *Angewandte Chemie*, 55: 8502-8527.

Sassone-Corsi P., Foulkes N.S., Whitmore D. (2000). Light acts directly on organs and cells in culture to set the vertebrate circadian clock. *Nature*, 404(6773): 87-91.

Saszik S., Bilotta J., Givin C.M. (1999). ERG assessment of zebrafish retinal

development. *Visual Neuroscience*, 16: 881-888.

Sato K., Yamashita T., Haruki Y., Ohuchi H., Kinoshita M., Shichida Y. (2016). Two UV-sensitive photoreceptor proteins, Opn5m and Opn5m2 in ray-finned fish with distinct molecular properties and broad distribution in the retina and brain. *PLoS One*, 11(5): e0155339.

Schibler U. and Sassone-Corsi P. (2002). A web of circadian pacemakers. *Cell*, 111(7): 919-922.

Schibler U., Gotic I., Saini C., Gos P., Curie T., Emmenegger, Y., Sinturel F., Gosselin P., Gerber A., Fleury-Olela F., Rando G., Franken P. (2015). Clock-talk: interactions between central and peripheral circadian oscillators in mammals. *Cold Spring Harbor Symposia on Quantitative Biology*, 027490.

Schluter D., Clifford E.A., Nemethy M., McKinnon J.S. (2004). Parallel evolution and inheritance of quantitative traits. *The American Naturalist*, 163: 809-822.

Seebacher F., Kazerouni E.G., Franklin C.E. (2016). Ultraviolet B radiation alters movement and thermal selection of zebrafish (*Danio rerio*). *Biology Letters*, 12(8).

Seeberg E., Eide L., Bjørås M. (1995). The base excision repair pathway. *Trends in Biochemical Sciences,* 20: 391-397.

Selby C.P. and Sancar A. (2006). A cryptochrome/photolyase class of enzymes with single-stranded DNA-specific photolyase activity. *Proceedings of the National Academy of Science U.S.A.,* 103: 17696-17700.

Serra E.L., Medalha C.C., Mattioli R. (1999). Natural preference of zebrafish (*Danio rerio*) for a dark environment. *Brazilian Journal of Medical and Biological Research,* 32: 1551-1553.

Servili A., Le Page Y., Leprince J., Caraty A., Escobar S., Parhar I.S., Seong J.Y., Vaudry H., Kah O. (2011). Organization of two independent kisspeptin systems derived from evolutionary-ancient kiss genes in the brain of zebrafish. *Endocrinology*, 152: 1527-1540.

Sharma A., Singh K., Almasan A. (2012). Histone H2AX phosphorylation: a marker for DNA damage. *DNA Repair Protocols*, pp. 613-626.

Siebeck U.E., Parker A.N., Sprenger D., Mathger L.M., Wallis G. (2010). A species of reef fish that uses ultraviolet patterns for covert face recognition. *Current Biology*, 20: 407- 410.

Sinha R.P. and Häder D.P. (2002). UV-induced DNA damage and repair: a review. *Photochemical and Photobiological Sciences,* 1: 225-236.

Song Y., Duan X., Chen J., Huang W., Zhu Z., Hu W. (2015). The distribution of kisspeptin (kiss)1- and kiss2- positive neurones and their connections with gonadotrophin-releasing hormone-3 neurones in the zebrafish brain. *Journal of Neuroendocrinology*, 27: 198-211.

Spence R., Gerlach G., Lawrence C., Smith C. (2008). The behaviour and ecology of the zebrafish, *Danio rerio*. *Biological reviews of the Cambridge Philosophical Society,* 83: 13-34.

Stemmer M., Schuhmacher L.N., Foulkes N.S., Bertolucci C., Wittbrodt J. (2015). Cavefish eye loss in response to an early block in retinal differentiation progression. *Development,* 142: 743-752.

Stich H.B. and Lampert W. (1981). Predator evasion as an explanation of diurnal vertical migration by zooplankton. *Nature*, 293: 396-398.

Szél A., Röhlich P., Caffe A. R., Van Veen T. (1996). Distribution of cone photoreceptors in the mammalian retina. *Microscopy Research and Technique*, 35: 445-462.

Takechi M. and Kawamura S. (2005). Temporal and spatial changes in the expression pattern of multiple red and green subtype opsin genes during zebrafish development. *Journal of Experimental Biology*, 208: 1337-1345.

Tamai T.K., Vardhanabhuti V., Foulkes N.S., Whitmore D. (2004). Early embryonic light detection improves survival. *Current Biology*, 14: 104-105.

Tang H., Liu Y., Luo D., Ogawa S., Yin Y., Li S., Zhang Y., Hu W., Parhar I.S., Lin H.,Liu

X., Cheng C.H.K. (2014). The kiss/kissr systems are dispensable for zebrafish reproduction: evidence from gene knockout studies. *Endocrinology*, 156: 589-599.

Tarttelin E.E., Bellingham J., Hankins M.W., Foster R.G., Lucas R.J. (2003). Neuropsin (Opn5): a novel opsin identified in mammalian neural tissue. *FEBS Letter*, 554: 410-416.

Tarttelin E.E., Frigato E., Bellingham J., Di Rosa V., Berti R., Foulkes N.S., Lucas R.J, Bertolucci C. (2012). Encephalic photoreception and phototactic response in the troglobiont Somalian blind cavefish *Phreatichthys andruzzii. Journal of Experimental Biology*, 215: 2898-2903.

Thoma F. (1999). Light and dark in chromatin repair: repair of UV-induced DNA lesions by photolyase and nucleotide excision repair. *EMBO Journal*, 18: 6585-98. Thompson C.L. and Sancar A. (2002). Photolyase/cryptochrome blue-light photoreceptors use photon energy to repair DNA and reset the circadian clock. *Oncogene,* 21: 9043-9056.

Thorndike E.L. (1911). A note on the psychology of fishes. *The American Naturalist,* 33: 923.

Timmerman C. and Chapman L. (2004). Hypoxia and interdemic variation in *Poecilia latipinna*. *Journal of fish biology*, 65: 635–650.

Tobler M., Palacios M., Chapman L.J., Mitrofanov I., Bierbach D., Plath M., Arias-Rodriguez L., de León F.J.G. and Mateos M. (2011). Evolution in extreme environments: replicated phenotypic differentiation in livebearing fish inhabiting sulfidic springs. *International journal of organic evolution*, 65: 2213-28.

Todo T. (1999). Functional diversity of the DNA photolyase/blue light receptor family. *Mutation research*, 434, 89-97.

Tomicic M.T., Reischmann P., Rasenberger B., Meise R., Kaina B., Christmann M. (2011). Delayed c-Fos activation in human cells triggers XPF induction and an adaptive response to UVC-induced DNA damage and cytotoxicity. *Cellular and Molecular Life Sciences*, 68: 1785-1798.

Tomonari S., Migita K., Takagi A., Noji S., Ohuchi H. (2008). Expression patterns of the

opsin 5–related genes in the developing chicken retina. *Developmental Dynamics*, 237: 1910-1922.

Uchida Y., Hirayama J., Nishina H. (2010). A common origin: signaling similarities in the regulation of the circadian clock and DNA damage responses. *Biological and Pharmaceutical Bulletin*, *33*: 535-544.

Vallone D., Gondi S.B., Whitmore D., Foulkes N.S. (2004). E-box function in a period gene repressed by light. *Proceedings of the National Academy of Science U.S.A.,*101: 4106-4111.

Vanselow K. and Kramer A. (2007). Role of phosphorylation in the mammalian circadian clock. *Cold Spring Harbor Symposia on Quantitative Biology*, 72(1): 167-176.

Vatine G., Vallone D., Appelbaum L., Mracek P., Ben-Moshe Z., Lahiri K., Gothilf Y., Foulkes N.S. (2009). Light directs zebrafish period2 expression via conserved D and E boxes. *PLoS Biology*, 7: e1000223.

Viitala J., Korpimaki E., Palokangas P., Koivula M. (1995). Attraction of kestrels to vole scent marks visible in ultraviolet light. *Nature*, 373: 425-427.

Watkins J., Miklósi Á., Andrew R.J. (2004). Early asymmetries in the behavior of zebrafish larvae. *Behavioural Brain Research,* 151: 177-183.

Weber S. (2005). Light-driven enzymatic catalysis of DNA repair: a review of recent biophysical studies on photolyase. *Biochimica et Biophysica Acta – Bioenergetics*, 1707: 1-23.

Weger B.D., Sahinbas M., Otto G.W., Mracek P., Armant O., Dolle D., Lahiri K., Vallone D., Ettwiller L., Geisler R., Foulkes N.S., Dickmeis T., (2011). The light responsive transcriptome of the zebrafish: function and regulation. *PLoS One* 6: e17080.

Wilkens H. (2001). Convergent adaptations to cave life in the *Rhamdia laticauda* catfish group (Pimelodidae, Teleostei). *Environmental Biology of Fishes*, 62: 251-261.

Wilkie S.E., Vissers P.M., Das D., Degrip W.J., Bowmaker J.K., Hunt D.M. (1998). The molecular basis for UV vision in birds: spectral characteristics, cDNA sequence and

retinal localization of the UV-sensitive visual pigment of the budgerigar (*Melopsittacus undulatus*). *Biochemical Journal*, 330: 541-547.

Yamashita T., Ohuchi H., Tomonari S., Ikeda K., Sakai K., Shichida Y. (2010). Opn5 is a UV-sensitive bistable pigment that couples with Gi subtype of G protein. *Proceedings of the National Academy of Science U.S.A.,* 107: 22084-22089.

Yamashita T., Ono K., Ohuchi H., Yumoto A., Gotoh H., Tomonari S., Sakai K., Fujita H., Imamoto Y., Noji S., Nakamura K., Shichida Y. (2014). Evolution of Mammalian Opn5 as a specialized UV-absorbing pigment by a single amino acid mutation. *Journal of Biological Chemistry*. 289: 3991-4000.

Yang Z. (1998). Likelihood ratio tests for detecting positive selection and application to primate lysozyme evolution. *Molecular Biology and Evolution,* 15: 568-573.

Yang Z. (2007). PAML 4: phylogenetic analysis by maximum likelihood. *Molecular Biology and Evolution,* 24: 1586-1591.

Yang Z. and Bielawski J.P. (2000). Statistical methods for detecting molecular adaptation. *Trends in Ecology and Evolution*, 15(12): 496-503.

Yang Z. and Nielsen R. (2000). Estimating synonymous and nonsynonymous substitution rates under realistic evolutionary models. *Molecular Biology and Evolution*, 17: 32-43.

Yewers M.S., McLean C.A., Moussalli A., Stuart-Fox D., Bennett A.T., Knott B. (2015). Spectral sensitivity of cono photoreceptors and opsin expression in two colour-divergent lineages of lizard Ctenophorus decresii. *Journal of Experimental Biology*. 218: 1556-1563.

Yokoyama S. and Yokoyama, R. (1996). Adaptive evolution of photoreceptors and visual pigments in vertebrates. *Annual Review of Ecology and Systematics,* 27: 543-567.

Yokoyama S., Radlwimmer F.B., Blow N.S. (2000). Ultraviolet pigments in birds evolved from violet pigments by a single amino acid change. *Proceedings of the National Academy of Sciences of the U.S.A.*, 97: 7366-7371.

Yokoyama S., Radlwimmer F.B., Kawamura S. (1998). Regeneration of ultraviolet pigments of vertebrates. *FEBS Letters*, 423: 155-158.

Yoshida M., Nagamine M., Uematsu K. (2005). Comparison of behavioral responses to a novel environment between three teleosts, bluegill *Lepomis macrochirus*, crucian carp *Carassius langsdorfii*, and goldfish *Carassius auratus*. *Fisheries Science,* 71: 314-319.

Zhong P.D. (2015). Electron transfer mechanisms of DNA repair by photolyase. *Annual Review of Physical Chemistry*, 66: 691-715.

Zohar Y., Muñoz-Cueto J.A., Elizur A., Kah O. (2010). Neuroendocrinology of reproduction in teleost fish. *General and Comparative Endocrinology*. 165: 438-455.

Acknowledgments

I would like to express my gratitude to my supervisors Prof. Cristiano Bertolucci for giving me the opportunity to do my PhD in his laboratory. I want to thank Dr. Elena Frigato and Dr. Silvia Fuselli for their advices and for helping and teaching me many techniques during my studies. I would like to thank my PhD coordinator Prof. Guido Barbujani for his comprehension and confidence to address my research interest. I am very grateful to Prof. Nicholas Simon Foulkes and Dr. Daniela Vallone who gave me the chance to work nine months in their laboratory at Karlsruhe Institute of Technology (KIT), Institute of Toxicology and Genetics (ITG).

I want to thank all the members at the University of Ferrara, Roberto Biello, Patricia Santos, Gloria Gonzales Fortez, Andrea Brunelli, Roberta Susca, Elisa Morbiato, Emiliano Trucchi, Giorgio Bertorelle, Silvia Ghirotto, Andrea Benazzo and Francesca Tassi, for friendly support during this career.
I would like to thank all the members of the ITG, Andrea Maria Guarino, Gennaro Ruggiero, Felicia Sangermano, Nathalie Geyer, Rima Siauciunaite, Halina Dora, Juan Du and Haiyu Zhao, for their help and friendship.

Last but not least I want to thanks my family and Bologna crew for all their strong support and love during my PhD life.

Pubblications during the PhD

- **Di Mauro G.**, Perez M., Lorenzi M.C., Guerrieri F.J., Millar J.G., d'Ettorre P. (2015). Ants discriminate between different hydrocarbon concentrations. ***Frontiers in Ecology and Evolution****.* 3: 133.

- Zhao H., **Di Mauro G.**, Lungu-Mitea S., Negrini P., Guarino M., Frigato E., Braunbeck T., Ma H., Lamparter T., Vallone D., Bertolucci C., Foulkes N.S. (2018). Modulation of DNA repair systems in blind cavefish during evolution in constant darkness. ***Current Biology***. 28(20): 3229-3243.

- Guarino A.M., **Di Mauro G.**, Ruggiero G., Geyer N., Delicato A. Foulkes N.S., Vallone D., Calabrò V. (2019). YB-1 recruiment to stress granules reveals a differential adaptive response to stress in Zebrafish. ***Scientific Reports***. Revised on 11/02/19.

- **Di Mauro G.**, Lucon-Xiccato T., Bisazza A., Bertolucci C. (2018). Chemical alarm cues mediate antipredator behaviour and learning in Zebrafish larvae. ***Manuscript in preparation***.

- Zhao H., Du J., **Di Mauro G.**, Negrini P., Vallone D., Bertolucci C., Foulkes N.S. (2018). Differential control of cavefish ddb2 reveals the evolution of DNA repair regulation in an extreme environment. ***Manuscript in preparation***.